USGS
science for a changing world

# Kīlauea's 2008–2018 Summit Lava Lake—Chronology and Eruption Insights

Chapter A of
**The 2008–2018 Summit Lava Lake at Kīlauea Volcano, Hawai'i**

Professional Paper 1867

**U.S. Department of the Interior**
**U.S. Geological Survey**

**Cover.** Photograph of the lava lake in late October 2012. Hawaiian Volcano Observatory (HVO) and Jaggar Museum are visible on the skyline in the upper right. Photograph from the Halema‘uma‘u Overlook by David Dow, HVO volunteer.

# Kīlauea’s 2008–2018 Summit Lava Lake—Chronology and Eruption Insights

By Matthew Patrick, Tim Orr, Don Swanson, Bruce Houghton, Kelly Wooten, Liliana Desmither,
Carolyn Parcheta, and David Fee

Chapter A of

**The 2008–2018 Summit Lava Lake at Kīlauea Volcano, Hawai‘i**

Edited by Matthew Patrick, Tim Orr, Don Swanson, and Bruce Houghton

Professional Paper 1867

**U.S. Department of the Interior**
**U.S. Geological Survey**

**U.S. Department of the Interior**
DAVID BERNHARDT, Secretary

**U.S. Geological Survey**
James F. Reilly II, Director

U.S. Geological Survey, Reston, Virginia: 2021



Suggested citation:
Patrick, M., Orr, T., Swanson, D., Houghton, B., Wooten, K., Desmither, L., Parcheta, C., and Fee, D., 2021, Kīlauea's 2008–2018 summit lava lake—Chronology and eruption insights, chap. A *of* Patrick, M., Orr, T., Swanson, D., and Houghton, B., eds., The 2008–2018 summit lava lake at Kīlauea Volcano, Hawai‘i: U.S. Geological Survey Professional Paper 1867, 50 p., https://doi.org/10.3133/pp1867A.

ISSN 1044-9612 (print)
ISSN 2330-7102 (online)

# Acknowledgments

The entire U.S. Geological Survey (USGS) Hawaiian Volcano Observatory (HVO) staff, in addition to dozens of USGS volunteers, contributed to monitoring the 2008–2018 lava lake. Jim Kauahikaua and Tina Neal were HVO Scientists-in-Charge during the summit eruption, and supervised monitoring and research. Steve Brantley, the Deputy Scientist-in-Charge, oversaw field operations and logistics. The HVO electronics and information technology groups are thanked for their work maintaining the summit monitoring equipment and datastreams. USGS staff, including David Wilson, Wes Thelen, Brian Shiro, Tamar Elias, Jeff Sutton, Mike Poland, Asta Miklius, Kyle Anderson, and Ingrid Johanson, contributed to interpretations of seismic activity, gas emissions, and ground deformation. We also thank USGS staff at other observatories who assisted with the 24-hour watch during the first 4 months of the eruption: Dan Dzurisin, Wendy McCausland, Ed Brown, Kristi Wallace, Nicole Lautze, Rick Hoblitt, Jim Dixon, Larry Mastin, Dina Venezky, and Matt Haney. Data and interpretation shared by Milton Garces at the Infrasound Laboratory of the University of Hawaiʻi were essential in tracking the early phases of the eruption. Pilot David Okita provided superb airborne views of the eruption. We thank the Alaska Volcano Observatory and the Hawaiʻi Institute of Geophysics and Planetology at the University of Hawaiʻi at Mānoa for use of handheld thermal cameras during 2008–9. Light detection and ranging (lidar) data were kindly shared by Todd Eriksen (University of Hawaiʻi at Mānoa), Adam LeWinter and David Finnegan (U.S. Army Corps of Engineers), and Gerald Bawden (USGS). Physical volcanology students from University of Hawaiʻi aided the tephra studies. Reviews by Jim Kauahikaua and Matt Loewen improved the manuscript. Lastly, we thank Hawaiʻi Volcanoes National Park and the National Park Service for facilitating HVO work in the closed regions of the park.

# Contents

## Figures

## Table

# Conversion Factors

International System of Units to U.S. customary units

| Multiply | By | To obtain |
|---|---|---|
| | Length | |
| centimeter (cm) | 0.3937 | inch (in.) |
| meter (m) | 3.281 | foot (ft) |
| kilometer (km) | 0.6214 | mile (mi) |
| meter (m) | 1.094 | yard (yd) |
| | Area | |
| hectare (ha) | 2.471 | acre |
| hectare (ha) | 0.003861 | square mile ($mi^2$) |
| | Volume | |
| cubic meter ($m^3$) | 264.2 | gallon (gal) |
| cubic meter ($m^3$) | 35.31 | cubic foot ($ft^3$) |
| cubic meter ($m^3$) | 1.308 | cubic yard ($yd^3$) |
| | Flow rate | |
| meter per second (m/s) | 3.281 | foot per second (ft/s) |
| | Mass | |
| metric ton (t) | 1.102 | ton, short [2,000 lb] |
| metric ton (t) | 0.9842 | ton, long [2,240 lb] |
| | Density | |
| kilogram per cubic meter ($kg/m^3$) | 0.06242 | pound per cubic foot ($lb/ft^3$) |
| gram per cubic centimeter ($g/cm^3$) | 62.4220 | pound per cubic foot ($lb/ft^3$) |

Temperature in degrees Celsius (°C) may be converted to degrees Fahrenheit (°F) as follows:

$$°F = (1.8 \times °C) + 32.$$

Temperature in degrees Fahrenheit (°F) may be converted to degrees Celsius (°C) as follows:

$$°C = (°F - 32) / 1.8.$$

# Abbreviations

| | |
|---|---|
| a.s.l. | above sea level |
| cm | centimeter |
| DI | deflation-inflation |
| ERZ | East Rift Zone |
| FTIR | Fourier transform infrared spectrometry |
| GPS | Global Positioning System |
| HVO | Hawaiian Volcano Observatory |
| km | kilometer |
| lidar | light detection and ranging |
| m | meter |
| $m^3$ | cubic meter |
| m/s | meter per second |
| RSAM | real-time seismic amplitude measurement |
| t/d | metric ton per day |
| UAS | unmanned aircraft system |
| USGS | U.S. Geological Survey |
| VLP | very long period |

# Kīlauea’s 2008–2018 Summit Lava Lake—Chronology and Eruption Insights

By Matthew Patrick,[1] Tim Orr,[1] Don Swanson,[1] Bruce Houghton,[2] Kelly Wooten,[1] Liliana Desmither,[3] Carolyn Parcheta,[1] and David Fee[4]

## Abstract

The first eruption at Kīlauea’s summit in 25 years began on March 19, 2008, and persisted for 10 years. The onset of the eruption marked the first explosive activity at the summit since 1924, forming the new “Overlook crater” (as the 2008 summit eruption crater has been informally named) within the existing crater of Halemaʻumaʻu. The first year consisted of sporadic lava activity deep within the Overlook crater. Occasional small explosions deposited spatter and small wall-rock lithic pieces around the Halemaʻumaʻu rim. After a month-long pause at the end of 2008, deep sporadic lava lake activity returned in 2009. Continuous lava lake activity began in February 2010. The lake rose significantly in late 2010 and early 2011, before subsequently draining briefly in March 2011. This disruption of the summit eruption was triggered by eruptive activity on the East Rift Zone. Rising lake levels through 2012 established a more stable, larger lake in 2013, with continued enlargement over the subsequent 5 years. Lava reached the Overlook crater rim and overflowed on the Halemaʻumaʻu floor in brief episodes in 2015, 2016, and 2018, but the lake level was more commonly 20–60 meters below the rim during 2014–18. The lake was approximately 280×200 meters (~42,000 square meters) by early 2018 and formed one of the two largest lava lakes on Earth.

A new eruption began in the lower East Rift Zone on May 3, 2018, causing magma to drain from the summit reservoir complex. The lava in Halemaʻumaʻu had drained below the crater floor by May 10, followed by collapse of the Overlook and Halemaʻumaʻu craters. The collapse region expanded as much of the broader summit caldera floor subsided incrementally during June and July. By early August 2018, the collapse sequence had ended, and the summit was quiet. The historic changes in May–August 2018 brought a dramatic end to the decade of sustained activity at Kīlauea’s summit.

The unique accessibility of the 2008–18 lava lake provided new observations of lava lake behavior and open-vent basaltic outgassing. Data indicated that explosions were triggered by rockfalls from the crater walls, that the lake consisted of a low-density foamy lava, that cycles of gas pistoning were rooted at shallow depths in the lake, and that lake level fluctuations were closely tied to the pressure of the summit magma reservoir. Lava chemistry added further support for an efficient hydraulic connection between the summit and East Rift Zone. Notwithstanding the benefits to scientific understanding, the eruption presented a persistent hazard of volcanic air pollution (vog) that commonly extended far from Kīlauea’s summit.

## Introduction

The first eruption at the summit of Kīlauea on the Island of Hawaiʻi in 25 years began on March 19, 2008, and continued for slightly more than 10 years. The eruption onset marked the first explosive activity other than Hawaiian fountaining at the summit since 1924, with sporadic lava lake activity in its first 2 years (Wilson and others, 2008). The subsequent 8 years consisted of continuous lava lake activity, evolving to form one of the two largest lava lakes on Earth (along with the lake at Nyiragongo Volcano, Democratic Republic of the Congo) (Patrick and others, 2016a, 2018; Valade and others, 2018).

The lava lake was unique for its combination of a robust monitoring network and accessibility. Scientists could reach the crater rim in a 5-minute drive and the crater was directly visible from the Hawaiian Volcano Observatory (HVO) facility. This ready accessibility provided an array of new insights into lava lake behavior and open-vent basaltic activity. Despite the benefits to science and tourism afforded by the summit activity, the eruption presented prolonged hazards to human health and challenges to the local economy. The increased gas emissions from the summit created persistent problems with volcanic air pollution (vog) across the Island of Hawaiʻi.

This chapter presents a chronology of the lava lake during its 10-year lifespan. We focus on the general activity and geologic observations to develop context for other, more focused studies,

[1]U.S. Geological Survey.

[2]University of Hawaiʻi at Mānoa.

[3]University of Hawaiʻi at Hilo.

[4]Infrasound Laboratory at the University of Hawaiʻi at Mānoa; now at the Alaska Volcano Observatory at the University of Alaska Fairbanks.

as well as discuss some notable aspects of the eruption and new insights provided by observing the lava lake. The scope of this chapter encompasses a chronology of lava lake activity, ending with the draining and termination of the lake on May 9, 2018. Other studies describe in detail the May–August 2018 collapses of the caldera floor that occurred at the summit after the lava lake drained (for example, Anderson and others, 2019; Neal and others, 2019).

# Background

## History of Kīlauea's Summit Activity

Kīlauea's summit caldera (fig. 1*B*) formed around 1500 common era (C.E.) (Swanson and others, 2012; Swanson, 2008), after the decades-long eruption of the ʻAilāʻau shield (Holcomb, 1987; Clague and others, 1999). The formation of the caldera was followed by approximately 300 years of episodic, mostly phreatomagmatic explosions, which produced the Keanakākoʻi Tephra (Swanson and others, 2012; Swanson and Houghton, 2018). These deposits blanket the summit region and have a total thickness of as much as 11 meters (m) around the caldera (McPhie and others, 1990; Swanson and Houghton, 2018). This prolonged explosive period involved considerable water-magma interaction, possibly because the caldera floor was near the level of the water table (Mastin, 1997). The 1790 C.E. eruption, which killed scores of Hawaiian warriors that were traveling past the summit at the time, was one of the closing episodes of this explosive period (Ellis, 1825; Swanson, 2008; Swanson and others, 2015).

The first westerners to document activity at Kīlauea's summit arrived in 1823 and observed lava lake activity across parts of the caldera floor (Ellis, 1825). This activity continued, with several interruptions, for the next 100 years (Wright and Klein, 2014). Most of the activity was centered near the current location of Halemaʻumaʻu Crater (figs. 1–3). Several episodes of lava lake drainage and (or) caldera floor subsidence occurred during the 1800s caused by eruptions on the rift zones (Finch, 1940; Wright and Klein, 2014). Lava lake activity ceased with explosions at Halemaʻumaʻu in May 1924 (Jaggar and Finch, 1924), which were triggered by magma withdrawal into the lower East Rift Zone (ERZ). The explosions were theorized to be driven by infiltration of the water table into hot zones around the crater as it enlarged by collapse (Jaggar, 1924), although recent modeling and observations during the 2008 and 2018 collapses and explosions have called this model into question (Houghton and others, 2011; Hsieh and Ingebritsen, 2019; Neal and others, 2019). The 1924 subsidence doubled the width of Halemaʻumaʻu to about 1 kilometer (km) (Jaggar and Finch, 1924). Summit activity after 1924 was characterized by occasional, typically brief, fountaining and effusive eruptions (Wright and Klein, 2014). The longest, in 1967–68, lasted for 254 days and significantly infilled Halemaʻumaʻu (Kinoshita and others, 1969). The most recent before onset of the 2008–18 eruption was in late September 1982, when fissures opened in the south part of the caldera and fed fountains for 14 hours (Banks and others, 1983; Wright and Klein, 2014).

The summit remained quiet for more than two decades after 1982 (Wright and Klein, 2014). After the January 1983 onset of the Puʻu ʻŌʻō eruption on the ERZ (fig. 1), the summit began a prolonged period of deflation, presumably caused by magma withdrawal from the summit reservoir to the ERZ eruption site. This long-term deflation ended, and an inflation period began around 2003, associated with an increase in the magma supply rate that persisted for several years (Poland and others, 2012). Inflation was briefly interrupted in June 2007, when the Father's Day intrusion occurred with abrupt deflation, but was followed immediately by a resumption of inflation (fig. 4) (Poland and others, 2008). Deflation returned to the summit after July 21, 2007, with the opening of new ERZ vents near Puʻu ʻŌʻō (Poland and others, 2008). The deflation rate slowly decreased through the end of 2007 and 2008 (fig. 4). Modest outgassing at the summit continued in the decades after 1982, with sulfur dioxide ($SO_2$) emission rates of about 100–300 metric tons per day (t/d) prior to 2007 (Elias and others, 1998; Elias and Sutton, 2002, 2007; Sutton and Elias, 2014). Halemaʻumaʻu was a popular visitor stop in Hawaiʻi Volcanoes National Park, and the large parking lot allowed access for many visitors to walk the 300 m to the fenced Halemaʻumaʻu Overlook.

## Monitoring Network

HVO operates a robust monitoring network across Kīlauea that has dense instrumentation at the summit (Guffanti and others, 2010). Seismic monitoring consists of a network of broadband stations on the caldera floor as well as several short-period and strong-motion stations in the summit area (Dawson and others, 1998; Okubo and others, 2014). Ground deformation is tracked by a network of Global Positioning System (GPS) instruments and borehole tiltmeters and augmented by satellite interferometry (Miklius and others, 2005; Poland and others, 2012). Gas emission rates are measured using an array of ultraviolet spectrometers installed in 2011 (Horton and others, 2012; Elias and others, 2018), which augment regular campaign measurements of $SO_2$ using vehicle-based instruments (Sutton and others, 2003; Sutton and Elias, 2014). Campaign Fourier transform infrared spectrometry (FTIR) is used to track changes in gas chemistry (Sutton and Elias, 2014). The first webcam at the summit was installed just a day before the March 19, 2008, eruption onset, and by 2018 this had expanded to three webcams and two thermal cameras (Orr and others, 2013; Patrick and others, 2014), as well as two non-telemetered time-lapse cameras, augmented by infrequent deployments of high-speed video cameras at high temporal and spatial resolutions (Gaudin and others, 2016). Other webcams and time-lapse cameras were installed temporarily during the 2008–18 eruption in response to specific episodes of activity. A four-element infrasound array operated at the University of Hawaiʻi Infrasound Laboratory was installed in 2006 and routinely recorded

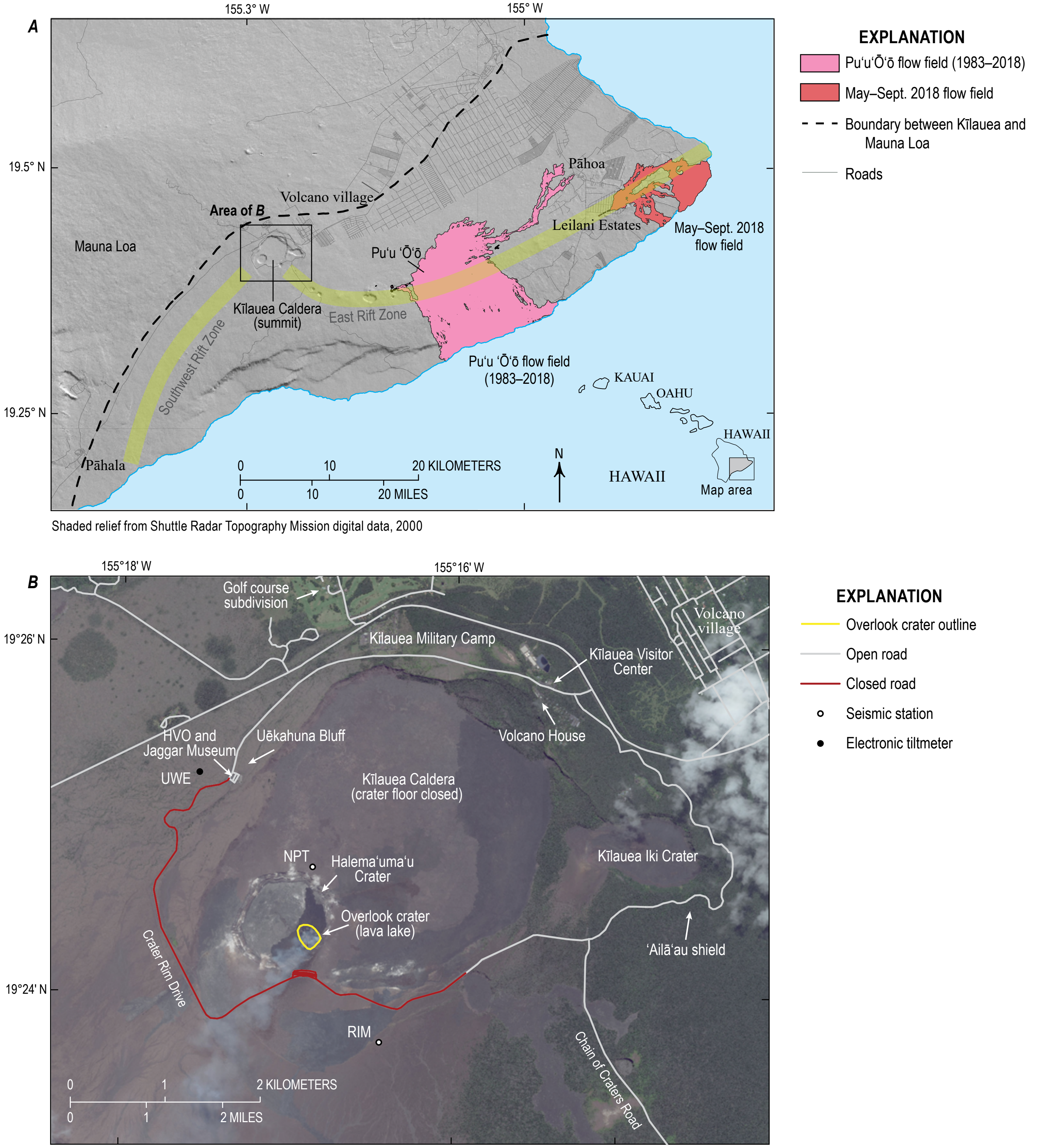


Shaded relief from Shuttle Radar Topography Mission digital data, 2000

Base image © 2016 DigitalGlobe, NextView license

**Figure 1.** Maps showing the location of Kīlauea Volcano and the 2008–18 lava lake. *A*, Kīlauea forms the southeast portion of the Island of Hawai‘i. Two rift zones extend down the flanks of the volcano (yellow areas). The Pu‘u ‘Ō‘ō eruption, on the East Rift Zone, was active during 1983–2018 and produced a 144-square-kilometer lava flow field (pink). The lower East Rift Zone eruption of May–September 2018 is shown in red and is 36 square kilometers in area. The summit eruption, the focus of this chapter, was present in Kīlauea Caldera. *B*, Map of Kīlauea Caldera from a WorldView satellite image collected on June 25, 2016. The summit lava lake was contained in what became known as the “Overlook crater” (yellow outline) within Halema‘uma‘u Crater in the southwest part of Kīlauea Caldera. Seismic and tiltmeter stations used in this analysis are shown. Part of Crater Rim Drive was closed to the public because of the summit eruption. HVO is the Hawaiian Volcano Observatory.

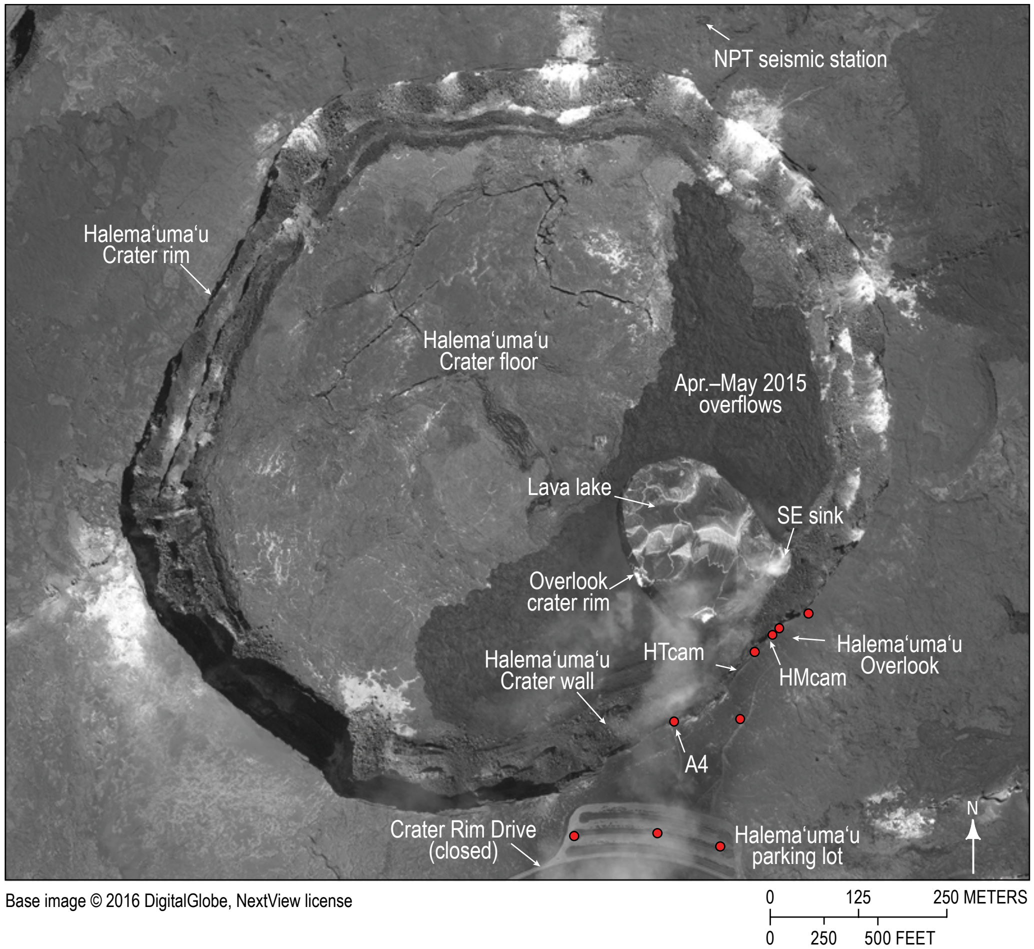


**Figure 2.** WorldView satellite image of Halemaʻumaʻu in November 2016. What became known as the "Overlook crater" and its lava lake were in the southeast part of Halemaʻumaʻu Crater. The Halemaʻumaʻu Overlook, on the crater rim, was the most common observation site of the lava lake. Cameras HMcam (visual) and HTcam (thermal) were nearby. A4 was another site of common observation. Red dots show locations of tephra collection buckets. The dark area on the crater floor was formed primarily in April–May 2015 when the lava lake overflowed. The southeast (SE) sink was the most common site of spattering in the lake.

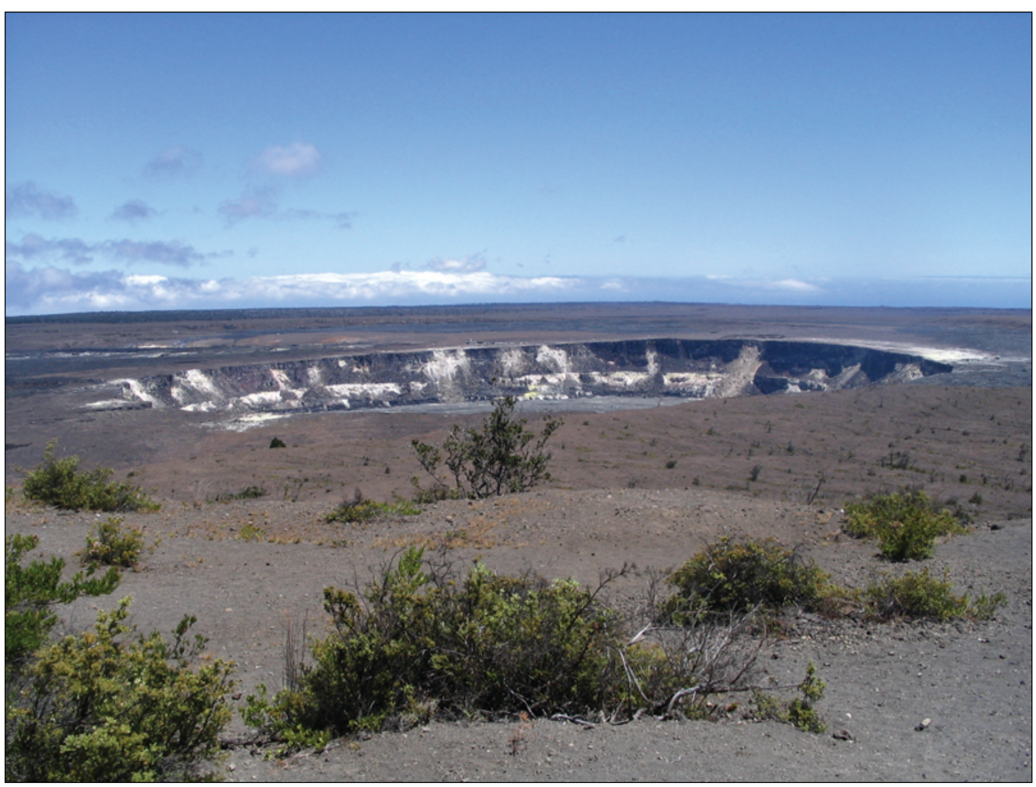

**Figure 3.** Photograph of Halemaʻumaʻu prior to eruption. Photograph taken near Jaggar Museum on August 3, 2006, by Matt Patrick.

acoustic signals from activity within the ERZ (Fee and others, 2011) and summit region (Fee and others, 2010).

A unique aspect of Kīlauea's recent lava lake activity is that it was directly observed and documented by geologists almost daily. Tephra collection from sample buckets occurred each workday (fig. 2; Swanson and others, 2009), and lava level was measured with a laser rangefinder nearly daily from 2013 to 2018 (Patrick and others, 2015a, 2019a). Other visits to the Halemaʻumaʻu Crater rim were made for equipment maintenance (for example, time-lapse camera card changing), deformation surveying, tephra sampling, and observations of eruption processes.

## Precursory Activity

Gravity surveys suggest gradual accumulation of magma in the Halemaʻumaʻu region in the three decades prior to the 2008 summit onset (Johnson and others, 2010), despite long-term deflation throughout most of this interval. This apparent discrepancy has been explained by magma occupying voids, such as cracks (Johnson and others, 2010). After the July 2007 onset of summit deflation, which was associated with a new vent on the ERZ (Poland and others, 2008; Orr and others, 2015a), the number of small earthquakes beneath Halemaʻumaʻu increased above typical levels. This elevated earthquake activity continued into early 2008. The small earthquakes were likely related, at least in part, to subsurface changes that led to the onset of the summit eruption and formation of the Overlook crater on March 19, 2008.

The first clear precursory changes began in early November 2007, when seismic tremor rose above background levels (fig. 4, table 1; Wilson and others, 2008; Johnson and Poland, 2013). $SO_2$ emission rates rose above the background range in late 2007, but the precise onset of this change was obscured by heavy rainfall in early December that scrubbed $SO_2$ from the system, triggering a brief drop in apparent emission rates (Elias and Sutton, 2012; Sutton and Elias, 2014). After the December rainfall, $SO_2$ emission rates rose steadily—presumably caused by both a recovery from the scrubbing episode and a real increase in source emission.

As 2008 began, seismic tremor and $SO_2$ emission rates continued to climb (fig. 4). We use real-time seismic amplitude measurement (RSAM; Endo and Murray, 1991) as a proxy for seismic tremor. RSAM at the summit reached a plateau at a level about 4–5 times the background level in January (Wilson and others, 2008). $SO_2$ emissions reached approximately 1,000 t/d by February (Elias and Sutton 2012; Sutton and Elias, 2014). These increased gas emissions created respiratory problems for some visitors to the Halemaʻumaʻu area, and Hawaiʻi Volcanoes National Park closed the west section of Crater Rim Drive to the public on February 20, 2008. Ground-based surveys using a handheld thermal camera in January and February showed only known, long-term heat sources and no new or anomalous thermal features in Halemaʻumaʻu (Wilson and others, 2008).

On March 12, 2008, a large fumarolic area abruptly appeared on the southeast wall of Halemaʻumaʻu, directly below the Halemaʻumaʻu Overlook (figs. 5, 6; Wilson and others, 2008; Sutton and Elias, 2014). This new fumarolic area was the first visible sign of developing changes at Halemaʻumaʻu. The area was approximately 50 m long and emitted a thick white plume to a height of several hundred meters. HVO geologists on the Halemaʻumaʻu rim could hear rock cracking sounds originating from the fumarolic area. Numerous incandescent spots, visible only at night, were present in the fumarolic area, indicating surface temperatures >525 °C (Draper, 1847). These high surface temperatures, along with the greatly increased $SO_2$ emission rates, were further evidence that magma might be close to the surface and an eruptive event could occur soon. The incandescent spots increased in number and spread across a broader area throughout the following week, becoming too numerous to count by March 18.

Despite these changes in seismic activity, $SO_2$ emission, and fumarolic activity, the rate and style of ground deformation showed no change through the precursory phase. Ground tilt continued the steady deflationary trend that had begun with the onset of the new vent at Puʻu ʻŌʻō in July 2007 (Poland and others, 2009), and there was no obvious change in the rate of deflation. Even in hindsight, the lack of deformation precursors is striking and puzzling.

## Chronology of the Eruption

### 2008: An Explosive First Year

The eruption began at 02:58 (all times are Hawaii Standard Time [HST]) on March 19, 2008, with several small earthquakes associated with the collapse of the fumarolic area into a large cavity and the subsequent ejection of lithic blocks and lapilli (Wilson and others, 2008; Fee and others, 2010; Houghton and others, 2011; table 1). The explosion deposited a near-continuous layer of lithic lapilli and ash that extended south across the Halemaʻumaʻu parking lot and adjacent spans of Crater Rim Drive. Coarse lapilli and blocks were scattered around the Halemaʻumaʻu Overlook, which broke and burned the wooden fencing (fig. 7). Many of the blocks were found surrounded by a flat circular zone lacking small particles (fig. 7*B*), which were presumably displaced by the impact. The largest block observed was 0.9 m in diameter located near the Halemaʻumaʻu Overlook, approximately 70 m horizontal distance from the new explosion crater. Larger blocks may have been deposited on the inaccessible Halemaʻumaʻu Crater floor (Houghton and others, 2017). The tephra had no juvenile component and was mostly lithic, originating from talus blocks derived from dense solidified lava flows that formed the Halemaʻumaʻu Crater walls (Houghton and others, 2011). In addition, ash and fine lapilli of white sulfate minerals, dominantly anhydrite, were presumably derived from areas of fumarolic alteration in the talus and crater wall. Residents of Pāhala, 30 kilometers from the summit (fig. 1), reported a dusting of fine white ash on vehicles that morning (Wooten and

**Table 1.** Notable events of Kīlauea’s 2008–2018 summit lava lake.

[ERZ, East Rift Zone; NPS, National Park Service; m, meter]

| Date | Event |
|---|---|
| Early November 2007 | Seismic tremor starts increasing above long-term background levels at Kīlauea summit |
| December 2007 | $SO_2$ emissions begin increasing above background at Kīlauea summit |
| February 20, 2008 | Western part of Crater Rim Drive closed to public by NPS because of volcanic gas |
| March 12, 2008 | Fumarolic area appears on south wall of Halemaʻumaʻu Crater; incandescence appears a few days later |
| March 19, 2008, 02:58 | Fumarolic area collapses, creating Overlook crater; small lithic explosion; onset of the 2008–2018 eruption |
| March 22, 2008 | Start of several days of spattering from crater; cored bombs reach Halemaʻumaʻu Overlook; first juvenile lava of the eruption |
| April 2008 | Brief closures of Hawaiʻi Volcanoes National Park owing to high $SO_2$ levels; voluntary evacuations of Volcano village |
| April–October 2008 | Several additional small explosions, ejecting juvenile and lithic material |
| September 5, 2008 | First sighting of lava lake within the Overlook crater |
| December 4, 2008 | Large crater wall collapse; start of month-long pause in surface activity; decrease in $SO_2$ emissions |
| February–May 2009 | Repeated Overlook crater floor collapses, episodic lava lake activity and gas pistoning |
| June 2009 | One month of continuous lava lake activity |
| June 30, 2009 | Large crater wall collapse; start of month-long pause in surface activity; decrease in $SO_2$ emissions |
| August 2009–January 2010 | Sporadic lava lake activity deep in Overlook crater |
| February 11, 2010 | Collapse of floor of Overlook crater; rise of lava lake; onset of continuous lava lake activity |
| February to early March 2011 | Rise in lava lake level; collapses of crater walls trigger small explosions |
| March 5, 2011 | Onset of Kamoamoa eruption on ERZ, lake drains over next few days |
| April–July 2011 | Rise of lava lake to levels obtained in February and March 2011 |
| August 3, 2011 | New vent opens on Puʻu ʻŌʻō on ERZ; summit lava lake drops 80 m |
| October 26, 2012 | Brief inflationary period culminates in highest level of lava lake to that point, at 22 m below the Halemaʻumaʻu Crater floor; small intrusion on October 28 produces rapid drop in lake level |
| January 2013 | Brief peak in lava lake levels, as high as 25 m below Halemaʻumaʻu Crater floor |
| June 27, 2014 | June 27th vent opens on Puʻu ʻŌʻō with no immediate effect on summit lake |
| August–November 2014 | Changes in lake level and summit tilt correlated with ERZ lava flow advance rate |
| April–May 2015 | Brief inflationary period culminates in lake rise; first overflows of lake onto floor of Halemaʻumaʻu Crater; May 10th intrusion causes lake level to drop to previous levels |
| October–November 2016 | Long-term peak in lake level; small brief overflow on Halemaʻumaʻu Crater floor |
| March–April 2018 | Summit inflation accompanies rise in lake level |
| Late April 2018 | Lake reaches Overlook crater rim, numerous overflows of lava lake onto Halemaʻumaʻu Crater floor |
| April 30, 2018 | Crater floor collapse at Puʻu ʻŌʻō, small Puʻu ʻŌʻō fissure; onset of intrusion toward lower ERZ |
| May 2, 2018 | Lake level begins rapid drop; onset of rapid summit deflation |
| May 3, 2018, 17:00 | Onset of lower ERZ eruption |
| May 4, 2018 | Magnitude 6.9 earthquake on south flank triggers brief lake sloshing; small crater wall collapses |
| May 9, 2018 | Final day of lava lake activity; lake surface approximately 330 m below Halemaʻumaʻu Crater floor |
| May 10, 2018 | Field visit confirms lava has drained below crater floor; lava lake activity terminated |
| Middle to late May 2018 | Continued collapse of the Overlook crater and Halemaʻumaʻu Crater floor; small explosions |
| June–August 2018 | Episodic collapse events of caldera floor; final event August 2; summit quiescence follows |

**Figure 4.** Plots of time series data of the 2008–18 Kīlauea summit eruption. Green dashed lines show intrusion events; red dashed lines show East Rift Zone vent openings. *A*, Elevation of the lava lake surface. During most of 2008 and early 2009, the lake was intermittently active and very deep in the crater, and lake level measurements were not possible. *B*, Surface area of the Overlook crater (black) and the lava lake (red). In May 2018, the Overlook crater enlarged and was consumed by broad crater floor collapse; the last data point shown here is from May 2018. *C*, North-south position of Global Positioning System (GPS) station UWEV. Increasing values may be viewed as a proxy for summit inflation and decreasing values for deflation. *D*, $SO_2$ emission rate from Kīlauea’s summit. Data compiled from Elias and Sutton (2012), Elias and others (2018, 2020), and Kern and others (2020). *E*, Real-time seismic amplitude measurement (RSAM) from station RIM. *F*, Located earthquakes (greater than magnitude 1.5) per week..

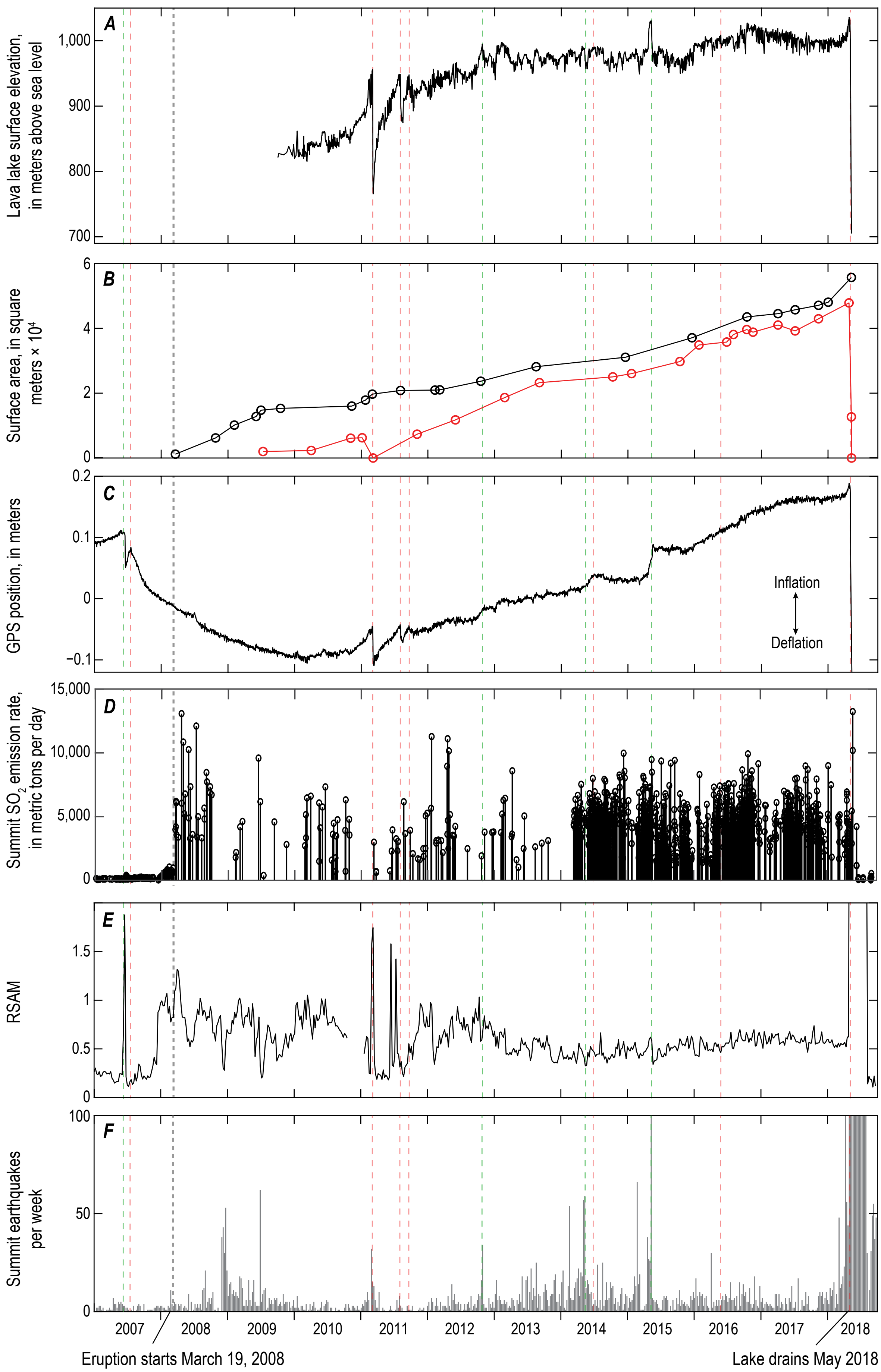
A
B
C
D
E
F
Lava lake surface elevation, in meters above sea level
1,000
900
800
700
Surface area, in square meters × 10^4
6
4
2
0
GPS position, in meters
0.2
0.1
0
−0.1
Inflation
Deflation
Summit SO2 emission rate, in metric tons per day
15,000
10,000
5,000
0
RSAM
1.5
1
0.5
0
Summit earthquakes per week
100
50
0
2007
2008
2009
2010
2011
2012
2013
2014
2015
2016
2017
2018
Eruption starts March 19, 2008
Lake drains May 2018

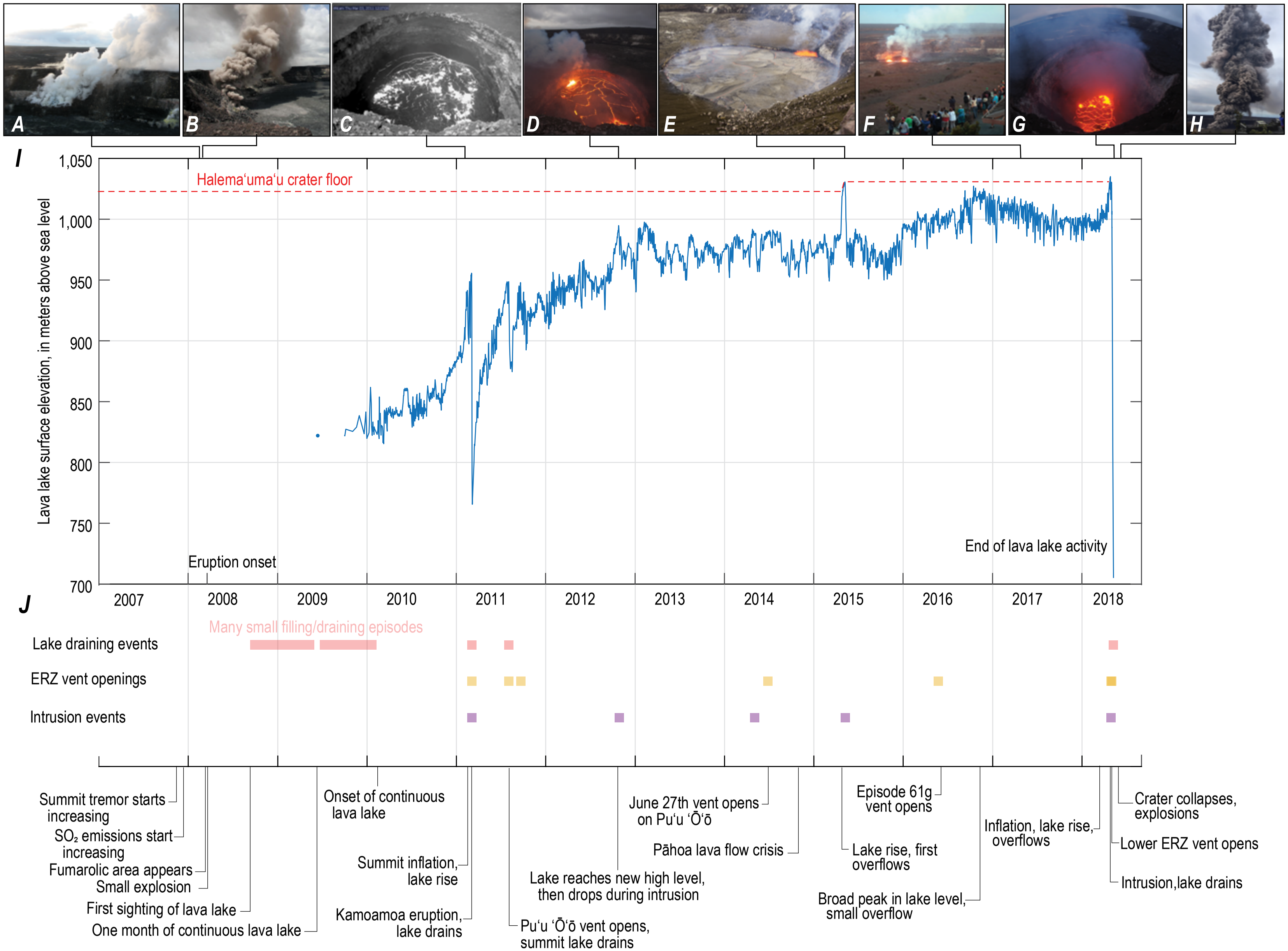


**Figure 5.** Timeline of the 2008–18 Kīlauea summit lava lake. Photographs (*A–H*) show selected snapshots of the activity. The general trend of the eruption is shown by the overall rise in lava lake elevation, terminated in May 2018 by sudden lake draining (*I*). Other draining events, East Rift Zone (ERZ) eruptions, and intrusions (summit or ERZ) are also shown (*J*). At the bottom, key events in the 10-year eruption are noted. Photograph credits and dates: *A*, Jeff Sutton, U.S. Geological Survey (USGS), March 14, 2008; *B*, Christina Heliker, USGS, March 24, 2008; *C*, HMcam webcam, March 3, 2011; *D*, David Dow, Hawaiian Volcano Observatory (HVO) volunteer, October 22, 2012; *E*, Tim Orr, USGS, April 26, 2015; *F*, Matt Patrick, USGS, April 27, 2017; *G*, Kyle Anderson, USGS, May 6, 2018; and *H*, Gail Ferguson, HVO volunteer, May 9, 2018.

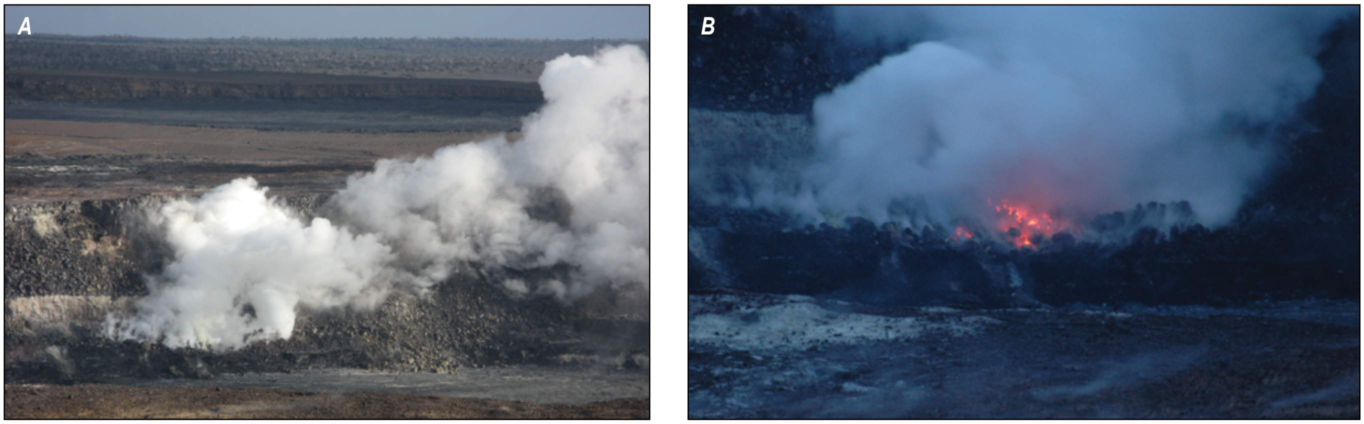

**Figure 6.** Photographs of the fumarolic area on the southeast wall of Halemaʻumaʻu. *A*, The fumarolic area formed abruptly on March 12, 2008, and was the first visual sign of changes at the summit. Its appearance was associated with a significant increase in $SO_2$ gas emission, and marked the beginning of a robust plume at the summit. For scale, the wall of Halemaʻumaʻu was about 85 meters high. Photograph by Jeff Sutton, U.S. Geological Survey, on March 15, 2008. *B*, Incandescence at the fumarolic area was visible at night and was approximately 30 meters in diameter. Photograph by Steve Lundblad, University of Hawaiʻi at Hilo, on March 16, 2008, at 19:00.

**Figure 7.** Photographs of deposits from the March 19, 2008, vent-opening explosion. *A*, Wooden fencing at the Halemaʻumaʻu Overlook was broken and burned by hot ejected blocks. Photograph by Kelly Wooten. *B*, Some blocks were surrounded by a circular zone that lacked fine particles. Photograph by Tim Orr. *C*, Crater Rim Drive, in the area around the Halemaʻumaʻu parking lot, was carpeted by small lithic lapilli. Photograph by Tim Orr. *D*, The largest ejected block on the Halemaʻumaʻu rim was 0.9 meters in diameter and landed on the fence along the trail to Halemaʻumaʻu Overlook. Photograph by Tim Orr. All photographs from March 19, 2008.

others, 2009). This event marked the first explosive eruption other than Hawaiian fountaining at Kīlauea’s summit since 1924. In response, the national park closed the area around Jaggar Museum and Uēkahuna Bluff (fig. 1) to the public for approximately 2 weeks while HVO assessed the new activity. The March 19 vent-opening explosion marked the onset of sustained harmonic infrasonic tremor at Halemaʻumaʻu (Fee and others, 2010).

The new crater, later informally named the “Overlook crater” because of its position below the Halemaʻumaʻu Overlook, had a diameter of 35 m and was perched low on the southeast wall of Halemaʻumaʻu (fig. 8). The approximately 400 cubic meter ($m^3$) volume of the explosive deposit was much smaller than that of the Overlook crater, indicating that the crater formed primarily by collapse into an underlying void, not explosive excavation (Swanson and others, 2009; Houghton and others, 2011). The void was presumably forming during the months of precursory activity, but the process of its formation is obscure. Views inside the crater, both to the naked eye and using a thermal camera, were blocked by a wide, hot, pulsating gas plume. The white to dusty-brown plume rose to several hundred meters above the crater and was advected southwestward by the prevalent trade winds. A glow in the crater could be seen at night, suggesting the shallow presence of magma.

Beginning on the evening of March 22, time-lapse camera images captured sparse incandescent particles ejected from the Overlook crater. The abundance of particles increased throughout the following day, and on the evening of March 23, HVO volunteers at the Jaggar Museum viewing area could see a nearly continuous ejection of incandescent particles rising vertically from the new crater, reaching the height of the Halemaʻumaʻu rim (fig. 9). The next day, HVO geologists found a sparse deposit of cored bombs and lapilli—that is,

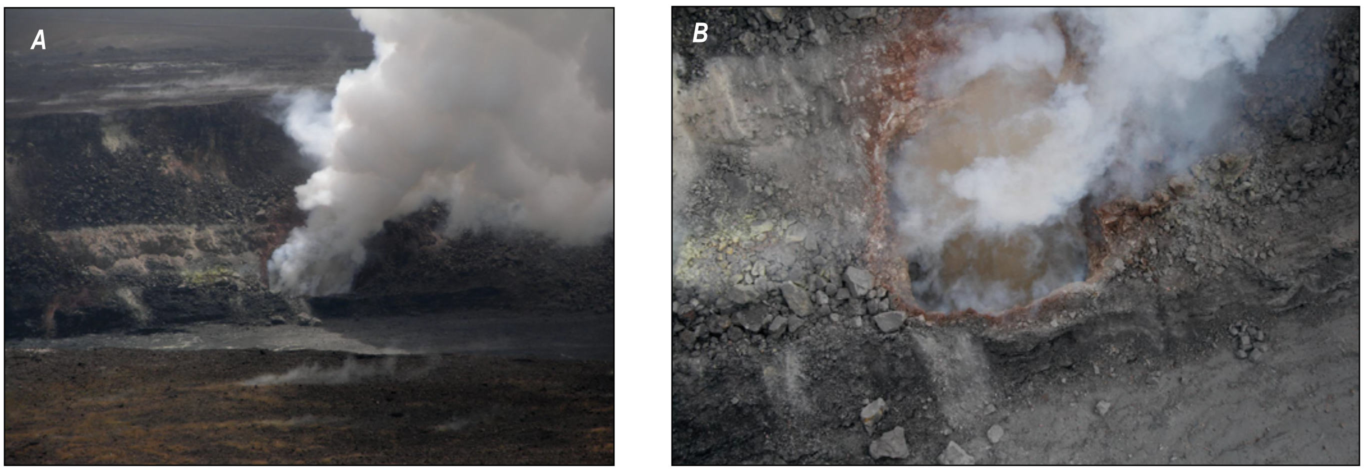


**Figure 8.** Photographs of the new Overlook crater formed on March 19, 2008. The crater formed in the early morning explosion and was approximately 35 meters in diameter. At this time, the crater was limited to the Halemaʻumaʻu Crater wall. Thick, pulsating fume prevented views inside the crater. *A*, View from the Hawaiian Volcano Observatory (HVO) and Jaggar Museum. Photograph from March 21, 2008, from a time-lapse camera in the HVO observation tower. *B*, Even from a helicopter, views inside the crater were not possible because of opaque fume. Photograph by Tim Orr on March 19, 2008.

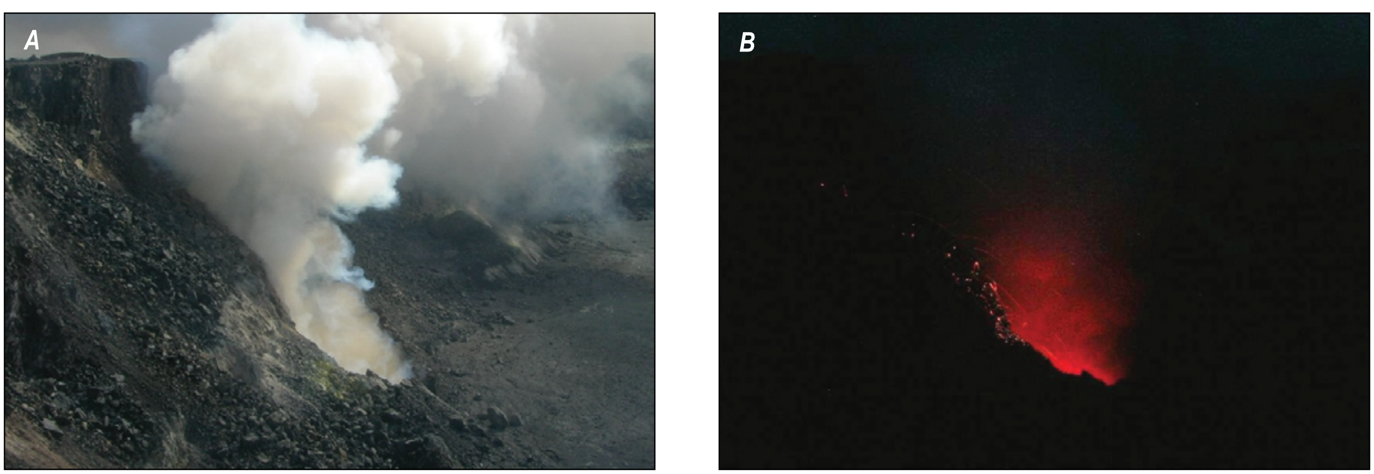


**Figure 9.** Photographs of spattering that occurred in the first weeks of the eruption and ejected cored bombs and lapilli around the Halemaʻumaʻu Overlook. The juvenile veneer that coated the lithic particles marked the first juvenile material erupted at Kīlauea’s summit since 1982. *A*, Frame from a time-lapse camera on the northeast rim of Halemaʻumaʻu. *B*, Composite of nighttime images from the same time-lapse camera to highlight the arcs of incandescent particles. Images from March 23, 2008. For scale, the wall of Halemaʻumaʻu is 85 meters high.

dense lithic particles surrounded by a coating of glassy juvenile lava (Wooten and others, 2009; Carey and others, 2015). This marked the first juvenile lava of the eruption. Ejection of molten material continued into the first week of April, when abundant deposits of Pele's hair and fine to medium juvenile ash were found adjacent to Halemaʻumaʻu. The sound of rocks cracking or falling against the crater walls could be heard starting in early April, but views were still obscured by thick fume, though a red glow could be seen deep in the crater. The juvenile nature of the ejecta and the red glow indicated that an exposed lava surface, albeit out of view, was present deep in the crater during the first months of the eruption (Carey and others, 2015).

The normally white, translucent plume occasionally turned an opaque brown caused by the entrainment of lithic material derived from wall collapses within the crater. At night, these brown plumes would cause the glow to briefly cease. A sustained brown plume, from March 23 to 28 (fig. 10), presumably represented nearly continuous rockfalls deep in the crater. The tephra content of brown plumes was very small and fine grained, as determined by first-hand experience during tephra fallout (Swanson and others, 2009).

HVO began a 24-hour watch on March 24 because of the rapidly changing nature of the eruption, with particular concern for the possibility of more explosive activity. This 24-hour watch persisted until August 9.

The new crater continued to emit a dense gas plume (Spampinato and others, 2012) and $SO_2$ emissions remained high. A shift in wind direction in April carried an $SO_2$-rich plume into busy areas of the national park, causing the park administration to close and evacuate visitors for several days on two occasions that month. Hawaii County Civil Defense Agency also called for voluntary evacuations of Volcano village (Dayton, 2008) (fig. 1). Two additional small explosions occurred in April, each associated with a collapse of part of the Overlook crater rim, which enlarged the crater (Wooten and others, 2009; Fee and others, 2010). The explosions deposited lithic and juvenile clasts downwind from the Halemaʻumaʻu rim. Collapses of the crater walls triggered spattering throughout the eruption on various scales, but we refer to explosions during this eruption as those events that were large enough to deposit lapilli (or larger) clasts on the Halemaʻumaʻu rim.

Fluctuating vent behavior occurred throughout mid-2008. The normally white plume continued to occasionally turn brown and opaque in brief episodes, caused by collapses within the Overlook crater. Intense periodic bursts of seismic tremor that had intervals of several minutes were frequently observed in June and July (fig. 11). Orange glow in the crater was visible at night (fig. 12) and tremor bursts corresponded with fluctuations in the glow and apparent temperature. Similar fluctuations were observed later (in September 2008) to be associated with gas pistoning of the lava surface (Patrick and others, 2008). The apparent gas pistoning of mid-2008 was another suggestion of an open, but still unseen, lava surface deep in the crater.

Although views deep into the Overlook crater were not possible in mid-2008, HVO geologists could see the upper part of the crater well enough to observe that the rim was severely overhung and potentially unstable (fig. 13). Collapses of the Overlook crater rim occurred frequently in the first year, enlarging the crater significantly (fig. 14). By early September, the Overlook

**Figure 10.** Photograph of a brown, tephra-laden plume that was common in the first weeks of the eruption. The small particles were likely sourced from collapse debris in the crater; brown plumes presumably represent periods of instability in the crater. View from Volcano House. Photograph by Christina Heliker, U.S. Geological Survey, on March 24, 2008.

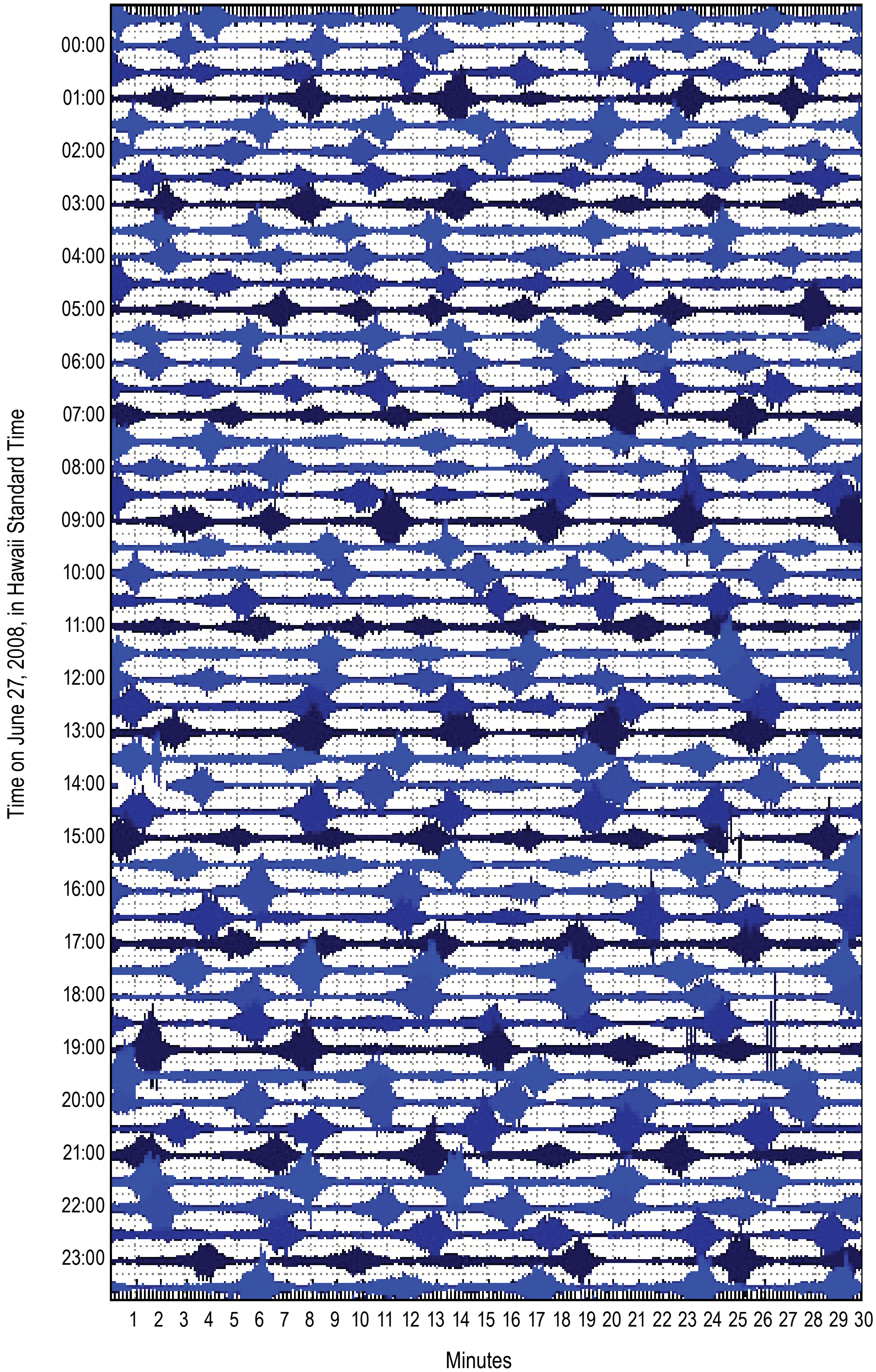


**Figure 11.** Plot of periodic bursts of seismic tremor at intervals of several minutes that were common in June and July 2008. Later visual observations confirmed that tremor bursts like these corresponded with gas-piston cycles in the lava lake. The quiet intervals corresponded with a rising, less active lava lake surface, whereas the bursts occurred with spattering and abrupt drop in lava level. This periodic behavior was also expressed by changes in infrasound, vent temperature, vent glow, plume vigor, and tephra production. Data from seismic station NPT on June 27, 2008.

**Figure 12.** Photograph of glow that was present on most days during the first months of the eruption. View from Jaggar Museum. Photograph by Dan Dzurisin, U.S. Geological Survey, on April 27, 2008.

**Figure 13.** Photograph of the large overhang on the north rim of the Overlook crater on September 3, 2008. These overhung sections occasionally collapsed, triggering composite seismic events, brown plumes, and sometimes explosive events. View from the Halemaʻumaʻu Overlook. Photograph by Tim Orr.

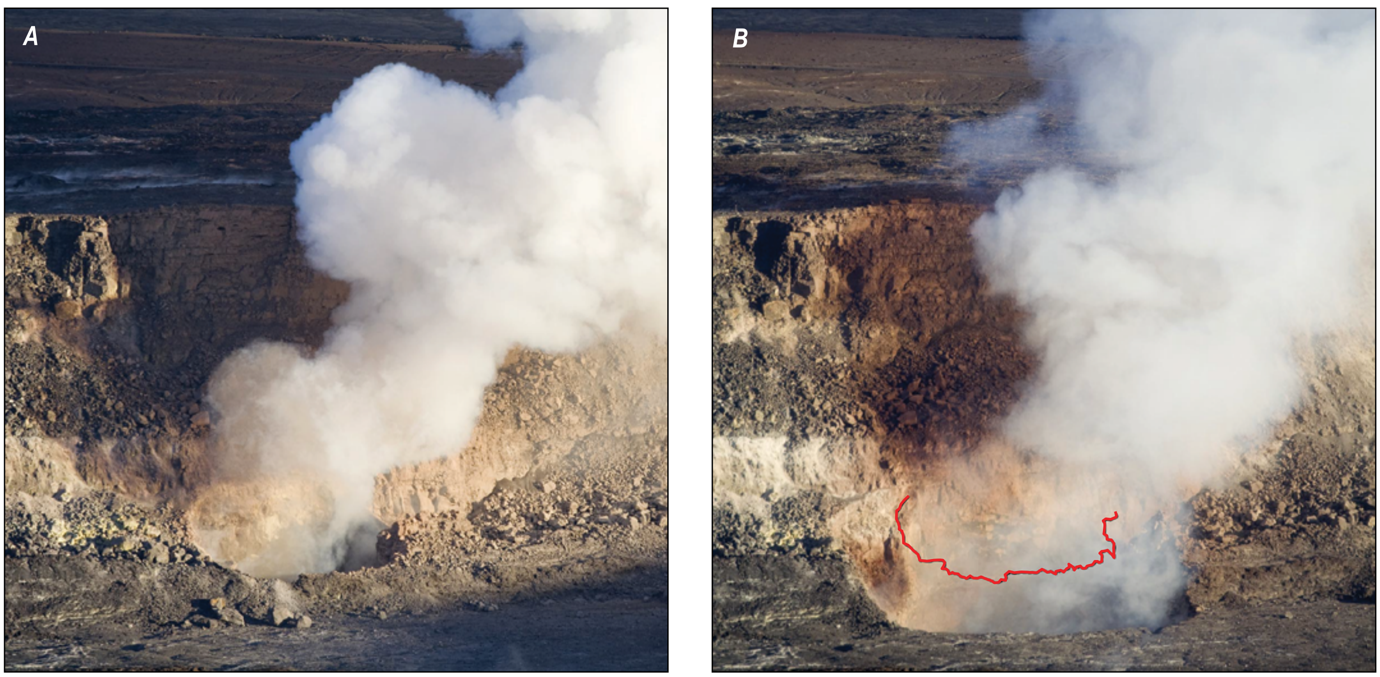


**Figure 14.** Photographs of the Overlook crater showing significant enlargement caused by occasional collapses of the crater rim during the first months of the eruption. *A*, View of the Overlook crater from Hawaiian Volcano Observatory (HVO) on April 1, 2008, when the crater (approximately 40 meters in diameter) was limited to the wall of Halemaʻumaʻu. *B*, By September 3, 2008, when this photograph was taken from about the same location, the crater was about 70 meters in diameter and extended onto the Halemaʻumaʻu Crater floor. The red line shows the crater outline in *A* for reference. Photographs by David Dow, HVO volunteer.

crater had doubled in diameter to approximately 70 m. Some of the collapses were associated with explosive events, including two in August (Wooten and others, 2009).

These early explosive events, as well as all subsequent explosions during the eruption, were recorded by seismometers as composite seismic events (fig. 15; Chouet and others, 2010; Patrick and others, 2011; Orr and others, 2013). Each began with a burst of high frequency energy, followed seconds later by long-period oscillations, with a tail of very long period seismicity that lasted several minutes. The explosive events also exhibited a distinctive infrasound signature (Fee and others, 2010).

The second-largest magmatic explosion of this eruption occurred on September 2, creating a deposit of ejecta that reached Crater Rim Drive near the Halemaʻumaʻu parking lot (fig. 16; Fee and others, 2010; Houghton and others, 2013). The ragged juvenile spatter had small lithic particles embedded in it (Wooten

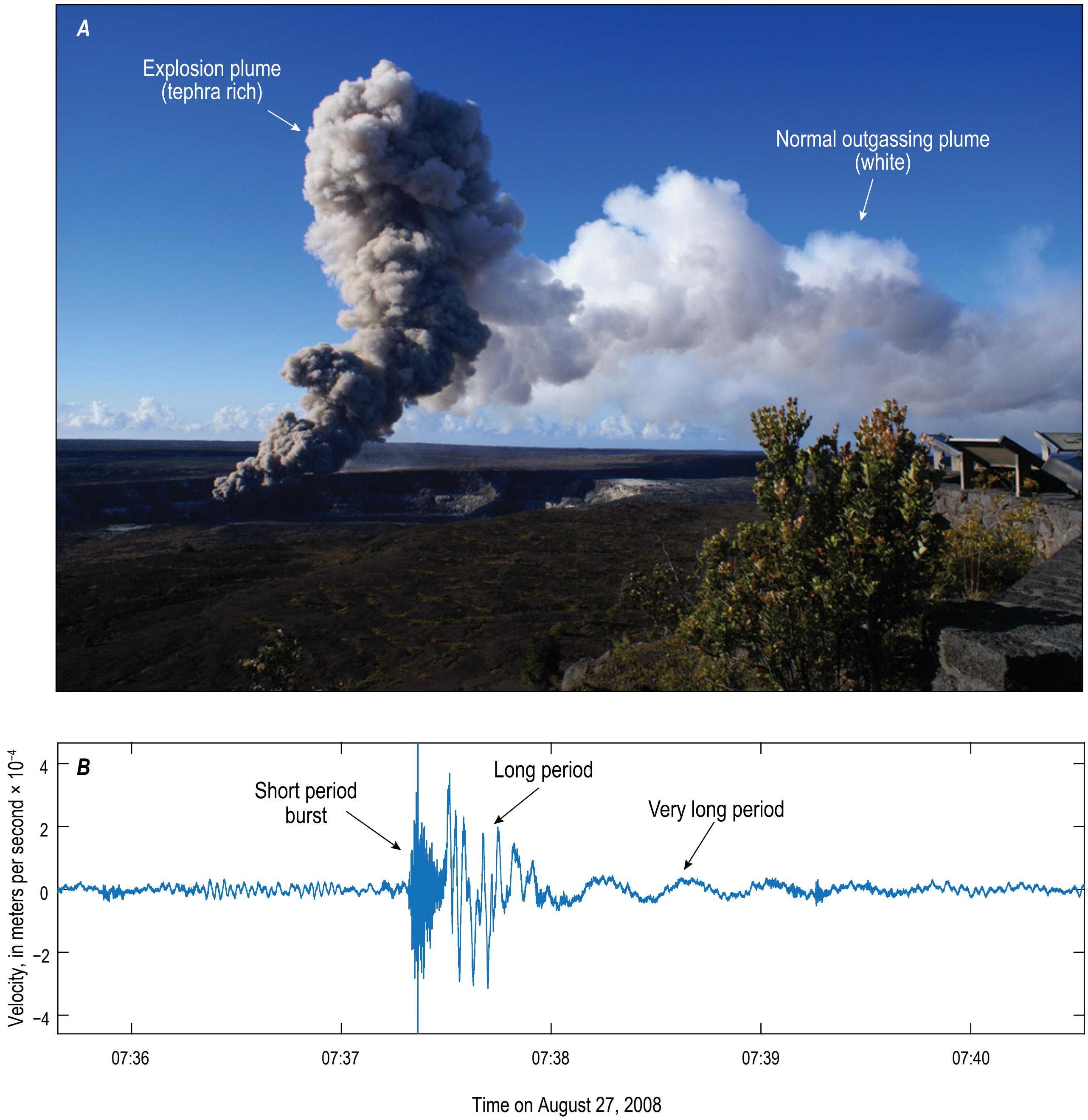


**Figure 15.** Photograph and plot of the August 27, 2008, explosion and composite seismic event. *A*, View from the Jaggar Museum of the brown plume produced by the explosion. The normal, white outgassing plume is being carried southwestward by the trade winds. Photograph by Jim Kauahikaua, U.S. Geological Survey. *B*, Accompanying composite seismic event recorded at station NPT (location in fig. 2), consisting of an initial short-period burst, followed by long-period and very-long-period oscillations.

and others, 2009), a feature characteristic of pyroclasts in every rockfall-induced explosion during the eruption.

A helicopter overflight on September 5 gave the first view of lava within the crater (fig. 17). The surface of a large, roiling lava lake was visible deep in the crater, with numerous zones of bubble bursting. The lake became more placid and lake level rose during intervals between tremor bursts or became highly agitated and fell during tremor bursts (timing of tremor bursts was noted in real time via radio from HVO). This timing confirmed that the tremor bursts were related to gas-piston activity. The rise of the lake surface that day, into view for the first time, corresponded with the inflation phase of a large deflation-inflation (DI) event (Anderson and others, 2015), offering the first suggestion that the lava level might be coupled with inflation and deflation of the summit.

Deflation predictably followed peak inflation in early September, and the lava lake appeared to drop, as it was no

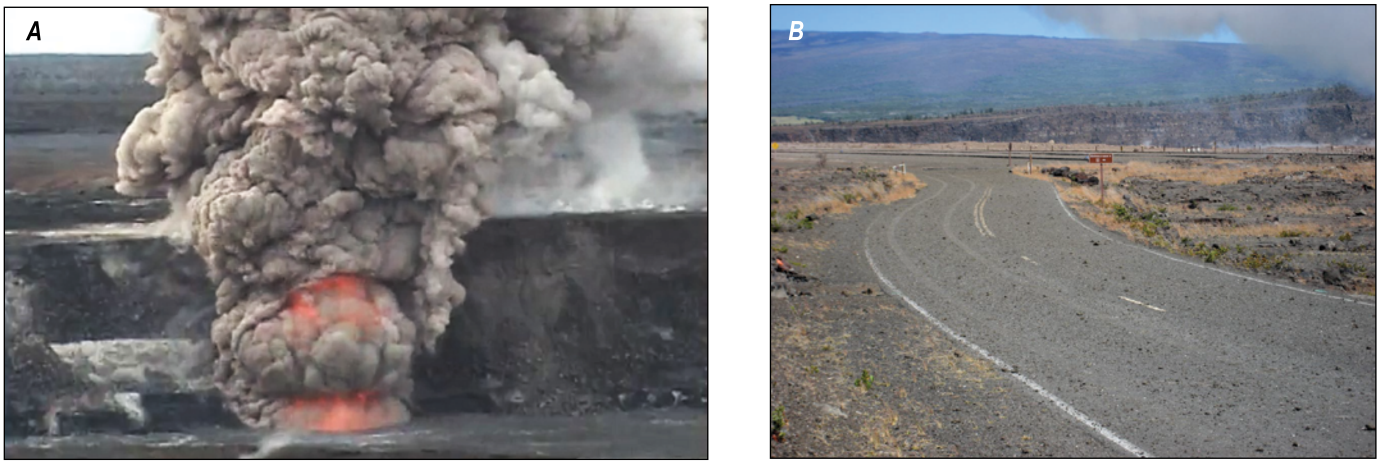


**Figure 16.** Images of two explosive events that occurred in 2008. *A*, Video frame showing the October 12, 2008, explosion at 07:29. A robust tephra-laden plume rises above the crater; incandescent pulsing occurs at the base. For scale, the floor of Halemaʻumaʻu (bottom of image) was about 85 meters below the Halemaʻumaʻu rim (midline of image). *B*, View of Crater Rim Drive, adjacent to the Halemaʻumaʻu parking lot, after the September 2, 2008, explosion. Juvenile bombs and lapilli were scattered on the pavement several hundred meters from the Overlook crater. The September 2 event was the second largest explosive event of the eruption in terms of juvenile mass output. Photograph by Kelly Wooten on September 3, 2008.

**Figure 17.** Photograph of the first clear view of lava in the Overlook crater, September 5, 2008. Hawaiian Volcano Observatory geologists viewed the lake for several minutes from a hovering helicopter and observed cycles of gas pistoning that corresponded with seismic tremor bursts. The lake surface was highly active, with roiling and bubbling activity. It was difficult to estimate the depth of lava below the rim, but it was more than 50 meters, and potentially much greater. Photograph by Tim Orr.

longer clearly visible that month. Two notable explosions and other collapses occurred in October (fig. 16; Fee and others, 2010; Patrick and others, 2011; Carey and others, 2012), but November was relatively quiet (fig. 18). Thermal camera images taken from a helicopter in late November showed that a small opening, and possibly lava, was present at the bottom of the Overlook crater. Infrasound during 2008 suggested that the lava surface was ~219 m below the Overlook crater rim (Fee and others, 2010).

Bright glow from the crater in late November and early December was abruptly terminated by a series of large collapses of the Overlook crater rim on December 4–6 (fig. 19). The collapses were associated with composite seismic events and emission of opaque brown plumes, followed by a dramatic weakening of the plume intensity and large drop in $SO_2$ emission rates (Elias and Sutton, 2012). The normal gas rushing sounds were no longer present after the collapses, and glow was absent. Infrasound also abruptly ceased at this time (Fee and others, 2010). It appeared that the collapses had choked the vent with rubble (Fee and others, 2010), and views into the crater with a thermal camera supported this interpretation (fig. 20*A*). The collapses ushered in a pause in the eruption that persisted through the end of the year; some researchers wondered if the eruption had ceased.

Throughout this first calendar year of summit activity, the ERZ eruption at Puʻu ʻŌʻō continued with no obvious reaction to the new summit events. Episode 58 of the Puʻu ʻŌʻō eruption began in July 2007, and slow moving pāhoehoe flows gradually migrated south to the ocean in early 2008 (Orr and others, 2015a). However, there were indications of coupled behavior at the summit and Puʻu ʻŌʻō. First, a brief surge in inflation in July 2008

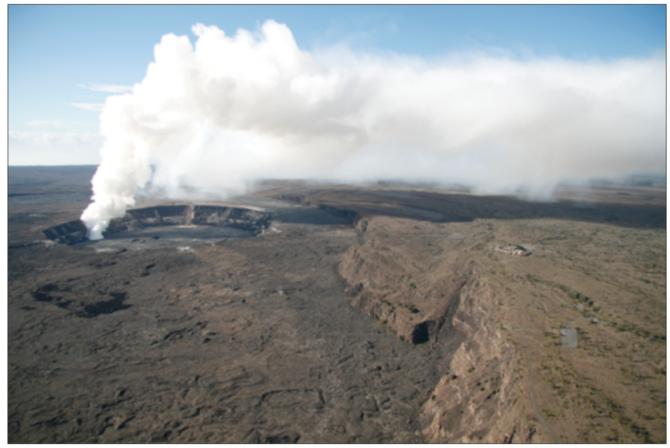

**Figure 18.** Photograph of typical behavior of the outgassing plume from Halemaʻumaʻu during 2008. Hawaiian Volcano Observatory and Jaggar Museum are on the right, perched on Uēkahuna Bluff along the rim of Kīlauea Caldera. View is from a helicopter, looking toward the southwest. Photograph by Tim Orr on November 28, 2008.

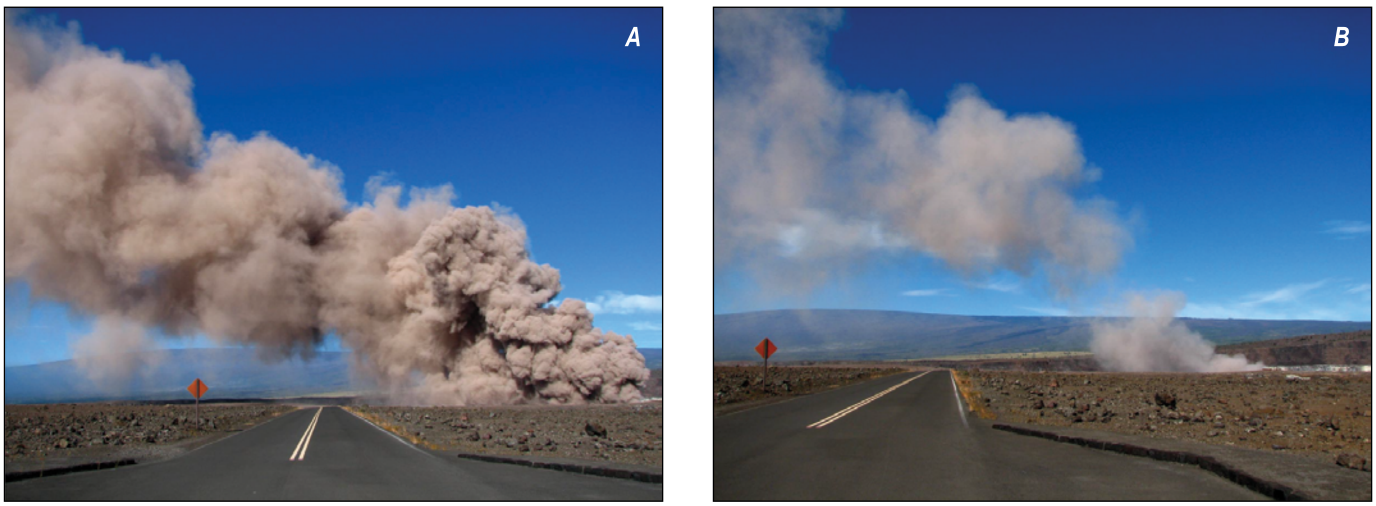


**Figure 19.** Photograph of the brown plume and subsequent pause in vent activity that persisted for several weeks after a series of large collapses of the Overlook crater walls on December 4, 2008. *A*, Thick brown plume moments after one of the collapses. Taken at approximately 09:20. *B*, Shortly after, at approximately 10:00, the reduction in gas emission is already evident by the weak plume. Photographs by Desiree Roerdink, Hawaiian Volcano Observatory volunteer.

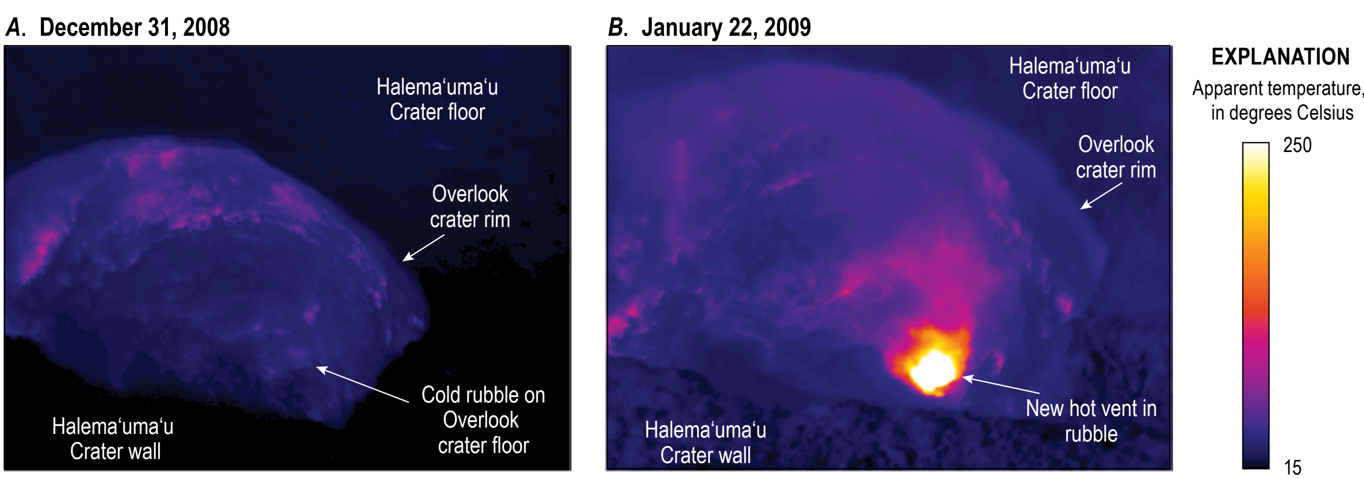


**Figure 20.** Thermal images showing views inside the Overlook crater taken from a helicopter. *A*, After the collapse of the Overlook crater that occurred in early December 2008, thermal images appeared to show cold rubble on the floor of the crater, presumably choking the vent. *B*, A hot, outgassing vent on the floor of the Overlook crater was reestablished in mid-January, when activity resumed. Images by Matt Patrick using a FLIR PM595 camera.

fed vigorous breakouts from the episode 58 lava tube, driving large explosions at the ocean entry. During this apparent increase in lava supply at Puʻu ʻŌʻō, the glow at the summit intensified in a manner mirroring increasing summit tilt. In hindsight, this increase in glow likely reflected rising of lava deep in the Overlook crater. Second, a large DI event in early August created a brief pause in effusion at Puʻu ʻŌʻō during the deflation and a subsequent surge in tube breakouts during the inflation. Glow from the Overlook crater peaked during this August DI event, again likely caused by fluctuating lava level.

## 2009: Sporadic, Deep Lava Lake Activity

The eruptive pause continued into the first 2 weeks of 2009. After a resumption in detectable infrasound from the vent reported by the Infrasound Laboratory of the University of Hawaiʻi on January 14 (Fee and others, 2010), glow and gas venting sounds returned on January 20 and thermal camera images showed a new hot hole deep in the crater on January 22 (fig. 20*B*). The hot hole presumably represented reestablishment of the vent, which opened through the rubble fill at the bottom of the crater.

On February 4, during the deflation part of a DI event, a composite seismic event occurred and was associated with emission of a brown plume. The thermal camera revealed that the floor of the Overlook crater had collapsed away, and the next day a crusted lava lake rose into this space as the inflation part of the DI event ensued (fig. 21). As inflation peaked the following day, episodic tremor bursts appeared and were associated with gas pistoning of the lake. By February 9, the gas pistoning had ceased and the lava lake was crusted over. In its place, one or two small spattering holes were present on the Overlook crater floor for the remainder of the month and through most of March.

On March 25, however, a pattern occurred that was similar to that of early February. During the deflation part of a DI event, a composite seismic event occurred, and a brown plume rose from the crater. This event was associated with further collapse of the floor of the Overlook crater, followed shortly after by the rise of a lava lake into the base of the crater. Episodic tremor again returned as gas pistoning ensued. The common pattern of February and March 2009 suggested that the lava column retreated during the deflation part of a DI event, removing support from the floor of the Overlook crater, which then collapsed. The collapses triggered

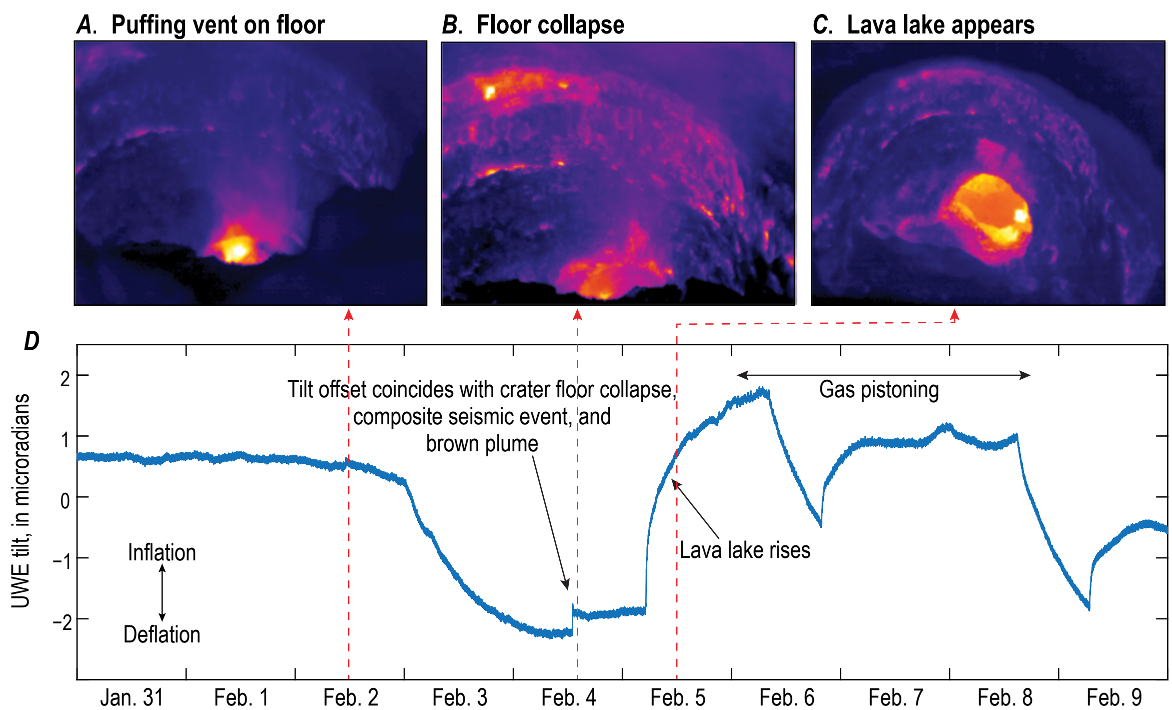


**Figure 21.** Plot showing an example of Overlook crater floor collapse in 2009. Tilt is measured at tiltmeter station UWE on the northwest rim of Kīlauea Crater. This example is from February 2009 and involved these events: (1) large deflation as part of a deflation-inflation (DI) event, (2) composite seismic event, (3) emission of a brown plume, (4) observation of crater floor collapse, (5) sharp inflation as part of the DI event, (6) lava lake rising into view, and (7) gas pistoning of the lava lake. It is presumed that deflation led to a drop in the lava column, which removed support for the Overlook crater floor, triggering a collapse and associated composite seismic event and brown plume. Reinflation resulted in lava column rise, filling the bottom of the Overlook crater with a small lava lake, which then began gas pistoning. This pattern occurred five times during 2009 and early 2010. Thermal images by Matt Patrick using a FLIR PM595 camera. Purple and black colors represent cool temperatures, yellow and white colors represent hot temperatures.

composite seismic events and emission of a brown ash-bearing plume. When the inflation part of the DI event followed, the lava column rose, filling the base of the Overlook crater with a small lava lake that then began gas pistoning. This pattern offered further support for the tie between lava level and ground tilt.

The lake that was established in late March soon crusted over, and small outgassing holes were present at the bottom of the crater through April and May. On May 31, crater floor collapse occurred again, followed the next day by the appearance of a lava lake deep in the crater. Unlike the previous lava lakes of February and March, which were only active for several days, this lava lake persisted for a month and marked the longest period of observable lava lake activity yet during the eruption.

In the first 3 weeks of June, the lake was very active, with a roiling, agitated surface and swift flow from one side of the lake to the other (fig. 22). Light detection and ranging (lidar) scans by the Pacific GPS Facility at the University of Hawai‘i at Mānoa on June 11 showed that the lake was approximately 60 m in diameter (fig. 23) and about 200 m below the Overlook crater rim (the Overlook crater rim at this time was at 1,023 meters above sea level [m a.s.l.]). The walls of the Overlook crater were significantly undercut, with an impressive 80 m of horizontal overhang on the north wall. Gas pistoning was common (Patrick and others, 2011). The lake rose after June 22 and the surface became more sluggish, consisting of large crustal plates. Views of the lake through

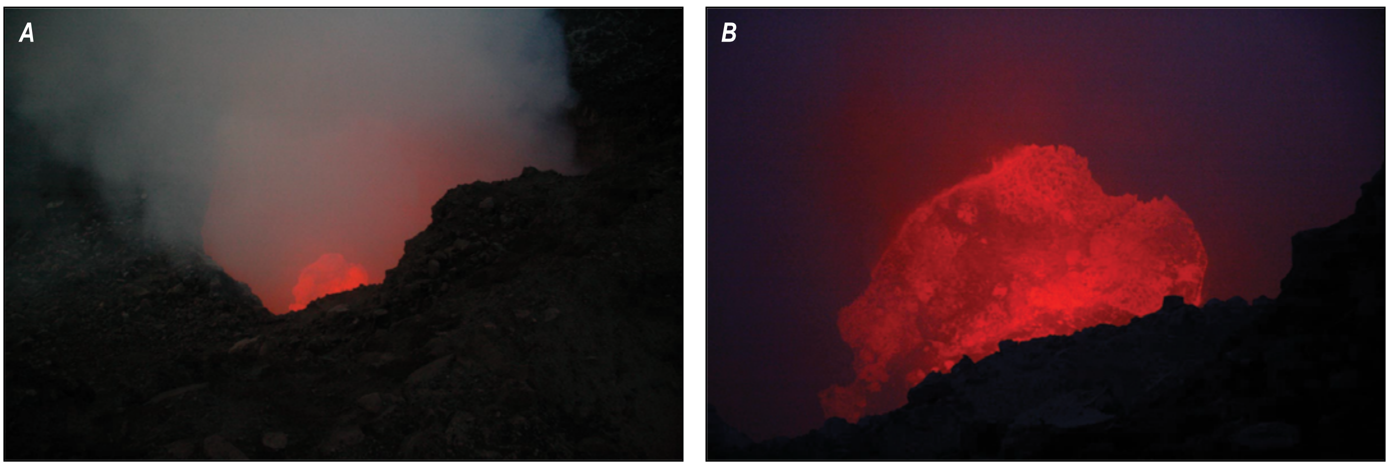


**Figure 22.** Photograph of the first sustained lava lake activity, which occurred in June 2009. The highly agitated, roiling lake was approximately 60 meters (m) in diameter and 200 m below the floor of Halema‘uma‘u. Photographs from 70 m west of the Halema‘uma‘u Overlook by Tim Orr on June 3, 2009.

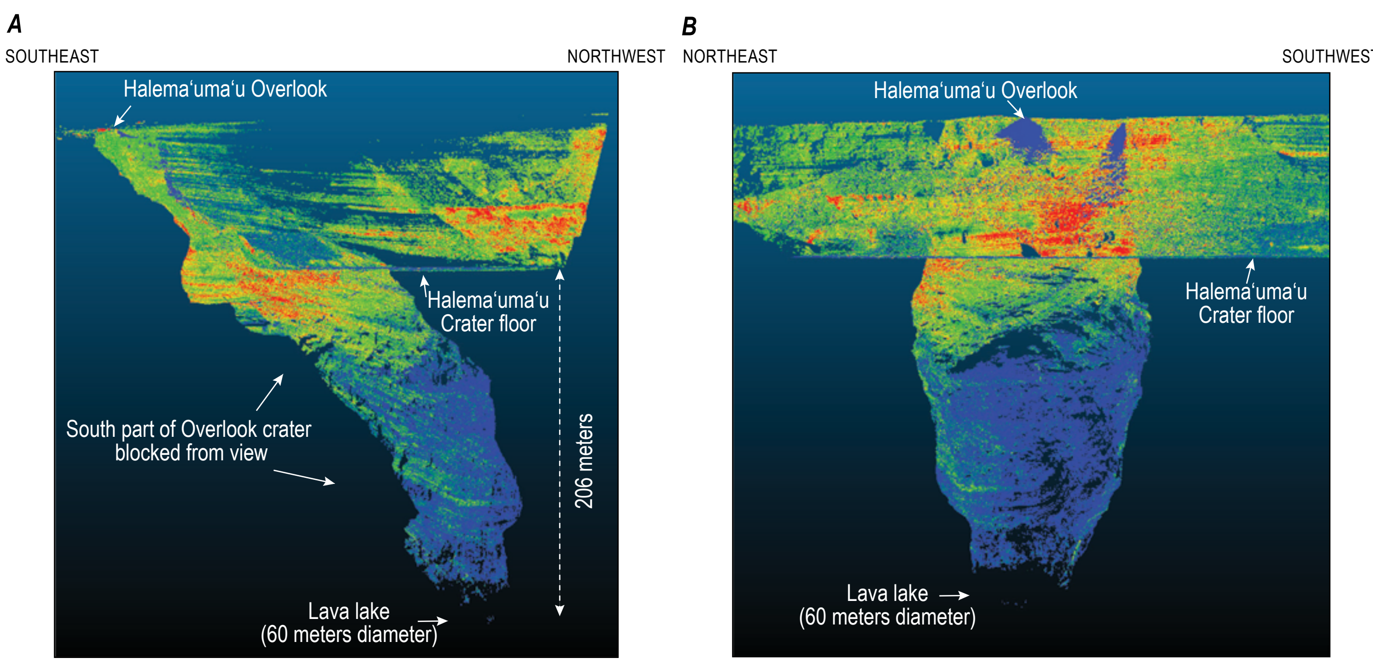


**Figure 23.** Cross sections of light detection and ranging (lidar) data from the Overlook crater in June 2009. Lidar scans provided the first precise constraints on lake and crater geometry. *A*, Southeast-northwest profile. *B*, Northeast-southwest profile. Data provided by Todd Eriksen and the Pacific GPS Facility at the University of Hawai‘i at Mānoa.

the thick fume were still sporadic; they were augmented by a video camera on night-shot (near-infrared) mode, which saw through the fume better than the naked eye. On several occasions, rockfalls were seen to hit the lake and trigger vigorous spattering and bubble bursting, originating at the point of impact.

On June 30, a series of large collapses of the walls and rim of Overlook crater ended the lava lake and appeared to again clog the vent with rubble, similar to what occurred in December 2008. Ground shaking caused by these collapses was felt 2 km away by staff at HVO. $SO_2$ emissions were again low (Elias and Sutton, 2012), the vent was dark and quiet, and infrasound ceased (Fee and others, 2010), indicating another pause in the eruption.

This second pause lasted through July and was terminated in early August with the appearance of a new hot hole in the rubble on the floor of the Overlook crater. Significant infrasound returned on August 9, as reported by the Infrasound Laboratory of the University of Hawaiʻi (Fee and others, 2010), and glow and gas rushing sounds were observed. Two small outgassing holes were present through the remainder of August and into September. An explosive event on September 17 deposited spatter around the Halemaʻumaʻu Overlook.

Another sequence of crater-floor collapse occurred on September 26, similar to those of February, March, and May, accompanied by a composite seismic event and brown plume. Two days later, lava again rose into the crater, with slow gas-piston cycles each lasting an hour or more. The lava lake was active into the first week of October but crusted over and was replaced again by several small outgassing holes on the crater floor. Minor collapses and rebuilding from spatter deposits modified the geometry of these outgassing holes and the floor of the Overlook crater through November and December. The Overlook crater remained deep, with the floor about 200 m below the rim, and activity remained obscured by thick fume, with the near-infrared video camera providing the only reliable views. When the outgassing holes enlarged sufficiently, small roiling lava lakes could be seen within them (fig. 24). By late December there was a dominant pit larger than most of the previous pits and holes on the crater floor. This pit hosted a small lava lake, with impressive gas-piston cycles in which the lava would rise sufficiently to cover much of the Overlook crater floor. By the end of 2009, the rim of the Overlook crater had a diameter of approximately 140 m.

## 2010: A Continuous Lava Lake Rises

The dominant pit from late 2009 continued to occupy the north part of the Overlook crater floor in early January 2010 and a smaller pit formed in the south part of the crater. On January 7, HVO geologists on an overflight could see lava upwelling as a circular dome fountain in the south pit that flowed as a wide, swift river toward the north, plunging into the deeper, larger pit. Gas-piston cycles, lasting 1.5 hours each, resulted in repeated rising of the lava level in the larger pit, drowning of the south pit and lava river, and covering of the entire floor of the Overlook crater in brief episodes. This heightened activity occurred near peak inflation of a DI event, and subsequent deflation over the next few days resulted in a lowered lava level and more subdued activity in the two pits. Renewed inflation during the DI event on January 14 produced a resurgence in the lava river and gas pistoning. Again, during the low stand of gas pistoning, the wide lava river flowed from the south pit toward the north, pouring into the deeper north pit. During rise phases, lava upwelled from the north pit and covered the Overlook crater floor. The transition from high stand to low stand triggered a large vortex, about 40 m in diameter, in which lava drained as a giant whirlpool into the north pit (fig. 25) with a loud roaring sound. This whirlpool remains one of the most visually impressive events of the entire eruption.

Subsequent deflation resulted in lower lava levels for the remainder of January and early February, where a small lava lake was normally confined within one of the pits. By February 10, at least three small pits perforated the Overlook crater floor; the largest (and northmost) pit hosted a small sloshing lava lake (fig. 26*A*). Most of the Overlook crater floor consisted of a large mound cut by hot fractures, surrounded by rubbly slopes that were also cut by hot cracks and reached the Overlook crater walls.

On February 11, during the deflation part of a major DI event, the floor of the Overlook crater collapsed in a pattern resembling the episodes of February, March, and May 2009. The collapse was associated with a composite seismic event and emission of a brown plume and was followed shortly thereafter by the appearance of a lava lake at the bottom of the Overlook crater (fig. 26*B*) that was larger than what had previously been observed. This collapse marked the end of periods of alternating small outgassing holes and transient lava lakes on the crater floor that typified activity in 2009 and was the start of continuous lava lake activity that continued for 8 years.

Through the remainder of February, all of March, and most of April, the Overlook crater floor consisted of a lava lake on the north end and a small outgassing hole in the south. On April 26, a composite seismic event associated with collapse of the septum between the outgassing hole and the lava lake (fig. 27*A*) created a small explosive event that deposited juvenile lapilli on the Halemaʻumaʻu Overlook. The collapse enlarged the lake toward the south, creating a kidney-bean-shaped lake elongate along a north-south axis and covering most of the Overlook crater floor (fig. 27*B*). This basic geometry was maintained through the rest of the year. The lake surface consisted of large crustal plates, where lava upwelled near the north lake margin, flowed south to a spattering and bubble bursting site, and downwelled along the south margin. The downwelling zone approximately coincided with the location of the south pit observed in early January.

Gas pistoning was common throughout the rest of 2010 (fig. 28; Nadeau and others, 2015; Patrick and others, 2016b). In May, gas pistoning began to exhibit more pronounced drops in seismic tremor during the lava rise periods (Nadeau and others, 2015). These periods of tremor stagnation, most


**Figure 24.** Photographs of typical activity in 2009. *A*, Views inside the Overlook crater with the naked eye (or camera) were commonly obscured by a thick plume. Photograph taken from a helicopter by David Dow, Hawaiian Volcano Observatory volunteer, on October 8, 2009. *B*, Using the night-shot (that is, near-infrared) mode on a video camera provided improved views through the thick fume. During much of 2009 there were small pits of outgassing, spattering holes on the floor of the Overlook crater; pits were at a depth of approximately 200 meters below the floor of Halemaʻumaʻu. Sometimes these pits were filled with roiling lava. Image taken from the Halemaʻumaʻu rim by Matt Patrick, September 13, 2009.

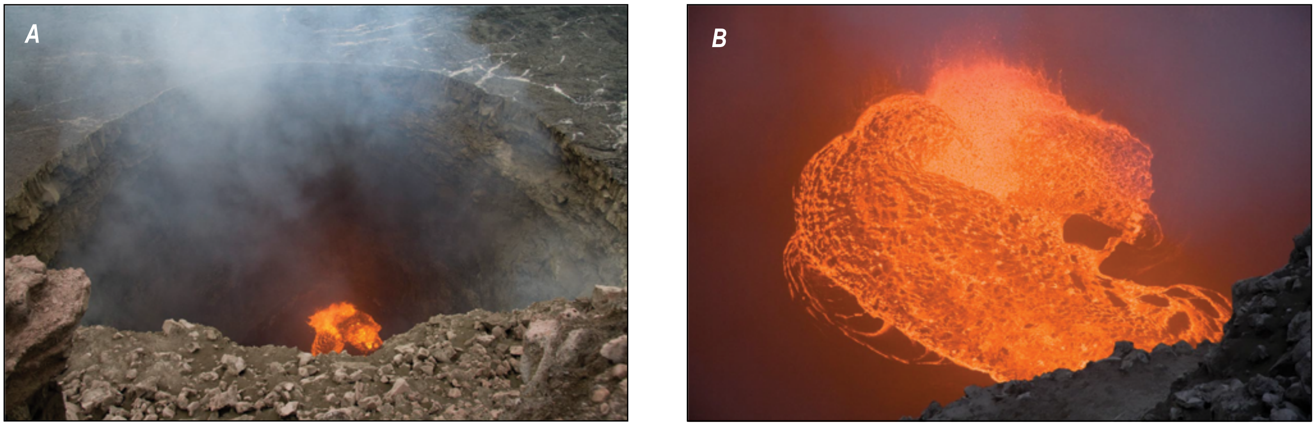


**Figure 25.** Photographs of a brief phase of whirlpool draining deep in the Overlook crater in January 2010. The lava was approximately 190 meters (m) below the floor of Halemaʻumaʻu. Lava upwelling from a perched vent in the south part of the crater floor (bottom of image) flowed toward a deeper pit in the north part of the floor. The lava went through cycles of gas pistoning, where draining formed a large vortex of pouring lava about 40 m wide. *A*, Wide view from the Halemaʻumaʻu Overlook, showing the Overlook crater rim. January 7, 2010. *B*, Close-up view of the lava whirlpool. Photographs by Tim Orr on January 14, 2010.

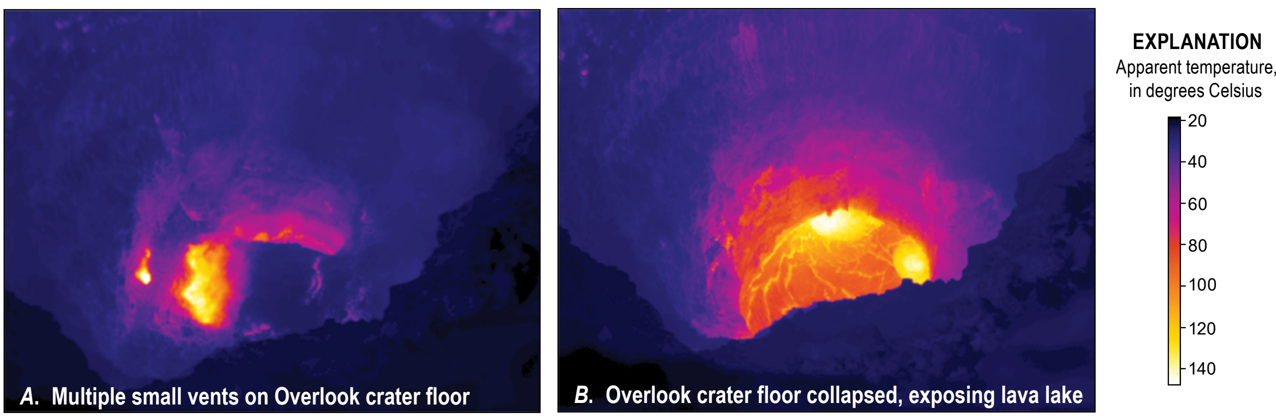


**Figure 26.** Thermal images of the onset of continuous lava lake activity in February 2010. *A*, On February 10, the Overlook crater floor was mostly solid, with small outgassing holes and hot cracks. *B*, After deflation, the floor of the Overlook crater collapsed, revealing an open lava lake surface (approximately 60 meters in diameter). Image taken at 16:30 on February 11, 2010. This pattern of deflation and crater floor collapse was similar to several events in 2009 (such as occurred on February 4 and March 25) but had longer lasting consequences. Thermal images collected from the Halemaʻumaʻu rim by Matt Patrick using a FLIR SC620 camera.

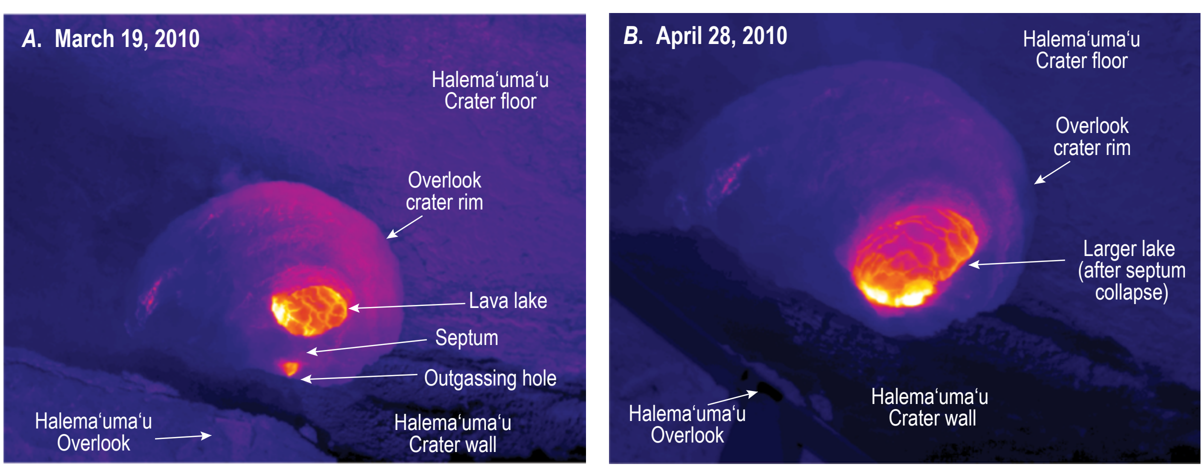


**Figure 27.** Thermal images taken from a helicopter showing enlargement of the lava lake in April 2010. On April 26, the septum between the lake and a small outgassing hole on the Overlook crater floor collapsed, enlarging the lake. Purple and black colors represent cool temperatures, yellow and white colors represent hot temperatures. Images by Matt Patrick using a FLIR SC620 camera.

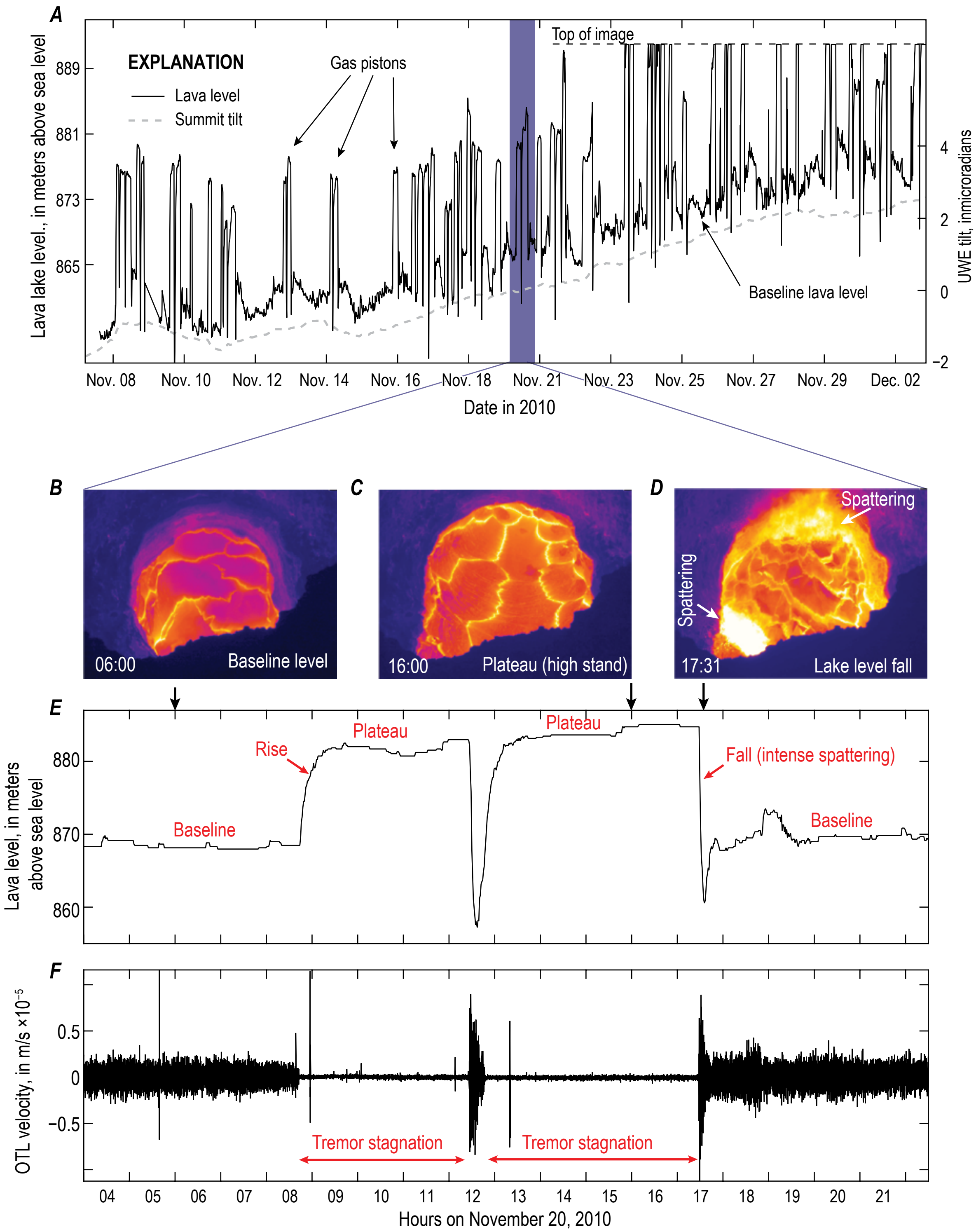


**Figure 28.** Plots showing gas pistoning during November 2010. *A*, Plot of lava lake level and ground tilt as measured at tiltmeter station UWE on the northwest rim of Kīlauea Crater. The baseline lake level rose gradually during November 2010 but had brief rises caused by gas pistoning superimposed on this trend. The rise in baseline lake level tracked inflationary ground tilt at the summit. *B–D*, Thermal images from the HTcam (location in fig. 2) on November 20 showing the lake at a baseline level (*B*), a high level caused by gas pistoning (*C*), and during a rapid drop at the end of the gas-piston cycle (*D*). The lake is approximately 80 meters (m) in diameter. The time each image was taken is in the lower left corner. Purple and black colors represent cool temperatures, yellow and white colors represent hot temperatures. *E*, Plot of lava level on November 20, showing two gas-piston cycles, each 3–5 hours long. The lake rose about 15 m during the gas-piston events. *F*, Plot of velocity (in meters per second [m/s] ×$10^{-5}$) as measured at station OTL, near the southwest rim of the caldera, on November 20. Seismic tremor dropped during the rise and plateau phases of the gas-piston events and increased during the rapid fall phase. Modified from Patrick and others (2019a).

evident in the high-pass (>1 hertz) seismic data, corresponded with a termination of spattering and bubble bursting in the lake, referred to as nonspattering periods (Patrick and others, 2016b). Unlike the gas-piston events of 2009 and early 2010, which seemed to occur only during the peaks of summit inflation, gas pistoning in the later part of 2010 bore no obvious relation with ground tilt. This change in behavior might reflect the presence of a continuously active lava lake after February 2010, whereas previously the emergence of the lake required inflation and lava rise.

A sharp rise in lake level, associated with significant summit inflation, began in November (Orr and others, 2015a). The lake surface rose from a baseline of about 850 m a.s.l. (about 170 m below the Overlook crater rim) in early November to a level of about 880 m a.s.l. (about 140 m below the rim) by the end of the year (fig. 29). Short-term fluctuations in lake level associated with gas pistoning were superimposed on this long-term rise (Patrick and others, 2016b). A continuously operating thermal camera was installed on the Halemaʻumaʻu rim at the end of October and provided improved views of the lake (Patrick and others, 2014); the camera ran continuously until it was destroyed in the May 2018 collapses.

## 2011: Lava Lake Draining and Disruption

The lava level continued to rise with summit inflation in January and February 2011. Superimposed on this trend were two cycles of fall and rise associated with unusually large DI events that had amplitudes of about 50 m and periods of approximately 7 days (Anderson and others, 2015). Gas pistoning continued to create short-term fluctuations in lava level, where intense bubble bursting and spattering occurred at the lake margins during falls.

The high lava level provided clear views of the stoping process on the walls of the Overlook crater. High lava levels increased heating of the crater walls, particularly on the undersides of overhangs, triggering many rockfalls. From the Halemaʻumaʻu Overlook, loud rock-cracking sounds were audible, ranging from high pitched pops to deep cannon-like booms. Many of these thermal cracking events were associated with spallation of rocks off the crater walls at high velocity. Others were internal to the walls themselves. During lake level fall as part of gas-piston cycles, vigorous spattering emitted intense heat, which promoted rockfalls and crater wall disintegration, sometimes creating a constant rain of rocks from the crater wall just above the spattering site. The erosion of rock near the base of the Overlook crater walls temporarily increased the extent of rock overhang and removed support for the upper crater walls, leading to several large collapses of the crater rim during January, February, and early March. Long, arcuate slices of the crater wall and rim as wide as 12 m fell, enlarging the Overlook crater significantly in the first 2 months of 2011. By early March, the crater was approximately 150 m (in the northeast-southwest direction) by approximately 165 m (in the northwest-southeast direction).

Rim collapses triggered several explosions during this period, large enough to deposit lithic and juvenile tephra around the Halemaʻumaʻu Overlook on January 17 and 21. Other large collapses occurred on February 14 and 15 and March 3. The webcam at the Halemaʻumaʻu Overlook captured these events in unprecedented detail (fig. 30; Orr and others, 2013). Each event began with the passive collapse of the Overlook crater wall. Because of the overhang, the rockfalls impacted the lake surface directly, and a burst of incandescent spatter was ejected from the impact site, along with a dense tephra plume. This sequence provided unambiguous evidence that the explosions were triggered by rockfalls rather than by rising gas slugs (Orr and others, 2013). Deep (1 km below the surface), very long period seismicity was also associated with the explosions, and the time-synchronized webcam video showed that these oscillations started after the rockfall impact, adding further support to the interpretation that

***A*. November 1, 2010** ***B*. December 31, 2010**

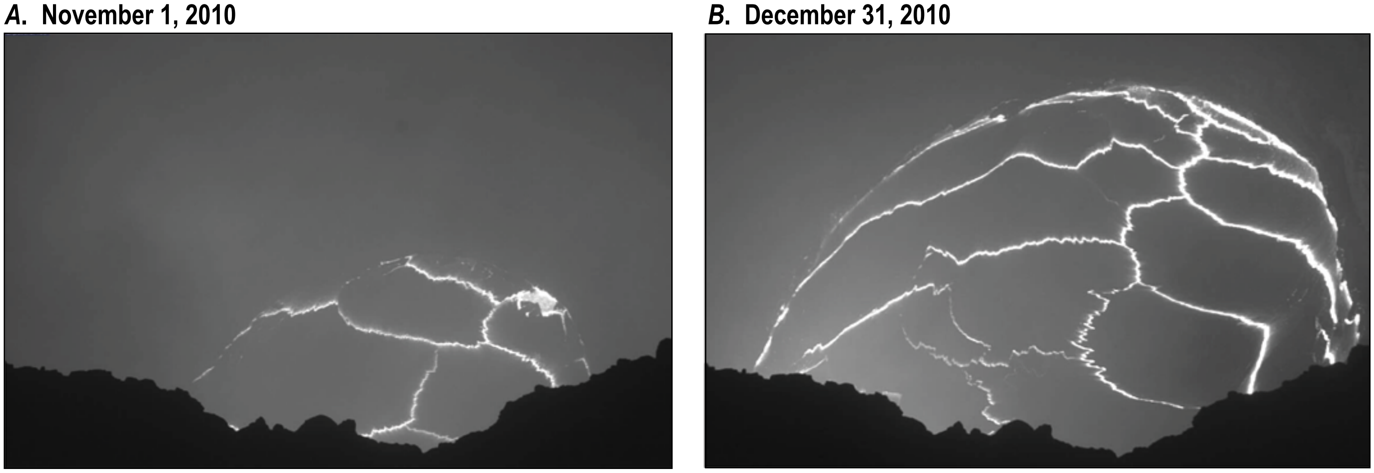

**Figure 29.** Webcam images (HMcam; location in fig. 2) showing the rise of the lava lake in late 2010. *A*, On November 1, the lake was approximately 180 meters below the Overlook crater rim. *B*, By the end of the year, the lava lake rose to about 140 meters below the Overlook crater rim and was larger in area owing to the flaring crater shape.

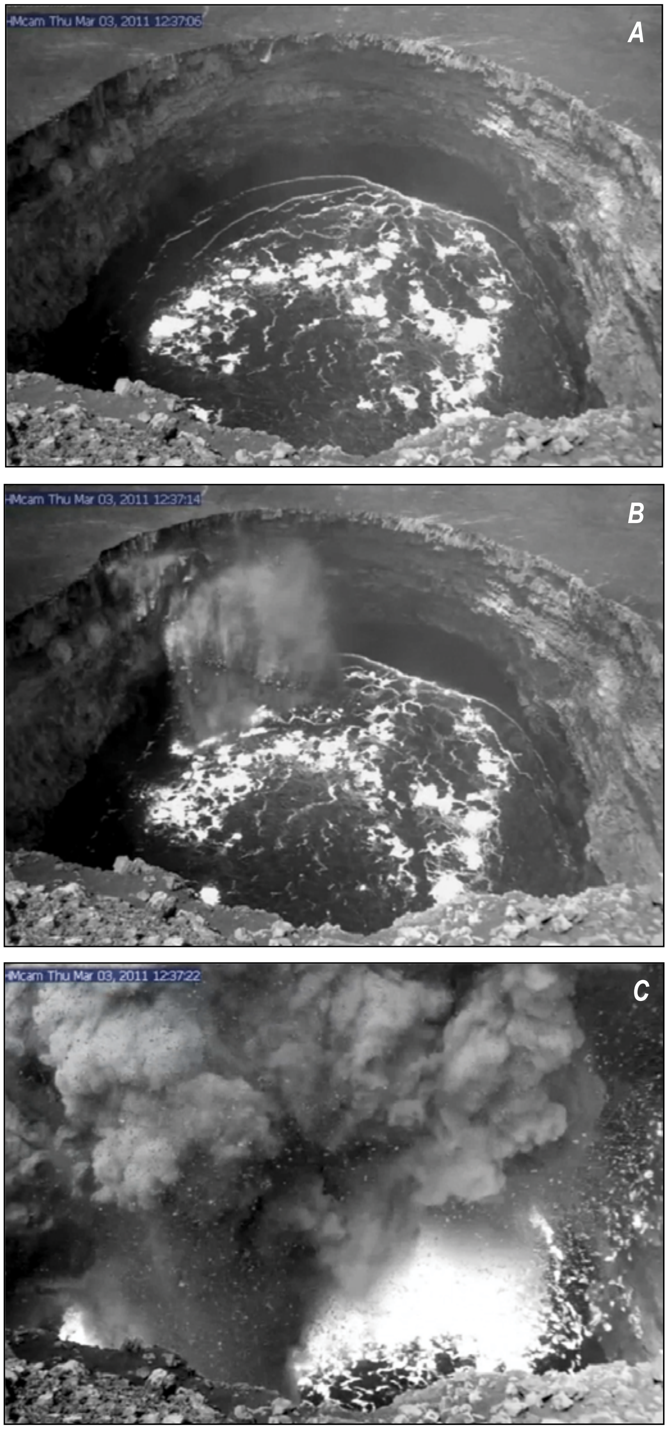


**Figure 30.** Images of explosions triggered by rockfalls from the Overlook crater walls. A webcam at the Halema‘uma‘u Overlook captured conclusive evidence that explosive events during the eruption were triggered by rockfalls that impacted the lake surface (Orr and others, 2013). This example is from March 3, 2011. *A*, Video frame from 12:37:06, about 10 seconds before the explosion. The lake is approximately 75 meters below the Overlook crater rim. *B*, Video frame from 12:37:14. A rockfall from the overhanging northwest wall of the Overlook crater impacts the lake surface. *C*, Video frame from 12:37:22. Hot spatter (white spots) is ejected as a dark, tephra-laden plume rises and fills the field of view. The lake surface is extremely agitated and sloshing. Images *B* and *C* also published by Orr and others (2013).

the explosive process and seismicity were driven by a top-down process (rockfalls) (Patrick and others, 2011; Chouet and Dawson, 2013; Orr and others, 2013; Dawson and Chouet, 2014).

As the lava lake rose to high levels in January and February, ground tilt showed continued inflation and the rate of small earthquakes in the upper ERZ increased well above background levels (Orr and others, 2015a). HVO provided a hazard assessment to the national park stating that this pattern, based on previous activity, indicated there was an increased likelihood of a change on the volcano, such as an intrusion or new vent opening on the ERZ (Sur, 2011).

At 13:42 on March 5, a rapid increase in seismic tremor at station STC, about 2 km west of Pu‘u ‘Ō‘ō on the ERZ, triggered automated alarms. The increase in tremor coincided with the onset of sharp deflation at Pu‘u ‘Ō‘ō, and the floor of Pu‘u ‘Ō‘ō crater began subsiding shortly after 14:00, dropping 85 m over the next few hours. The Kamoamoa eruption began at 17:09 with fissures opening approximately 2 km west of Pu‘u ‘Ō‘ō, and intermittent fountaining continued for the next 4 days in this area (Orr and others, 2015a).

At the summit, sharp deflation began at approximately 14:20 on March 5, along with a simultaneous drop in the lava lake level. Given the frequent small fluctuations in lava level common to the lake, it is difficult to place an exact time on when draining began. Over the next 24 hours, the lake dropped approximately 200 m, leaving only a tiny pond between March 7 and 9 (fig. 31; Carbone and others, 2013; Orr and others, 2015a). Numerous small collapses occurred in the Overlook crater as the level dropped, but the crater remained mostly intact with no large-scale failures.

Views inside the crater with the naked eye were blocked by thick fume, but images taken with a thermal camera from a helicopter provided a clear picture of the structure and activity in the drained crater over the next week (fig. 32). The uppermost 60 m of the crater was a large elliptical cavity (170×150 m in map view), below which extended a narrow shaft (120×90 m) to the floor at approximately 260 m below the rim. Active lava was absent in the crater during the March 10 overflight, was present on March 14, and was absent again on March 17. Small lava ponds reappeared episodically over the next few weeks, modulated by DI events—lava rose and filled the bottom of the crater during the inflation part of a DI event, forming a small pond, but then drained partly or completely during deflation. Gradually, as the summit inflated, the lava level rose, and the brief draining events ended after April 5, when the lake remained continuously in view from the Halema‘uma‘u Overlook. As the lava level rose in May and June, the lake built a solidified ledge around itself, so that the lake was contained within an inner pit. In addition to the main lake, two channelized streams of lava occasionally appeared from a smaller upwelling area southeast of the lake. These two streams flowed northwest and cascaded into the lake. Lake circulation was also highly variable during this time, sometimes abruptly switching from north-south directed flow to south-north directed flow (fig. 33). The cascades and shifting flow directions suggested two competing lava upwelling sites, one in the lake itself in the northwest part of the crater, and another in the small hole in the southeast.

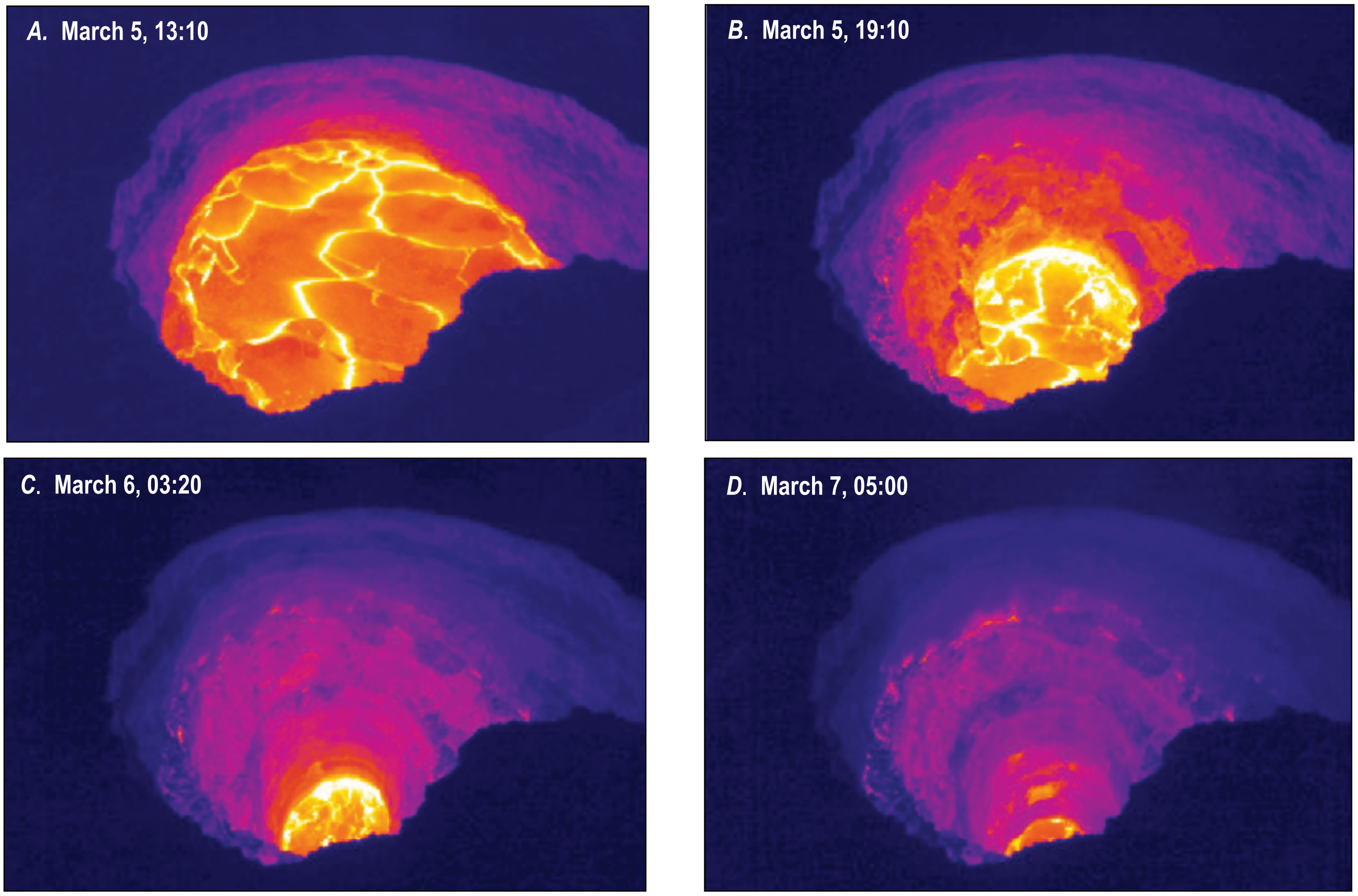


**Figure 31.** Thermal images of the summit lava lake draining during the Kamoamoa eruptive event on the East Rift Zone in March 2011. The lake drained over the course of approximately 24 hours. Images from the HTcam thermal webcam at the Halemaʻumaʻu rim (location in fig. 2). Date and times are given. *A*, The lava lake before the onset of the Kamoamoa event. The lake began draining shortly after 14:00. *B*, About 5 hours after the onset of draining, the lake level had dropped approximately 60 meters. *C*, Early the next day, most of the lake had drained, leaving a small lava lake at the bottom of the Overlook crater. Small rockfalls occurred from the crater walls, but the crater remained mostly intact. *D*, One day later, a small amount of residual ponded lava remained at the bottom of the crater, but the lake was mostly drained. Purple and black colors represent cool temperatures, yellow and white colors represent hot temperatures.

The lake continued rising through July, and by the start of August it had reached approximately the high level attained before the Kamoamoa eruption in March. Rock cracking sounds were common, many loud enough to be heard inside the HVO building about 2 km away. On August 3, rising lava levels in Puʻu ʻŌʻō crater led to the opening of fissures on the west flank of the Puʻu ʻŌʻō cone, draining lava from the crater in a couple of hours. These new fissures triggered another major drop in the lava lake in Halemaʻumaʻu, but the amplitude and rate of drop were not as dramatic as that of the March 5 draining. The summit lake level dropped approximately 80 m over the next 7 days, and briefly disappeared from the bottom of the Overlook crater on August 14–17. The draining at Puʻu ʻŌʻō was caused by the opening of a vent on the cone flank (Patrick and others, 2019b). The fact that this had a significant impact on summit lake level and tilt indicates how small changes along the ERZ can impact the summit via an efficient hydraulic connection (Patrick and others, 2019b).

As Puʻu ʻŌʻō stabilized and refilled with lava in late August, the summit reinflated and the level of lava in the Overlook crater rose. Puʻu ʻŌʻō crater rapidly refilled in September, and the summit lava level returned to approximately its previous high level by the middle of the month. On September 21, new fissures broke out on the upper flank of the Puʻu ʻŌʻō cone, partly draining Puʻu ʻŌʻō crater and sending a new flow (Peace Day flow; episode 61b) toward the southeast (Poland, 2014). The summit lava lake response to this event was muted because the change was obscured by ongoing DI events, and the drop was probably less than 20 m. The minor change at the summit was likely caused by the high elevation of the Peace Day vent, which did not efficiently drain the magmatic system.

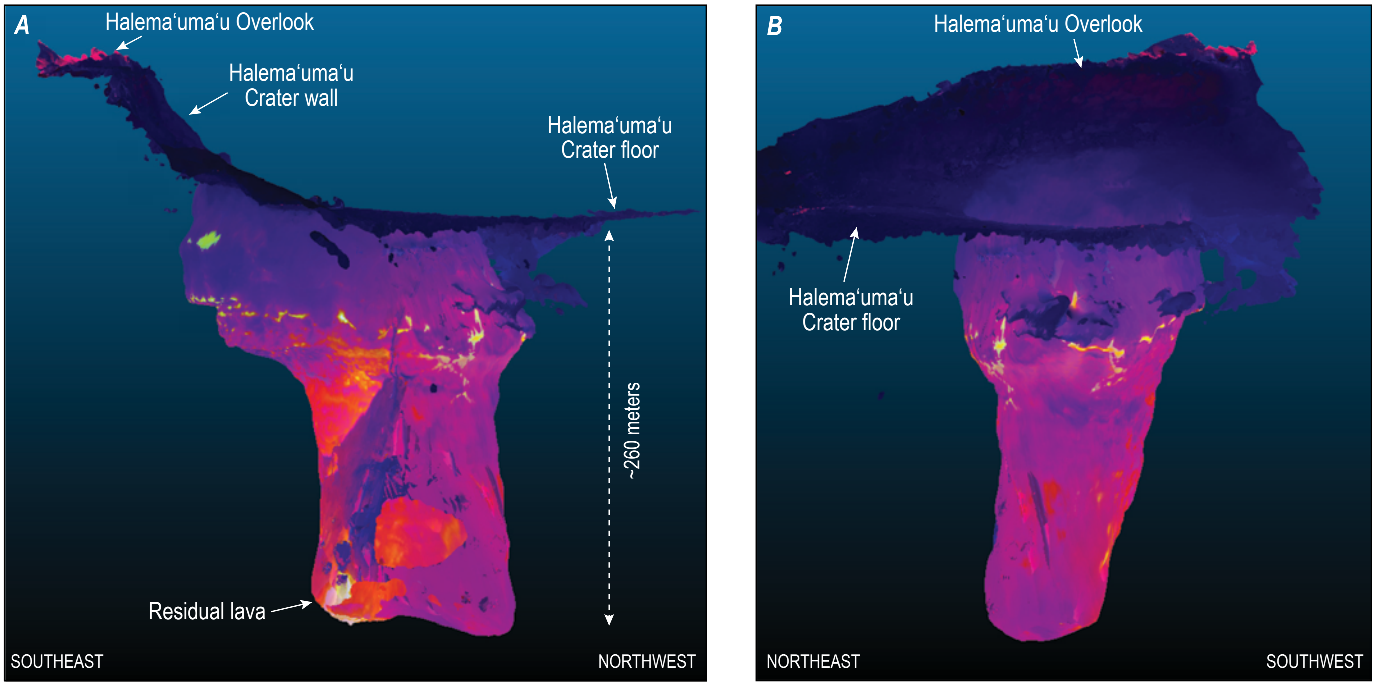


**Figure 32.** Three-dimensional reconstruction of the Overlook crater after the lava lake drained on March 5–7, 2011. The south part of the crater has several ledges and a deep shaft exists in the north part of the crater that reaches a maximum depth of approximately 260 meters. Model created from structure-from-motion software using thermal images (taken by Matt Patrick) collected from a circling helicopter on March 8 and 9, 2011. Warm and cool colors show hot and cool temperatures, respectively, in the thermal images.

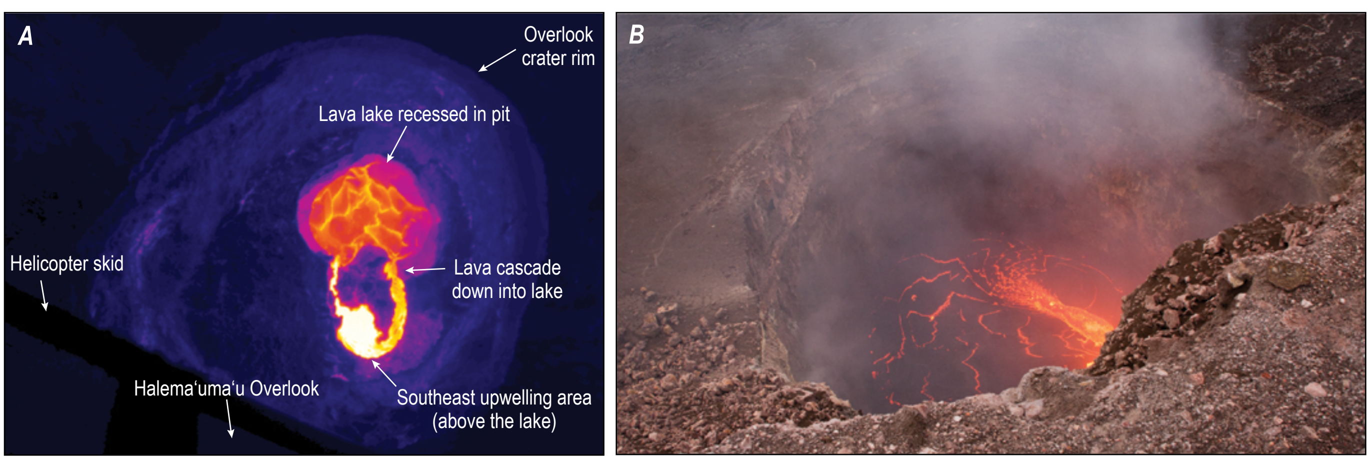


**Figure 33.** Photographs taken after the Kamoamoa eruptive event of March 2011, when the summit reinflated and the lava lake refilled. *A*, In May, the lava lake was often recessed in a pit. Occasionally, lava upwelled from a spot southeast of the lake, sending two lava streams cascading downward into the lake. Thermal image taken on May 11, 2011, by Matt Patrick using a FLIR SC620 camera. Purple and black colors represent cool temperatures, yellow and white colors represent hot temperatures. *B*, Lava pours from a vent in the south part of the crater and flows northward in a channel. The lake continued refilling until early August 2011, when it drained again during another East Rift Zone eruptive event. Photograph taken on June 2, 2011, from the Halemaʻumaʻu rim by Ben Gaddis, Hawaiian Volcano Observatory volunteer.

For the rest of 2011, the lava level at the summit was generally at a higher baseline level than that of 2010. Frequent DI events caused fluctuations in lake level of 10–20 m over the course of several days. The lake surface consisted of large crustal plates, with dominant surface flow from north to south. The final notable event of the year was an explosion at 16:55 on December 21. The explosion, triggered by a large collapse of the west wall of the Overlook crater, deposited juvenile lapilli and bombs west beyond the Halema‘uma‘u parking lot and Crater Rim Drive. Overall, the 2011 activity was notable not only for its highly dynamic nature but also for the coupled lava level changes at Halema‘uma‘u and Pu‘u ‘Ō‘ō, highlighting the close hydraulic connection between the summit and ERZ (Orr and others, 2015a; Patrick and others, 2019b).

## 2012: Approaching Stability

There was an overall rise in lava lake level during 2012, overprinted by day-to-day changes caused by DI events. In January and February, a series of DI events occurred that clearly showed the close correlation between ground tilt and lava lake level (fig. 34; Patrick and others, 2015a). Later in the year, two large DI events occurred simultaneously with summit deflation and a drop in lava lake level to low levels. The deflation part of these DI events corresponded with brief eruptive pauses on the ERZ lava flow field (Patrick and others, 2019b). These coupled cycles added further evidence of the hydraulic connection between the summit and ERZ—the low pressure in the summit magma reservoir during deflation produced both a drop in summit lava lake level and a reduction of lava supply to Pu‘u ‘Ō‘ō.

For the first half of 2012, the lake was nested within levees of solidified lava that formed ledges around most of the lake margin (fig. 35). These ledges grew vertically by the deposition of lava from overflows and spatter, particularly during short-term rises in lake level caused by gas pistoning and inflation during DI events. Parts of the ledges frequently failed, particularly during short-term lava level drops caused by deflation during DI events, which removed lateral support from the ledges. In late August, a large part of the inner ledges collapsed, allowing the lake to fill much of the Overlook crater from wall to wall, though a large ledge remained in the south part of the crater.

The most notable change in 2012 occurred in October and started with a steady rise of lava level at the beginning of the month (fig. 36). In early October, the lava lake level was approximately 60 m below the crater rim and by October 26 rose to a peak of about 22 m below the rim. As it rose, the lake overtopped the surrounding inner ledges of solidified lava and completely filled the Overlook crater wall to wall. High lake levels provided the clearest views of the lake surface thus far, and heating of the crater walls enhanced thermal cracking and crater wall collapses, with a cacophony of pops and booms audible at Jaggar Museum and HVO.

The higher lava levels of late October also corresponded with an increase in the number of low-magnitude earthquakes in the upper ERZ, in a pattern like that preceding the Kamoamoa eruption event (Orr and others, 2015a; Patrick and others, 2015a). Based on this pattern, HVO again recognized a higher likelihood of a change on the volcano, such as an intrusion or formation of a new vent. The former occurred around October 28, corresponding with a swift drop in lava level of 35 m over the next few days. The intrusion appeared to occur near Keanakāko‘i in the summit region (A. Miklius, written commun., 2012). This event further highlighted the role of the summit lava lake as a pressure gauge of the summit magma reservoir (Patrick and others, 2015a), where intrusions act as a pressure release valve that returns the system to baseline behavior.

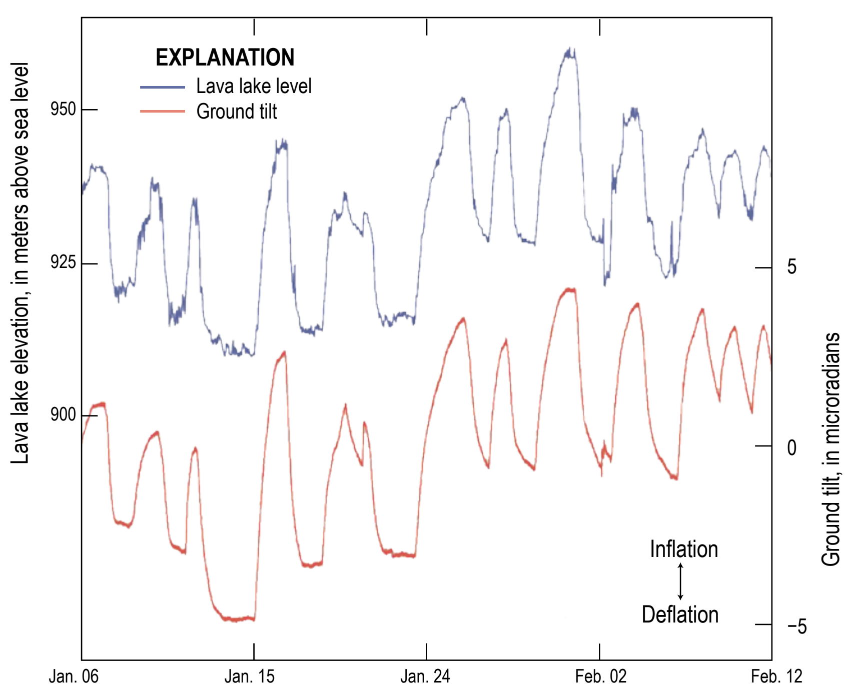


**Figure 34.** Plot showing the coupling of summit lava lake level and ground tilt during 2012. In the first 2 months of 2012, a series of deflation-inflation events occurred. This relation demonstrates that the lake behaved similar to a piezometer of the summit magma reservoir. Plot also published by Patrick and others (2015a).

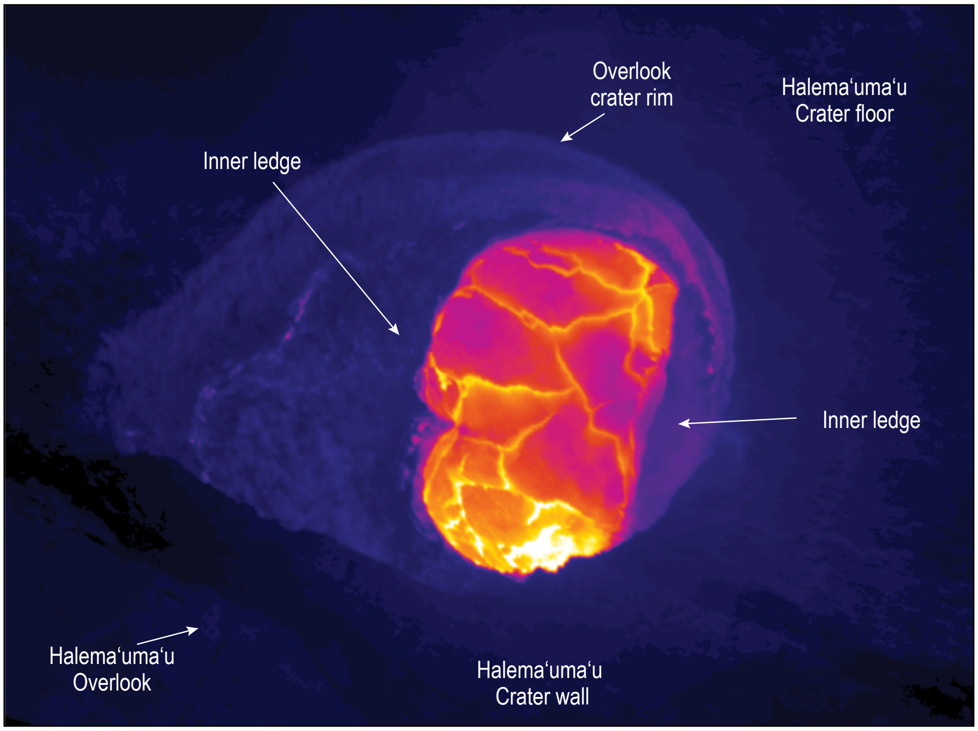


**Figure 35.** Thermal image showing a typical view of lava lake geometry during early 2012. Inner ledges surrounded the lake on the east and west margins. Upwelling was normally in the north part of the lake, and spattering present along the south margin. Thermal image collected from a helicopter by Matt Patrick on April 26, 2012, using a FLIR SC620 camera. Purple and black colors represent cool temperatures, yellow and white colors represent hot temperatures.

**Figure 36.** Photograph of the lava lake as it rose in late October 2012, when it peaked about 20 meters below the Overlook crater rim. Hawaiian Volcano Observatory (HVO) and Jaggar Museum are visible on the skyline in the upper right. Photograph from the Halemaʻumaʻu Overlook by David Dow, HVO volunteer, on October 22, 2012.

## 2013: A Rise in Lake Level and Increase in Crater Size

January 2013 began with lava at a very low level, approximately 80 m below the Overlook crater rim. Within days, however, sharp inflation corresponded with a rapid rise of lake level—by January 14, lava reached a level comparable to the October 2012 peak at about 20 m below the Overlook crater rim. The high level corresponded with small crustal plates and an apparent increase in surface velocity, which may suggest a magmatic pulse into the system (Swanson and others, 2016). Elevated seismicity in the upper ERZ suggested a pattern like that of October 2012, but lava levels eventually dropped by about 30 m through February and March without any obvious intrusion.

The January rise in lava level at the summit was mirrored at Puʻu ʻŌʻō, as lava filled the crater and began overflowing the east rim on January 19. These overflows eventually developed a tube and fed the slow-moving Kahaualeʻa 1 flow (episode 61c). Sustained high lake levels at Puʻu ʻŌʻō later in the year produced the Kahaualeʻa 2 flow (episode 61d), which persisted until mid-2014 (Patrick and others, 2015b).

The higher levels of 2013 resulted in the lake drowning the inner ledges that formed in 2012, leading to a larger lake that filled the Overlook crater wall to wall along the west, north, and east margins (fig. 37). A large ledge remained along the south lake margin (Burzynski and others, 2018), but higher lake levels occasionally produced overflows onto the ledge, building it higher. On July 25–26, during a large deflation episode and lava level drop, a large part of the south ledge collapsed, presumably because the lower lake level removed lateral support from the ledge.

Activity in 2013 highlighted two different styles of collapse—failure of a juvenile veneer versus large structural collapse of preexisting wall rock—in the Overlook crater and their relation with the changing state of magma reservoir pressure. During the deflation part of large DI events, when the lake would drop tens of meters over several days, large slabs or sheets of juvenile veneer adhering to the crater walls (left behind by the dropping lava level) would detach and fall into the lake, triggering spattering and bubble bursting on the lake margins. During the inflation part of large DI events, the lake could rise to unusually high levels, triggering heating of the overhanging crater wall and rock cracking. This heating and cracking would then lead to collapse of the upper walls of the Overlook crater, which were composed of lava erupted in 1967–68 and 1974. The wall-rock collapses, originating from higher on the crater walls than juvenile veneer collapses, would impact the lake with enough energy to trigger small explosive events that deposited spatter on the Halemaʻumaʻu floor or rim (Orr and others, 2013). Lidar scans (LeWinter, 2014) completed before and after a large collapse on January 15 showed it had a volume of 21,100 $m^3$.

Throughout the year, the lake surface was composed of large black crustal plates, with a dominant north to south migration. Spattering was common in the lake, most often in the southeast corner of the lake. We call this area the southeast (SE) sink, as it was an area of enhanced downwelling when bubble-bursting and spattering were active; the SE sink remained a common area of spattering to the end of the eruption. The position of the SE sink may have coincided with holes in the floor of the crater observed in previous years. Spattering continued to produce abundant Pele's hair and spheroidal tears and a semicontinuous carpet accumulated southwest of Halemaʻumaʻu. Nonspattering or weakly spattering periods (gas pistons) were still common and occurred during 21 percent of the year (Patrick and others, 2016b; Burzynski and

**Figure 37.** Photograph showing a typical view of the lava lake during 2013. A large inner ledge of solidified lava was present in the south part of the crater. Photograph taken from a helicopter by Tim Orr on August 16, 2013.

others, 2018). Gas-piston cycles produced changes in lava level of generally 5 m or less. These amplitudes were smaller than those of previous years, perhaps because of the larger surface area of the lake in 2013 (Patrick and others, 2016b).

Based on observations at the Halemaʻumaʻu Overlook, the sound of the lake seemed to be dominated by continuous outgassing and was commonly compared to ocean surf. During times of weak spattering, slow outgassing produced a hissing or sizzling sound. More vigorous spattering produced a louder sound resembling roaring or jetting. Some of these sounds may also have been produced by crustal plates sliding past one another, as well as by plates buckling and sliding past the crater wall. The continuous sound was often interrupted by sporadic rockfalls, which ranged from abrupt booming and crashing to more prolonged sessions resembling glass breaking. High lava stands often produced sharp reports caused by thermal cracking of the Overlook crater walls. These general audible characteristics continued through the rest of the lava lake phase that ended in 2018.

## 2014: Steady Lake Activity

The year 2014 was marked by highly stable behavior in the lake (fig. 38). Lava level had little net change, and the lake surface was normally 30–60 m below the Overlook crater rim. As in past years, day-to-day lava level changes resulted from frequent DI events. Large deflation episodes and lava level drops caused slabs of juvenile veneer on the crater walls to fall into the lake, triggering localized spattering. The most common site of spattering was in the SE sink, and nonspattering or weakly spattering (gas piston) periods occurred during 26 percent of the year. There were also good views of migrating spattering, in which spatter vents that formed in the north part of the lake drifted toward the south, presumably carried by lake currents (Patrick and others, 2015c, 2016a,b, 2018). Migrating spattering was a common occurrence in the lava lake throughout its lifespan and is similar to the "traveling fountains" observed at Halemaʻumaʻu in the early 1900s (Brigham, 1909; Perret, 1913a; Jaggar, 1947).

Several episodes in 2014 highlighted different styles of surface flow on the lake. The normal, stable flow direction was from the upwelling source in the north part of the lake. Occasionally, vigorous spattering and bubble bursting along the north margin of the lake triggered wholesale reversal of the lake surface flow direction. Presumably, this is because the spattering acts as a downwelling trigger. Spattering records the bursting of large gas bubbles, and the resulting void left by the burst creates a local sink into which the surrounding lava plunges, in the "siphon" effect of Perret (1913a,b) or "downsucking" of Jaggar (1947). Given that the spattering and bubble bursting appears to be shallowly rooted in the lake, this unstable, spatter-driven surface flow appeared to be a transient, superficial imprint on the stable, upwelling-driven flow that normally dominated in 2014 (Patrick and others, 2016a).

High lava levels (approximately 35 m below the Overlook crater rim) were sustained for 2 weeks in April and May but abruptly terminated on May 10 with a rapid drop in lava level of approximately 30 m. This drop in lava level accompanied a small earthquake swarm beneath the summit and may have resulted from a small intrusion in the summit caldera region that had no other obvious impact on the eruption (A. Miklius and M. Poland, written commun., 2014).

**Figure 38.** Photograph showing a typical view of steady lava lake activity in 2014. The lake mostly extended from wall to wall in the Overlook crater and was about 50 meters below the Overlook crater rim. Spattering occurred in the southeast (SE) sink (right side of lake). Photograph taken from the Halemaʻumaʻu rim at site A4 (location in fig. 2) by Matt Patrick on February 1, 2014. The photograph was taken at dusk and the exposure altered the colors slightly—a more realistic representation is shown in figure 43.

Two small explosions interrupted the steadiness of the summit eruption in 2014. The July 23 explosion occurred after a collapse of the Overlook crater wall near the SE sink, depositing spatter at the Halemaʻumaʻu Overlook and igniting some of the battered wooden fencing. Another collapse near the SE sink produced an explosion on October 19, again throwing juvenile bombs and lapilli around the Halemaʻumaʻu Overlook.

The steady activity at the summit during 2014 was welcomed by HVO staff, who were busy during the second half of the year responding to the ERZ lava flow crisis in the town of Pāhoa (Poland and others, 2016a; Patrick and others, 2017). The June 27 (episode 61e) lava flow started from a new vent at Puʻu ʻŌʻō on that date, and migrated northeast during July through October. In late October, the flow entered the outskirts of the town of Pāhoa. A large deflation episode associated with a DI event at the summit corresponded with the flow front stalling on October 30, presumably caused by a reduction in the lava supply rate, averting major destruction. At the summit, the lava lake dropped 16 m during this deflation episode. A subsequent lobe formed in November and stalled in January 2015 (Poland and others, 2016a; Patrick and others, 2017). The October 30 stalling event and its relation to summit deflation and lava lake level change again highlighted the connection between the summit and ERZ. Given that changes in rate of lava supply to the ERZ commonly occur about one day after the ground tilt changes at the summit (Orr and others, 2015b), this episode was a clear example of how the summit tilt and lava lake can be used to make short-term forecasts of lava flow vigor and associated hazards on the ERZ (Patrick and others, 2015a).

## 2015: Steady Activity Interrupted by Brief Overflows

The activity in the first few months of 2015 was similar to that of 2014 and was relatively steady. The lake was normally 40–60 m below the Overlook crater rim during January–March. Around April 20, however, sharp summit inflation began abruptly (Jo and others, 2015), and the lava lake rose concomitantly (fig. 39). Rates of earthquakes in the upper ERZ increased with the rising lava level, like the pattern observed in 2011 (Patrick and others, 2015a). For the first time during this eruption, the lava lake and its spattering became visible from public viewing areas at Jaggar Museum, and national park visitation rose dramatically.

The lava lake reached the Overlook crater rim early on April 28 and at 21:30 spilled onto the floor of Halemaʻumaʻu for the first time during the eruption. The lake overflowed episodically for the next few days, sending pāhoehoe flows several hundred meters northward and southwestward (fig. 40*A*). During overflow episodes, it was difficult to recognize the lake margin with the naked eye, as the lake surface blended into the overflows. With each overflow, the rim of the Overlook crater was built slightly higher, creating a subtle perched lava lake geometry. Eventually, the Overlook crater rim was built as much as 8 m above the original floor of Halemaʻumaʻu. The overflows ultimately covered 15.1 hectares, about 27 percent of the Halemaʻumaʻu floor (area excludes the lake itself) (figs. 2, 40*B*).

Heating and thermal cracking of the Overlook crater walls were enhanced by the high lava levels, though this was limited to the south wall, the only part that stood above lake level. This heating led to three large collapses of the crater wall in late April and early May, and the resulting explosive events deposited spatter around the Halemaʻumaʻu Overlook (fig. 41). The spatter deposits

**Figure 39.** Photograph of rapidly rising lava lake level in late April 2015. This photograph from April 26 shows the lake just 3 meters below the Overlook crater rim. The lake was sufficiently high that spattering was beginning to form small ramparts along the Overlook crater rim, on the floor of Halemaʻumaʻu. The largest spattering site was near the southeast (SE) sink. Photograph from the Halemaʻumaʻu rim at site A4 (location in fig. 2) by Tim Orr.

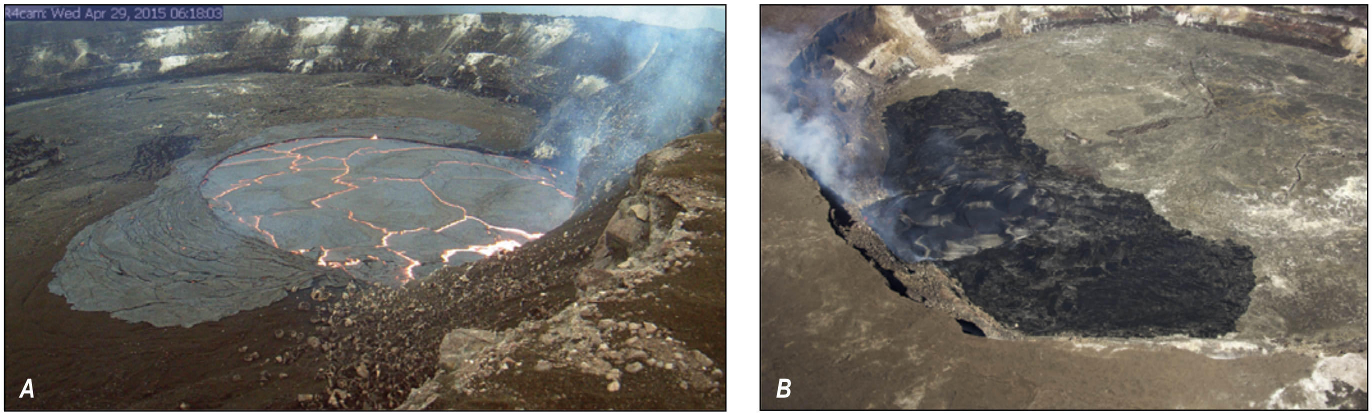


**Figure 40.** Images of lava spilling onto the floor of Halemaʻumaʻu in April–May 2015. *A*, Lava began overflowing the Overlook crater on the evening of April 28, and the next morning lobes of shelly pāhoehoe extended north and southwest from the crater rim. Webcam image from location A4 (fig. 2). *B*, By May 5, 2015, overflows were more extensive. The final area of overflows was about 15.1 hectares, covering 27 percent of the Halemaʻumaʻu floor (area excludes the lake itself). Photograph taken from a helicopter by Tim Orr.

were thicker and more strongly agglutinated than most previous ones because the spattering site was closer to the rim owing to the high lake level.

During this episode of overflows, the dynamics of the lake did not change significantly. As usual, lava upwelled in the north part of the lake and flowed toward the south, where there was often spattering and bubble bursting along the margin. However, the frequency of nonspattering phases (associated with gas pistoning) decreased during the high lava stand of late April and early May. Such a reduction was sometimes observed with other high lava level phases. The reason for less frequent nonspattering periods during high lava stands is unclear.

The high lava level continued until May 9, when sharp deflation accompanied a rapid drop in lava level over the next few days. This deflation was associated with a swarm of small earthquakes and presumed intrusion of magma beneath the south part of the caldera (W. Thelen and A. Miklius, written commun., 2015). Rapid lava level drops were associated with frequent collapses of juvenile veneer from the Overlook crater wall (fig. 42). As the slabs fell, they exposed the light-colored wall rock and provided a clear view of the 8-m-thick buildup of new lava along the rim (fig. 42). At times, these collapses involved parts of the Overlook crater wall behind the veneer, resulting in a slight enlargement of the crater area. By May 16,

**Figure 41.** Image of the May 3, 2015, explosion. A collapse of the south Overlook crater wall impacted the lake, triggering an explosion that deposited spatter on the Halemaʻumaʻu rim. For scale, the Halemaʻumaʻu Crater wall is 85 meters high. Image from a webcam in the Hawaiian Volcano Observatory observation tower, May 3, 2015, at 13:20.

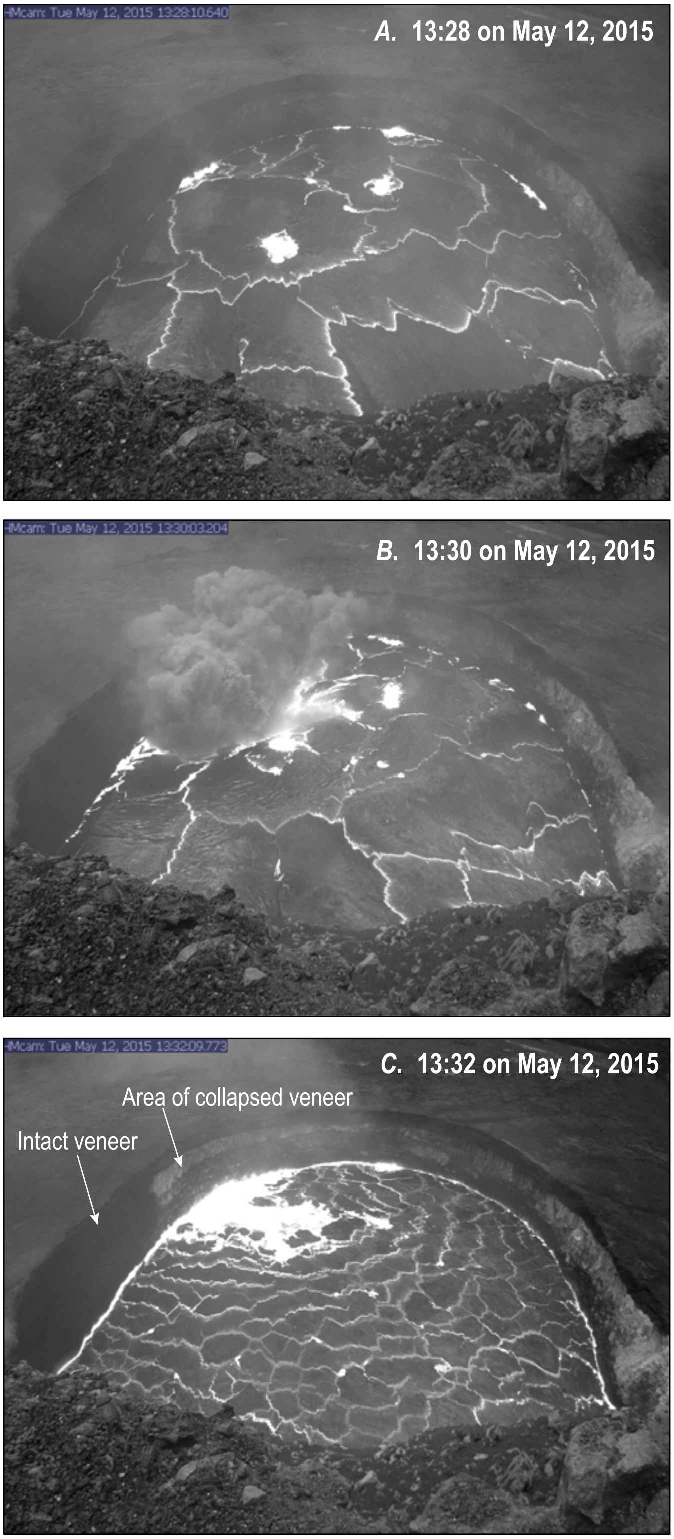


**Figure 42.** Photographs showing lava veneer falling from the Overlook crater wall during the May 2015 drop in lava lake level. Large drops in lake level removed support for lava veneer formed during high stands on the Overlook crater walls, resulting in large slabs of veneer plummeting into the lake. Falling veneer triggered composite seismic events as well as spattering and lake agitation. Images from the HMcam webcam (location in fig. 2) at the Halemaʻumaʻu Overlook on May 12, 2015.

the lake was about 62 m below the new Overlook crater rim (54 m below the former rim), now at 1,031 m a.s.l. This April–May peak in lava level appears to have resulted from a brief pulse in magma supply to the summit reservoir (Swanson and others, 2016).

After this brief overflow period, the lake level gradually declined until late October. A small explosion on July 1 was triggered by collapse of a part of the Overlook crater wall and rim but deposited insignificant tephra outside the crater. Lava level continued to fluctuate during DI events, superimposed on the generally declining lake level trend. Episodic spattering continued as usual, and juvenile veneer spalled from the Overlook crater walls during drops in lake level.

Starting in late October, lake level began to rise. During the final week of 2015, the lake level rose approximately 30 m, and by year's end it had reached a higher elevation than at any other time during the eruption, except for April–May 2015.

## 2016: A Rising, and More Visible, Lava Lake

Lake level remained high during the first months of 2016 (fig. 43), with the level at about 1,000 m a.s.l., or about 30 m below the new Overlook crater rim (1,031 m a.s.l.), by mid-February (Patrick and others, 2018). Spattering remained common (fig. 44). At this high level, spattering could occasionally be seen from HVO and the public overlook at Jaggar Museum, and more tephra (mostly Pele's hair) fell outside Halemaʻumaʻu. Accompanying this high lake level was a reduction in the frequency of nonspattering or weakly spattering (gas piston) periods. For the whole of 2016, gas-piston periods occurred just 4 percent of the time, compared to 20–30 percent during previous years.

By the middle of the year, the lava surface could be frequently seen from HVO and Jaggar Museum, providing improved views for park visitors (Patrick and others, 2018). The high lava levels also provided clearer views of the lake surface and its activity from the Halemaʻumaʻu Overlook, allowing HVO geologists to better document and classify the spattering, surface textures, spreading zones, and crustal plate interactions (Patrick and others, 2018).

In mid-September, a large part of the south ledge collapsed into the lake. The new scarp revealed that the interior of the south ledge was incandescent and semimolten, with glowing rubble occasionally sloughing off the face of the scarp (Patrick and others, 2018). These observations resemble those made of glowing material trickling out from the faces of collapsing ledges in the early 1900s lava lake in Halemaʻumaʻu (Jaggar, 1917).

The lava reached a high level on October 15, when it briefly overflowed parts of the Overlook crater rim, advancing a few tens of meters onto the floor of Halemaʻumaʻu. High lava levels seemed to be the reason for the increase in Pele's hair deposition downwind of Halemaʻumaʻu in 2016, producing a thick (as much as 10 centimeters [cm]) but loose carpet around the Halemaʻumaʻu rim and mats of hair in the parking lot (fig. 45).

**Figure 43.** Photograph showing a typical view of the lava lake in 2016. Spattering is in the southeast (SE) sink. The dark, 8-meter-thick overflows from mid-2015 cap the light-colored older (pre-eruption) flows in the Overlook crater wall. The Hawaiian Volcano Observatory and Jaggar Museum are on the skyline in the upper left. Photograph from the Halemaʻumaʻu rim at site A4 (location in fig. 2) by Tim Orr on January 7, 2016.

**Figure 44.** Photograph showing typical spattering from the southeast (SE) sink. The spattering area is about 30 meters long and is generated by bursting of many large bubbles. For scale, the spatter is ejected to a height of approximately 15 meters above the lake surface. Photograph from the Halemaʻumaʻu rim at site A4 (location in fig. 2) by Matt Patrick on June 27, 2016.

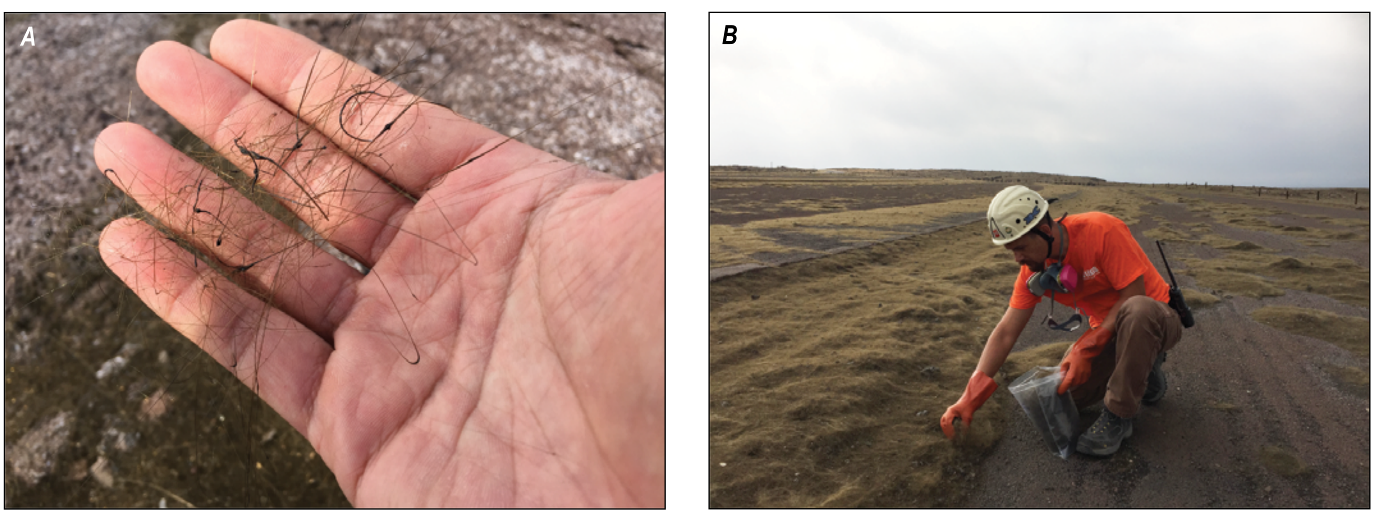


**Figure 45.** Photographs of Pele's hair, which was a common product from spattering in the lava lake in 2016. Accumulation of Pele's hair increased with the high lava lake levels of 2016. *A*, Close-up view of Pele's hair. Small Pele's tears (lava droplets) terminate many of the hairs. *B*, Hawaiian Volcano Observatory (HVO) geologist collecting Pele's hair for geochemical analysis among mats accumulated in the Halemaʻumaʻu parking lot. Photographs by Hannah Guo, HVO volunteer, on November 9, 2016.

On November 29, HVO geologists visited the floor of Halemaʻumaʻu for the first time during the eruption and walked to the north rim of the Overlook crater, collecting samples of the May 2015 and October 2016 overflows. The crater rim had a thin covering of fluid spatter. The overflows consisted of large sheets of shelly pāhoehoe. The shelly crust on these sheet flows was approximately 5–10 cm thick, which may be similar to the thickness of the crust on the lake.

The high lava level during the entire year promoted heating and thermal cracking of the Overlook crater walls, leading to nine explosive events, the most in any year of the eruption. Six of the explosive events occurred between August and December. The high stand of the lake meant that more spatter fell around the Halemaʻumaʻu Overlook than during low stands. On August 6, a section of the Overlook crater rim near the SE sink collapsed, triggering an explosion that deposited spatter along the Halemaʻumaʻu rim. The deposit was continuous and as thick as 20 cm along a 70 m stretch of the crater rim just east of the Halemaʻumaʻu Overlook. Spatter landed on the power system for a gravimeter (Carbone and others, 2013) and melted the plastic case and batteries. Three small explosions deposited sparse spatter at the Halemaʻumaʻu Overlook in September and October, and a larger explosion occurred on November 28. This explosion threw large (>1 m diameter) fluidal spatter bombs around the Halemaʻumaʻu Overlook (fig. 46); some clasts struck the thermal camera. The camera was protected by its plastic case, but bombs landed on the power and ethernet cables, melting through them and causing data interruptions. Another smaller explosive event on December 2 was triggered by a collapse along the south crater wall that deposited spatter around the Halemaʻumaʻu Overlook (Patrick and others, 2018).

The high lava levels also provided improved views of the quasi-periodic bubble bursts in the north part of the lake, which approximately coincided with the zone of lava upwelling (Orr and others, 2014). These bubble bursts were commonly observed in the last few years of the eruption (2015–18) and occurred at least as early as mid-2014. They appeared to be individual decimeter- to meter-sized bubbles or bubble clusters that abruptly burst at the surface, creating a small circular zone of fresh incandescent lava. The location of bubble bursting was relatively stable and coincided with the zone of upwelling; we presume the bursts were triggered by gas bubbles traveling upward from the conduit that feeds into the base of the lake (Orr and others, 2014; Patrick and others, 2016a, 2018). In early 2017, we measured the interval of bubble bursting at this site to be 30–45 seconds, which is close to that of the long-lived “Old Faithful” fountain at Halemaʻumaʻu in the early 1900s (Jaggar, 1947).

The late 2016 lava levels marked an overall high in the long-term trend until that point, disregarding the short-term April–May 2015 peak (fig. 4). A slow decline in lake level ensued after November. The year ended with the lake level varying between approximately 995 and 1,020 m a.s.l., or 10–35 m below the Overlook crater rim.

## 2017: Continued Steady Lake Activity

A slow overall drop in lava level characterized 2017 after the broad peak in lake levels in late 2016. At the start of the year, the lake and its spattering were still frequently visible from HVO and Jaggar Museum (fig. 47), particularly during the short-term rises associated with inflation during DI events. As the year went on, however, views of the lake from HVO and Jaggar Museum became less frequent or were limited to just the top part of spattering sites.

Nevertheless, the lake level remained high enough in 2017 that good visual observations were possible from the Halemaʻumaʻu Overlook (figs. 48, 49). The lake behavior remained similar to that of the previous few years. The surface was composed of large black crustal plates, with a dominant flow from the upwelling zone in the north part of the lake

**Figure 46.** Photograph of a large spatter bomb from the November 28, 2016, explosion. The bomb landed on the trail near the Halemaʻumaʻu Overlook and stretched and flattened upon impact. Photograph by Tim Orr on November 28, 2016.

**Figure 47.** Photograph showing the high lake level in late April 2017. Consistently high lake levels in late 2016 and early 2017 provided good views of the lake and spattering from the public viewing area at Jaggar Museum. Photograph taken from the Hawaiian Volcano Observatory observation tower by Matt Patrick on April 23, 2017.

**Figure 48.** Photograph of a typical view of the lava lake in 2017. Two spatter sites are active. Photograph from the Halemaʻumaʻu Overlook by Matt Patrick on November 18, 2017.

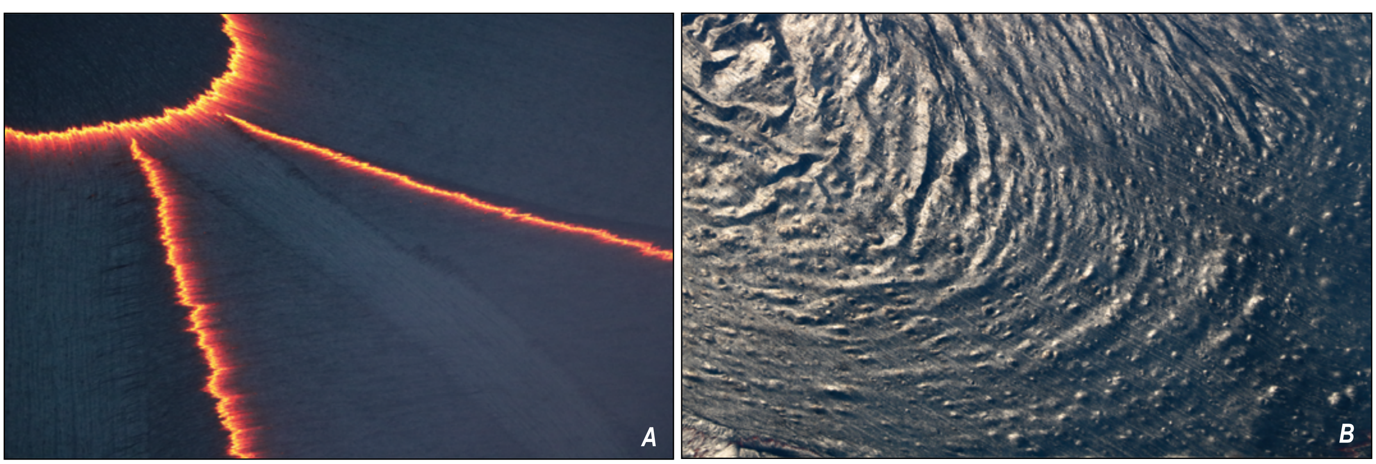


**Figure 49.** Photographs showing lake surface textures made visible by high lava levels in 2017. *A*, Evening view of spreading zones and crustal plate textures. Surface texture can be used to identify the spreading zone where different parts of crustal plates originated, which provides insight into lake surface dynamics (Patrick and others, 2018). The field of view is approximately 50 meters wide. Photograph by Matt Patrick on November 20, 2017. *B*, Daytime view of folds and blisters on the lake surface. Blister formation was abrupt, and presumably represented large bubbles or gas pockets that rose to the surface but failed to burst through the surface crust (Patrick and others, 2018). The field of view is approximately 20 meters wide. Photograph by Matt Patrick on June 4, 2017.

toward the south. Spattering and bubble bursting was still most frequently seen in the SE sink, but also occurred in other parts of the lake, normally at the margins (fig. 48).

## 2018: Historic Changes at Kīlauea's Summit

Activity during the first 3 months of 2018 was like that of 2017. The lake was normally 25–40 m below the Overlook crater rim. Spattering in the lake could occasionally be seen from Jaggar Museum and HVO during high levels associated with inflation during DI events, but the lake was normally out of direct view from public areas. Upwelling persisted in the north part of the lake and the SE sink remained the most common area of spattering. On January 19, a collapse of a part of the south wall of the Overlook crater triggered an explosion that deposited bombs as far as the Halemaʻumaʻu parking lot, with a dispersal range greater than that seen in the explosions of the previous few years.

As the 10-year anniversary of the eruption was marked in mid-March, the lava lake exhibited typical activity (fig. 50). Although the lava level had dropped slightly since the high stand of late 2016, there were otherwise no signs of diminishment in the lake behavior. Normal variations in lava level occurred, involving sporadic spattering and typical gas emission rates.

Inflation at the summit began gradually in mid-March and became prominent by the end of the month. It continued into April, with the rate of inflation increasing toward the end of the month. Shallow earthquakes in the summit and upper ERZ also increased during this period (Flinders and others, 2020), consistent with summit pressurization (Patrick and others, 2015a). The lava level rose with the inflation and the lake overflowed a little onto the Halemaʻumaʻu floor late on April 21, and further small overflows occurred the next day. On April 23, a large overflow covered approximately one-third of the Halemaʻumaʻu floor. Over the next several days, the lake maintained a high level, with numerous episodic overflows. Bubble-bursting and spattering were present along the lake margin, building low, discontinuous ramparts perched above the Halemaʻumaʻu floor. The scattered spattering sites also produced small spatter-fed flows around the lake margin. The largest overflow was on the morning of April 26, when approximately two-thirds of the Halemaʻumaʻu Crater floor was covered in shelly pāhoehoe (fig. 51). Deflation as part of a DI event began on April 27 and the lake dropped 15 m over the next 2 days. However, the lake level rebounded with the inflation part of

**Figure 50.** Photograph of the lava lake on March 19, 2018—the tenth anniversary of the start of the summit eruption. Photograph from approximately 100 meters east of the Halemaʻumaʻu Overlook by Janet Babb, U.S. Geological Survey.

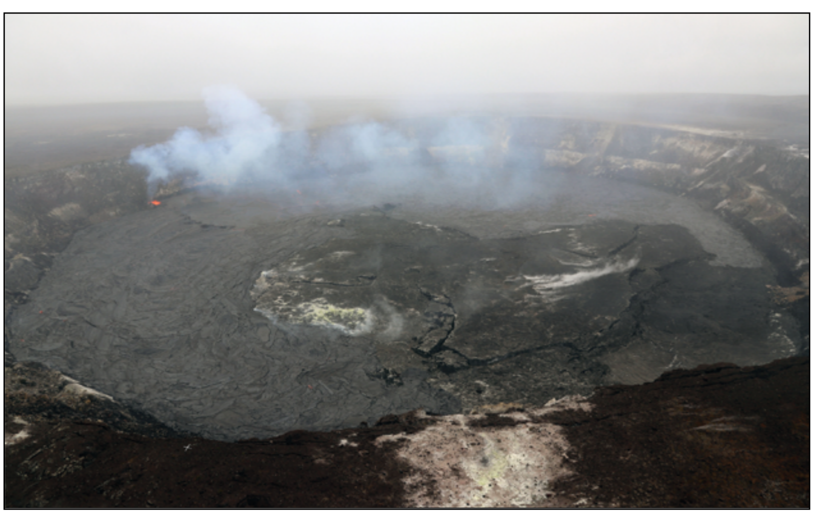

**Figure 51.** Photograph of the lava lake overflowing onto the floor of Halemaʻumaʻu on April 26, 2018. View is from a helicopter looking south across Halemaʻumaʻu. The lava lake and the Overlook crater are at the far left side of the crater. The lake overflows wrap around the slightly higher central floor of Halemaʻumaʻu. Photograph by Carolyn Parcheta.

a DI event starting on April 30; the lake level peaked on May 1 at 5 m below the high stand marked on April 26.

Inflation was also occurring at Pu‘u ‘Ō‘ō during March and April. A small lava lake, which had been active for more than 2 years in the west part of Pu‘u ‘Ō‘ō crater, rose gradually, building a perched lava lake. During March and April, the main crater floor, consisting of solidified lava flows, uplifted in a piston-like manner. Small lava flows were also erupted onto the crater floor, further testament to increasing pressure in the shallow magma system at Pu‘u ‘Ō‘ō. By late April, the crater floor had been uplifted endogenously about 15 m.

This increasing pressure culminated on April 30 in an intrusion from Pu‘u ‘Ō‘ō toward the east, accompanying a small and brief eruption of lava from a fissure on the west flank of the cone. Earthquakes migrated eastward into the lower ERZ over the next few days, indicating the intrusion was extending well beyond the bounds of the Pu‘u ‘Ō‘ō-Kupaianaha eruption area (Neal and others, 2019). Ground cracking appeared near Leilani Estates, in the lower ERZ, on May 2. Just before 17:00 on May 3, lava began erupting from a fissure in Leilani Estates, ushering in a 4-month eruption that covered a large part of lower Puna District with lava flows (Neal and others, 2019).

The reaction at the summit to these dramatic changes on the ERZ involved a significant drop in the lava lake level that appeared to begin on May 1 or 2; there was no obvious immediate reaction of the lake to the April 30 intrusion at Pu‘u ‘Ō‘ō. The precise onset of lake draining on May 1–2 is obscured by the typical short-term variations in lake level. Over the subsequent week, the lake dropped more than 300 m (fig. 52), with frequent collapses of the Overlook crater walls and several small explosive events (fig. 53). At 12:32 on May 4, a moment magnitude 6.9 earthquake occurred on the south flank of Kīlauea near Kalapana (Liu and others, 2018; Neal and others, 2019). Thermal images from the HTcam show apparent brief sloshing of the lake triggered by the earthquake, but no major or lasting changes in lake behavior as a result of the earthquake.

During visits to the Halema‘uma‘u Overlook on May 6 and 7, HVO geologists observed frequent rockfalls, where large slabs of thick veneer adhering to the Overlook crater wall collapsed into the lake. The collapse scars exposed incandescent, rubbly material that indicated the interior of the lava veneer was semimolten (like observations made in September 2016). As the lake level dropped between May 2 and 9, the surface became more agitated and disrupted by bubbling and spattering, perhaps owing to the increasing collapses of the crater wall as the lake level lowered. An explosion at 08:27 on May 9 (fig. 53), the largest magmatic explosion of the eruption, deposited spatter on the power system for the thermal camera (HTcam) and webcam (HMcam) at the Halema‘uma‘u Overlook, terminating their image streams. The lake was last observed during an overflight at 15:30 on May 9 (fig. 54). By 06:10 on May 10, the lake was no longer visible, having drained below the floor of the Overlook crater (fig. 55). Handheld thermal camera images that day showed only rubble near the bottom of the crater. May 9 therefore marks the end of the 2008–18 era of lava lake activity at Kīlauea's summit.

**Figure 52.** Photograph of the lava lake draining in early May 2018. Halema‘uma‘u spans the width of the photograph; Hawaiian Volcano Observatory is on the skyline at the top. The Overlook crater fills the center of the image, with the lake approximately 220 meters below the Halema‘uma‘u floor. Photograph taken by Kyle Anderson, U.S. Geological Survey, on May 6 from the Halema‘uma‘u Overlook using a wide-angle camera, which distorts the view.

**Figure 53.** Photograph of a dark tephra-rich plume rising above Halema‘uma‘u at 08:29 on May 9, caused by a collapse of the Overlook crater wall. The collapse was associated with a small explosion that deposited spatter around the Halema‘uma‘u Overlook. Photograph taken by Gail Ferguson, Hawaiian Volcano Observatory volunteer.

**Figure 54.** Photograph showing the last view of lava in Halema‘uma‘u during the 2008–18 lava lake. Roiling and spattering covers much of the lake surface, which is about 330 meters below the Overlook crater rim. The lake is partly obscured by the thick plume. Photograph taken on May 9, 2018, at 15:43 by Carolyn Parcheta.

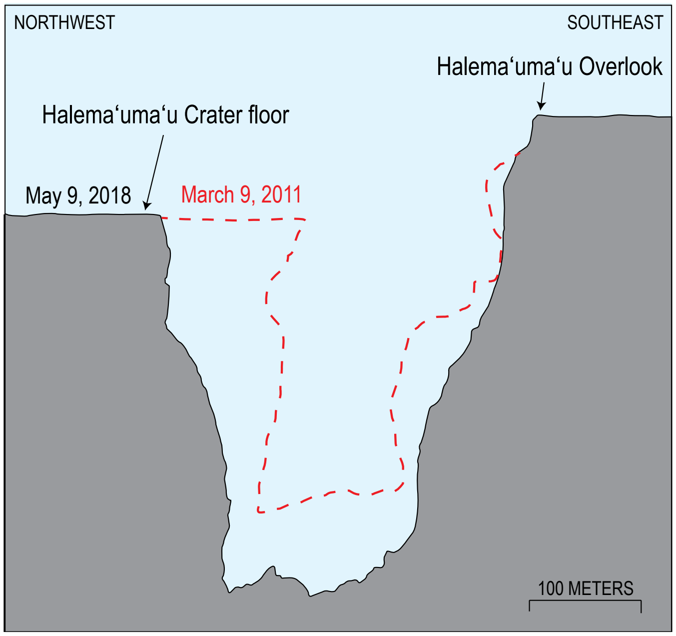


**Figure 55.** Cross section of the Overlook crater in March 2011 (dashed red line) and May 2018 (grey fill), after the lava lake draining events at those times. Figure also published by Patrick and others (2019a).

**Figure 56.** Photograph of Kīlauea’s summit in repose. Note the lack of any discernable gas plume. Photograph taken by Carolyn Parcheta from Volcano House, on the northeast caldera rim, on August 17, 2018.

Over the next 3 months, collapses consumed the Overlook crater and Halema‘uma‘u (Anderson and others, 2019). Several small explosive events occurred in the last half of May. Episodic collapse events through June and July expanded to involve the south part of Kīlauea’s caldera floor (Neal and others, 2019). Major effusion at the lower ERZ eruption abruptly ended on August 4, and the final summit collapse event occurred on August 2 (Neal and others, 2019). As of May 2020, no eruptive activity was present at the summit, Pu‘u ‘Ō‘ō, or the lower ERZ. For the first time in more than 35 years, Kīlauea was in a prolonged repose (fig. 56).

# Notable Aspects of the Eruption

## Conflicting Precursory Signals

Despite improvements in modeling magmatic systems, operational forecasting of volcanic activity still relies heavily on pattern recognition—comparing current activity to that previously exhibited by the volcano (Poland and others, 2016b; Lowenstern and others, 2017; Poland and Anderson, 2020). Kīlauea’s summit eruption was difficult to forecast as its precursory activity had no precedent in Kīlauea’s historical record and differed from those preceding previous summit eruptions. The seismic activity (increase in the rate of small shallow earthquakes beneath Halema‘uma‘u as well as unusually high summit tremor), coupled with the unprecedented $SO_2$ emissions at the summit (Sutton and Elias, 2014), indicated strongly that an eruption might occur. The lack of any change in the ongoing deflation was a strong argument against the arrival of significant volumes of new magma that might fuel a new eruption and placed constraints on the likely magnitude of any such eruption. This argument against an upcoming eruption was bolstered by Kīlauea’s own record—every summit eruption since at least 1954 was preceded by summit inflation (Wright and Klein, 2014).

HVO staff debated the meaning of the seismic tremor and $SO_2$ emission rate increases during the precursory period, as part of developing a hazard assessment for Hawai‘i Volcanoes National Park. Discussions focused on disruption to the hydrothermal system around Halema‘uma‘u, which could explain the seismicity and lack of deformation but was hard to reconcile with the high $SO_2$ emission rates that suggested outgassing of new magma. Overall, the expectation among staff for the occurrence of explosive activity was low, though several staff members did highlight the possibility of a small-scale phreatic explosion owing to the restive state of the hydrothermal system. Ultimately, the forecasting accuracy was hampered because there is no historical record, to our knowledge, of any large fumarolic area suddenly appearing at the summit, or any previous summit eruption occurring in the modern record in the absence of associated ground deformation.

## What Triggered the Summit Eruption?

The driving forces that triggered summit activity remain unclear, but it is likely that the onset of the summit eruption was related in some manner to the surge in magma supply that occurred from 2003 to 2007 (Poland and others, 2012). The surge drove summit inflation in this period that may have primed the shallow reservoir, allowing magma to rise and become poised for subsequent eruption. But why was there an absence of precursory inflation in the weeks to months before the eruption, as occurred in earlier summit eruptions? Long-term gravity surveys indicate net mass accumulation at the summit following the 1975 Kalapana earthquake, despite long-term deflation, which Johnson and others (2010) interpret as magma filling preexisting voids at the summit. It is possible that the terminal stages of the buildup to the summit eruption in late 2007 may have involved the cryptic rise of magma into shallow voids, or the widening and interconnection of existing voids, that created an open pathway for the magma to the surface, driving outgassing. The rapid deflation triggered after the opening of new ERZ vents on July 21, 2007, may also have played a role. The deflation may have enhanced outgassing of shallow magma poised beneath Halema‘uma‘u either through static decompression of the magma reservoir (Poland and others, 2009) or the opening of pathways between the shallow storage region and the surface. The presence of the 35-m-wide crater on March 19, 2008, revealed when its roof collapsed, is evidence for the development of large voids before the eruption began (see next section).

## Birth of a Crater and Lava Lake

Although pit craters are common features on volcanoes, crater formation and evolution have rarely been observed in detail (Okubo and Martel, 1998). We think it likely that a large void existed beneath the spot where the Overlook crater formed because the volume of ejecta on March 19, 2008, is very small relative to the volume of the crater after the explosion. We interpret the crater to have formed from collapse of the roof into that void (Swanson and others, 2009; Houghton and others, 2011). Lidar scans in 2009 showed that the north wall of the crater had a remarkable overhang (80 m), and rockfalls from the overhang were a common part of crater enlargement. This overhang was maintained in part through thermal cracking of the lower crater walls just above the lava surface, as best observed in February and March 2011 (Orr and others, 2013). Thermal erosion enhanced the overhang of the uppermost crater walls, removing support and enabling large collapses of the rim. In this manner, we observed directly that a process similar to magmatic stoping (Daly, 1903) was a major part of crater enlargement (Orr and others, 2013). Magmatic stoping in an intrusive scenario, however, would nevertheless have significant differences with the surface process observed here. For instance, in the Overlook crater there was a significant gap between the lava and collapsing wall rock, whereas such a gap would presumably not be present in an intrusive scenario under significant lithostatic pressure.

The development of the void prior to the Overlook vent opening remains puzzling. How could such a large, shallow feature develop without surface indications? Why was a gas plume only visible in the final week before roof collapse and vent opening? Where did the rock go that originally filled the void?

The formation of lava lakes is also rarely observed (Coppola and others, 2016; Aiuppa and others, 2018). At Halema‘uma‘u, we observed that the formation of the lake was closely tied to ground deformation and the pressure state of the summit magma reservoir, as this controlled the height of the lava column (Patrick and others, 2015a). The sporadic lava lake activity of 2009 was a function of the rise and fall of the lava column during DI cycles, where the lake appeared at inflation peaks and dropped and crusted over during deflation. Overall, we observed that the establishment of the lake was erratic, and its persistence seems to be tied to magma reservoir pressure, which in turn may be influenced by the ERZ as well as by magma supply rate (Patrick and others, 2019b).

## Hydraulic Connection to the East Rift Zone

The summit eruption in Halema‘uma‘u occurred during the Pu‘u ‘Ō‘ō eruption (1983 to 2018) on Kīlauea's ERZ (Heliker and Mattox, 2003; Orr and others, 2015a). This period marks the first time in the written historical record (since the early 1800s) of long-term (>1 year) concurrent summit and rift zone eruptions (Patrick and others, 2019b). Previous simultaneous summit and rift zone eruptions have occurred, but the overlap has normally been brief. Before the recent summit eruption, the longest measured concurrent period was 8 months, during the 1919–20 Mauna Iki eruption on the Southwest Rift Zone (Jaggar, 1947; Rowland and Munro, 1993).

These long-term coeval events provide a new opportunity to understand the hydraulic connection between the summit and ERZ. A subsurface connection between the summit and rift zones (flanks) was recognized by Hawaiians and western visitors in the early 1800s, based on the close timing of events in these locations (Bishop, 1827), and has been an integral part of volcanologic research at Kīlauea ever since (Eaton and Murata, 1960; Poland and others, 2014). More recent studies have added further evidence for a close connection between the summit and ERZ (Tilling, 1987). For example, DI events at the summit were often mirrored, with an apparent delay, at Puʻu ʻŌʻō (Cervelli and Miklius, 2003).

The 2008–18 summit lava lake provided improved constraints and further evidence of the link between the summit and ERZ. One of the clearest indicators of an efficient fluid connection between the summit and Puʻu ʻŌʻō is the similarity in lava chemistry. Lava samples from each eruption site show identical trace element geochemistry, indicating a shared magma source and efficient transport of magma between the summit and ERZ (Rowe and others, 2015; Thornber and others, 2015).

As further evidence, lava lake levels were closely coupled at the summit and Puʻu ʻŌʻō, mimicking the mirrored DI events at the summit and Puʻu ʻŌʻō recognized by Cervelli and Miklius (2003). Despite being 20 km apart, the lava lake level at the summit was normally a mere 100–150 m higher than that at Puʻu ʻŌʻō (Patrick and others, 2019b). Recent activity has shown that changes originating at the ERZ vent had the ability to influence summit behavior, demonstrating that the hydraulic connection is a two-way street (Patrick and others, 2019b). Magma flows from the summit to the ERZ, but the sustained fluid connection and fully engorged conduit allowed ERZ processes to regulate summit activity upstream. Summit fluctuations in tilt and lava level also correlated with, and shortly preceded, variations in lava flow vigor on the ERZ (Orr and others, 2015b; Patrick and others, 2015a, 2017; Poland and others, 2016a), providing a clear empirical tool for lava flow hazard forecasting.

## Shifting Dominance of Summit and East Rift Zone Outgassing

A remarkable aspect of the summit eruption was the accompanying change in gas emissions from the Puʻu ʻŌʻō eruption on the ERZ. Prior to the summit eruption, the Puʻu ʻŌʻō eruption produced $SO_2$ emissions typically of 1,000–3,000 t/d and the summit area emitted a small fraction of this, 180 t/d on average (Elias and Sutton, 2012; Sutton and Elias, 2014). When the summit activity began in 2008, summit $SO_2$ emissions had already jumped to more than 1,000 t/d (Sutton and Elias, 2014). An unsteady drop in $SO_2$ emissions at Puʻu ʻŌʻō began in 2009, with emission rates of just several hundred metric tons per day after 2010. Sutton and Elias (2014) and Sutton and others (2015) attribute the drop in $SO_2$ emissions at Puʻu ʻŌʻō to enhanced outgassing of magma at the summit, which subsequently reached Puʻu ʻŌʻō carrying less gas than it had at the summit. As both the summit and ERZ eruptions were jointly fed by the summit magma reservoir complex (Poland and others, 2014), outgassing at the summit had the potential to deplete the volatile content of magma being fed to Puʻu ʻŌʻō. It is not yet known how this large reduction in gas content affected the transport efficiency of magma to the ERZ, or the rheology of lava erupted at Puʻu ʻŌʻō.

## Lava Lake Piezometer

The Overlook crater lava lake presented the first opportunity to show conclusively the direct relation between magma reservoir pressure and lava lake level. Previous studies, such as by Tilling (1987) and Denlinger (1997), provided evidence to suggest that the lava level in open vents was related to pressure in the magmatic system. The recent eruption included a lake with a direct connection to the summit magma reservoir, providing a robust comparison. Halemaʻumaʻu's lava lake level had a strong linear correlation with summit ground tilt, indicating that the lava lake could be used as a liquid pressure gauge, or piezometer, of the summit magma reservoir (fig. 34; Anderson and others, 2015; Patrick and others, 2015a, 2019a; Poland and Carbone, 2016). Changes in summit pressure were directly related to the magma supply rate to the ERZ and its lava flows, providing a hazard forecasting tool. This relation between lava level and reservoir pressure has relevance for other open-vent volcanoes. Both Nyiragongo (Democratic Republic of the Congo) and Stromboli (Italy) experienced flank eruptions that were preceded by unusually high levels of lava in their summit craters (Tazieff, 1977; Calvari and others, 2005, 2010), indicating that high summit lava levels might be a common, perhaps universal, sign of increased flank hazard.

## Rockfall-Triggered Explosions and Top-Down Seismicity

The process driving the explosive events during the 2008–18 summit lava lake was initially debated, but Orr and others (2013) used webcam video and direct observations to show conclusively that the explosions were triggered by rockfalls from the Overlook crater walls impacting the lake. Other data suggest that the lake had a high bulk vesicularity (Carbone and others, 2013), and rockfalls into the lake might trigger a rapid release of gas stored in the lake. Also, the rockfalls may trigger nucleation and the rapid formation of new bubbles in the lake (Carey and others, 2012). The forces propelling spatter out of the lake may include this violent outgassing but may also involve the splashing process of a Worthington jet, representing the rebound of fluid after an impact (Orr and others, 2013). The recognition of this process provides a new mechanism for small explosive events at open-vent basaltic volcanoes.

Very-long-period (VLP) seismic signals were associated with all the explosions at Halemaʻumaʻu. At Stromboli, VLP signals have been explained using a bottom-up model, whereby large gas slugs ascend the conduit and trigger VLP signals at a conduit flare, then subsequently rise to burst on the surface and drive an explosion (James and others, 2006). At Halemaʻumaʻu, the origin of the VLP signal is quite deep, about 1 km (Dawson and others, 2010). Reconciling the timing of the explosions and VLP signals indicates that this bottom-up model cannot apply to these events; Patrick and others (2011) present a top-down conceptual model whereby the explosion at the top of the lava column (shown to be triggered by rockfalls by Orr and others [2013]) creates pressure changes that are transmitted down the lava column and couple with the surrounding rock at a depth of 1 km. A quantitative model of deep VLP signal generation via surficial rockfalls is presented by Chouet and Dawson (2013). VLP signals have also occurred in the absence of rockfall-triggered explosions; Dawson and Chouet (2014) present a review of VLP signal types and characteristics.

## A Foamy Lava Lake and Shallowly Driven Gas Pistoning

Gravity studies show that the bulk density of the Halemaʻumaʻu lava lake was much lower than that of dense rock, owing to a high amount of exsolved gas stored in the lake. Carbone and others (2013) estimated a bulk density of approximately 950 kilograms per cubic meter, suggesting that the lake, or parts of it, might be much like a foam. A foamy texture would be consistent with the high vesicularity of scoria ejected during explosive events and with the mechanism of the explosions themselves (Carey and others, 2012; Eychenne and others, 2015). Rockfalls impacting the lake might allow exsolved gas in the lake to be violently released, triggering an explosion (Orr and others, 2013). That the lake is a large gas repository is also consistent with the shallow origin of gas pistoning inferred for the lake (Patrick and others, 2016b; Poland and Carbone, 2018).

Gas pistoning is a cyclic, gas-driven, rise and fall of the lava lake surface that had been observed many times on Kīlauea prior to the recent summit eruption. Several competing theories existed as to the process driving it, ranging from gas accumulating near the top of the lava column (Swanson and others, 1979), to deep pressure balancing (Whitham and others, 2006), to the deep-seated rise of large gas slugs up the conduit (Vergniolle and Jaupart, 1990; Edmonds and Gerlach, 2007). The recent Halemaʻumaʻu lava lake commonly exhibited gas pistoning, providing a new opportunity to test these differing ideas. Examining the activity in 2010 and later, Patrick and others (2016b) showed that deep-seated drivers, such as gas slugs or deep pressure balancing, were not consistent with multidisciplinary observations, and that gas pistoning appeared to be driven by gas accumulation at or near the top of the lava lake. This gas accumulation might be controlled by the buildup and failure of foam near the lake surface (Orr and Rea, 2012), perhaps driven by evolving permeability and porosity in the lake (Patrick and others, 2016b; Poland and Carbone, 2018).

The gas pistoning and spattering variations that were common during the eruption highlighted the close relation between seismic tremor and outgassing from the lake (Elias and Sutton, 2012; Kern and others, 2015; Nadeau and others, 2015; Patrick and others, 2016b, 2018), similar to that observed at other basaltic volcanoes (Ripepe and others, 1996; Palma and others, 2008; Nadeau and others, 2011). At Halemaʻumaʻu, there was a clear and consistent scaling relation among spattering activity in the lake, $SO_2$ emission rates, and high-frequency (>1 hertz) seismic tremor. Presumably, the increased spattering and bubble bursting on the lake surface represented higher rates of gas release from the lake. At the same time, the spattering, bubble bursting, and lake disturbance created higher seismic tremor (Patrick and others, 2016a,b). The strong correlation may allow seismic tremor to be used as a proxy for gas emission rates during times, such as nighttime hours, when conventional tools for $SO_2$ emission rate measurements are not possible.

## Combining New and Old Monitoring Techniques

The 2008–18 summit eruption of Kīlauea highlighted the effectiveness of several monitoring tools. Thermal cameras were an essential tool for observing the lake activity because of their ability to see through the thick fume that often filled the Overlook crater, particularly during the first few years of the eruption when lava was far below the crater rim (Patrick and others, 2014; Burzynski and others, 2018). For the stationary thermal camera (HTcam; fig. 2), the capability to see through fume provided continuous observation of the crater that would not otherwise have been possible. Using the handheld thermal camera at a steep angle from a circling helicopter allowed us to image the geometry of the overhanging crater walls. The joint analysis of continuous thermal camera and webcam imagery with geophysical data streams, such as broadband seismic data, helped discriminate between competing models that were ambiguous in the geophysical data alone (Patrick and others, 2011, 2016b; Orr and others, 2013). Continuous gravimetry is not common at volcanoes but provided important constraints on the density of the lava in the lake (Carbone and others, 2013; Poland and Carbone, 2018), which is a primary input for modeling lava lake processes. Daily tephra collection, though time consuming, allowed for regular estimates of mass output from the lake and provided material for geochemical tracking of lake activity (Swanson and others, 2009). A hand-held laser rangefinder measured lava level to an accuracy of about 1 m and was especially useful when the lake level was out of view of the thermal camera. Sporadic scans of the Overlook crater and lava lake surface with a tripod-mounted lidar system provided unprecedented detail on the crater geometry and lake surface morphology (Anderson and others, 2014; LeWinter, 2014). Gas emission tracking was improved by using a novel spectrometer array (Horton and others, 2012; Elias and others, 2018), which provided high-rate measurements (every 10 seconds). Given the impact of volcanic air pollution (vog) on the local community, University of Hawaiʻi at Mānoa scientists, in collaboration with HVO, developed on online vog forecasting tool (Businger and others, 2015). Use of high-speed, high-resolution cameras focused on single spattering sites has greatly increased our understanding of the processes and rates of bubble rise and bursting (Gaudin and others, 2016).

In the final year of lake activity, two tools were tested, and one deployed, to provide automated measurements of lava lake level. A radar system developed by University of Cambridge (Peters and others, 2018) was successfully tested, and likely would have been deployed if the lake had persisted. An industrial laser rangefinder was tested by HVO and deployed for continuous measurement in April 2018, just before the lake drained (Patrick and others, 2019c). The continuous laser rangefinder performed well, providing highly precise measurements of lake level.

Unmanned aircraft systems (UAS) were not a part of monitoring the lava lake, limited in large part by regulatory restrictions. Routine helicopter flights allowed HVO geologists to obtain vertical imagery of the lake for structure-from-motion processing, though such views would have been more frequently possible, and less costly, with UAS. UAS probably would have been adopted as a routine tool if the lake had persisted.

Despite the importance of this modern instrumentation, we emphasize the vital role that direct visual observations played in furthering understanding of summit eruption processes during the decade of monitoring from 2008 to 2018. These routine visual and audible observations provided a richer context for unraveling the complex behaviors that occurred in the lake and provided important insights that were simply not available from instrumentation alone. Effectiveness in monitoring the eruption came from combining the decidedly “low-tech” field observations with the “high-tech” imagery and geophysical data, and analyses of lake behavior combined these complementary approaches together (for example, Orr and others, 2013). The daily observations of lake activity were enabled by the close proximity of HVO to the eruption site—which was the original intent of Thomas Jaggar and the founding philosophy of the Hawaiian Volcano Observatory (Tilling and others, 2014).

## Hazards

Hazards local to the Halemaʻumaʻu area included high concentrations of $SO_2$ (>100 parts per million) and the risk of ballistic impacts from blocks and spatter during occasional explosions (Houghton and others, 2013; Orr and others, 2013). The Halemaʻumaʻu area was closed throughout the eruption, however, and these hazards posed no threats to the general public. Scientists who worked in the Halemaʻumaʻu area were required to wear respirators and hard hats to minimize the threat and followed other safety protocols.

The primary hazard to the public was volcanic air pollution (vog) created by continuous gas emissions from the lava lake (Elias and Sutton, 2017). $SO_2$ emission at the summit was approximately 100–300 t/d before the eruption (Elias and others, 1998; Elias and Sutton, 2002, 2007; Sutton and Elias, 2014), and normally 1,000–8,000 t/d during the later years of the eruption (Elias and others, 2018). This increase in $SO_2$ emission, coupled with the location of the new vent, increased vog on the Kaʻū (south) and Kona (west) sides of the island beyond what was common during the previous years of Puʻu ʻŌʻō activity. Although vog is not thought to cause permanent problems, like asthma, in healthy individuals, it is an acute respiratory irritant that can cause significant discomfort to susceptible people (Longo and others, 2010; Longo, 2013; Tam and others, 2016). Individuals with compromised respiratory systems (for example, with asthma or chronic obstructive pulmonary disease) are more seriously affected, as vog can aggravate existing symptoms.

The increase in vog was also detrimental to agriculture and ranching on the Island of Hawaiʻi (Elias and Sutton, 2017). Farmers reported significant damage to sensitive crops, such as cut flowers. Metal infrastructure, such as fencing and gates, which is essential to ranching, experienced increased corrosion.

## Conclusions

Kīlauea’s summit eruption began in March 2008 and evolved into a state of persistent lava lake activity that abruptly ended in May 2018. By 2016, the lake was one of the largest on Earth, slowly enlarging within its growing crater. The lake exhibited highly dynamic activity with common fluctuations in lake level, outgassing rates, and small-scale explosive activity. Its behavior was also closely correlated with the activity on Kīlauea’s East Rift Zone, illustrating an efficient hydraulic connection. The recent activity marks the first time in the written historical record of sustained (>1 year) concurrent eruptions at the summit and along a rift zone, providing a unique opportunity to study Kīlauea’s magmatic system.

Although much has been learned about Halemaʻumaʻu’s lava lake, many questions remain. It is not clear precisely how or where gas accumulated in the lake, and how the presumed foam-like consistency related to lake circulation. Physical analog studies of viscous, convecting, bubble-rich mixtures might provide insight into this question, as would more detailed studies of gas geochemistry. Precise locations of the source of seismic tremor may provide constraints on lake and conduit dynamics. Joint analysis of gas emissions, bubble bursting, and lava level at the summit and Puʻu ʻŌʻō would provide further constraints on the hydraulic connection, a topic which would also benefit from refined modeling. Rockfalls added solid particles to the lake; did they melt, did they sink to the bottom of the lake and accumulate, and do they influence the chemical composition of the lake lava? How did the void form beneath the surface prior to the March 19, 2008, collapse? In terms of hazard, however, the greatest need for future research relates to the unknown impacts of long-term exposure to volcanic air pollution on human health.

The summit eruption could be regarded as having a mixed impact. It provided a windfall of data for scientific research on lava lakes and open-vent basaltic eruptions and served as a venue for such studies for a decade. The lake provided a boost for tourism and an impressive sight for residents. To many, Halemaʻumaʻu’s lava lake was a vivid reminder of the volcanic deity Pele. But the volcanic air pollution was a persistent challenge both for residents and the agriculture and ranching industries. Nevertheless, Island of Hawai‘i residents have shown impressive resilience when faced with the challenges of living on an active volcano.

During 2008–18, Kīlauea’s summit experienced a return to the continuous lava lake activity that characterized much of the 1800s and early 1900s. That early lake was a primary impetus for the founding of the Hawaiian Volcano Observatory in 1912 (Tilling and others, 2014), and it was a fitting coincidence that a lava lake was present again for the 100-year anniversary of the observatory’s beginning. During the decade of recent lava lake activity, scientists, residents, and visitors were granted the uncommon opportunity, as geologist James Dana and others had in the 1800s, to “witness the operations in the vast laboratory” (Dana, 1849).

## References Cited

Aiuppa, A., Maarten de Moor, J., Arellano, S., Coppola, D., Francofonte, V., Galle, B., Giudice, G., Liuzzo, M., Mendoza, E., Saballos, A., Tamburello, G., Battaglia, A., Bitetto, M., Gurrieri, S., Laiolo, M., Mastrolia, A., and Moretti, R., 2018, Tracking the formation of a lava lake from ground and space—Masaya Volcano (Nicaragua), 2014–2017: Geochemistry, Geophysics, Geosystems, v. 19, p. 496–515.

Anderson, K.R., Poland, M.P., Johnson, J., and Miklius, A., 2015, Episodic deflation-inflation events at Kīlauea Volcano and implications for the shallow magma system, *in* Carey, R., Poland, M., Cayol, V., and Weis, D., eds., Hawaiian Volcanism—From Source to Surface: American Geophysical Union Geophysical Monograph 208, p. 229–250.

Anderson, K.R., Johanson, I.A., Patrick, M.R., Gu, M., Segall, P., Poland, M.P., Montgomery-Brown, E.K., and Miklius, A., 2019, Magma reservoir failure and the onset of caldera collapse at Kilauea in 2018: Science, v. 366, no. 6470, 10 p.

Anderson, S.W., LeWinter, A.L., Finnegan, D.C., Patrick, M.R., and Orr, T.R., 2014, Repeat terrestrial LiDAR scanning at Kilauea Volcano reveals basaltic lava lake surface slope, structure and micro-pistoning [abs.]: American Geophysical Union Fall Meeting abstract no. V43A-4851.

Banks, N.G., Wolfe, E.W., Duggan, T.A., Okamura, A.T., Koyanagi, R.Y., Greenland, L.P., and Jackson, D.B., 1983, Magmatic events at Kīlauea Volcano, Hawaii, 1982: EOS Transactions, v. 64, p. 901–902.

Bishop, A., 1827, Journal of Mr. Bishop, while on a tour of Hiro: Missionary Herald, v. 23, p. 48–55.

Brigham, W.T., 1909, The volcanoes of Kilauea and Mauna Loa on the Island of Hawaii—Their variously recorded history to the present time: Honolulu, Hawaii, Bishop Museum Press, Memoirs of the Bernice Pauahi Bishop Museum, v. 2, no. 4, 222 p. plus plates.

Burzynski, A.M., Anderson, S.W., Morrison, K., Patrick, M.R., Orr, T., and Thelen, W., 2018, Lava lake thermal pattern classification using self-organizing maps and relationships to eruption processes at Kilauea Volcano, Hawai‘i, *in* Poland, M.P., Garcia, M.O., Camp, V.F, and Grunder, A., eds., Field Volcanology—A tribute to the distinguished career of Don Swanson: Geological Society of America Special Paper 538, p. 307–324.

Businger, S., Huff, R., Pattantyus, A., Horton, K., Sutton, A.J., Elias, T., and Cherubini, T., 2015, Observing and forecasting vog dispersion from Kīlauea Volcano, Hawaii: Bulletin of the American Meteorological Society, v. 96, p. 1,667–1,686, https://doi.org/10.1175/BAMS-D-14-00150.1.

Calvari, S., Lodato, L., Steffke, A., Cristaldi, A., Harris, A.J.L., Spampinato, L., and Boschi, E., 2010, The 2007 Stromboli eruption—Event chronology and effusion rates using thermal infrared data: Journal of Geophysical Research, v. 115, no. B04201, 20 p., https://doi.org/10.1029/2009JB006478.

Calvari, S., Spampinato, L., Lodato, L., Harris, A.J.L., Patrick, M.R., Dehn, J., Burton, M.R., and Andronico, D., 2005, Chronology and complex volcanic processes during the 2002–2003 flank eruption at Stromboli volcano (Italy) reconstructed from direct observations and surveys with a handheld thermal camera: Journal of Geophysical Research, v. 110, no. B02201, 23 p.

Carbone, D., Poland, M.P., Patrick, M.R., and Orr, T.R., 2013, Continuous gravity measurements reveal a low-density lava lake at Kīlauea Volcano, Hawai‘i: Earth and Planetary Science Letters, v. 376, p. 178–185.

Carey, R.J., Manga, M., Degruyter, W., Swanson, D., Houghton, B., Orr, T., and Patrick, M., 2012, Externally triggered renewed bubble nucleation in basaltic magma—The 12 October 2008 eruption at Halema‘uma‘u Overlook vent, Kīlauea, Hawai‘i, USA: Journal of Geophysical Research, Solid Earth, v. 117, no. B11202, 10 p., https://doi.org/10.1029/2012JB009496.

Carey, R.J., Swavely, L., Swanson, D.A., Houghton, B.F., Orr, T.R., Elias, T., and Sutton, A.J., 2015, Onset of a basaltic explosive eruption from Kīlauea’s summit in 2008, *in* Carey, R.J., Cayol, V., Poland, M., Weis, D., eds., Hawaiian Volcanoes—From Source to Surface: American Geophysical Union Geophysical Monograph 208, p. 421–437.

Cervelli, P.F., and Miklius, A., 2003, The shallow magmatic system of Kīlauea Volcano, *in* Heliker, C., Swanson, D.A., and Takahashi, T.J., eds., The Pu‘u ‘Ō‘ō–Kupaianaha eruption of Kīlauea Volcano, Hawai‘i—The first 20 years: U.S. Geological Survey Professional Paper 1676, p. 149–163.

Chouet, B.A., and Dawson, P.B., 2013, Very long period conduit oscillations induced by rockfalls at Kīlauea Volcano, Hawaii: Journal of Geophysical Research, Solid Earth, v. 118, p. 5,352–5,371, https://doi.org/10.1002/jgrb.50376.

Chouet, B.A., Dawson, P.B., James, M.R., and Lane, S.J., 2010, Seismic source mechanism of degassing bursts at Kīlauea Volcano, Hawaii—Results from waveform inversion in the 10-50 s band: Journal of Geophysical Research, Solid Earth, v. 115, no. B09311, 24 p., https://doi.org/10.1029/2009JB006661.

Clague, D.A., Hagstrum, J.T., Champion, D.E., and Beeson, M.H., 1999, Kīlauea summit overflows—Their ages and distribution in the Puna District, Hawai'i: Bulletin of Volcanology, v. 61, p. 363–381.

Coppola, D., Campion, R., Laiolo, M., Cuoco, E., Balagizi, C., Ripepe, M., Cigolini, C., and Tedesco, D., 2016, Birth of a lava lake—Nyamulagira volcano 2011–2015: Bulletin of Volcanology, v. 78, no. 20, 13 p.

Daly, R.A., 1903, The mechanics of igneous intrusion: American Journal of Science, v. 15, p. 269–298.

Dana, J.D., 1849, Geology, vol. X *of* United States Exploring Expedition 1838–1842: C. Sherman, Philadelphia, 756 p.

Dawson, P.B., Benitez, M.C., Chouet, B.A., Wilson, D., and Okubo, P.G., 2010, Monitoring very-long-period seismicity at Kīlauea Volcano, Hawai'i: Geophysical Research Letters, v. 37, 6 p., https://doi.org/10.1029/2010GL044418.

Dawson, P.B., and Chouet, B., 2014, Characterization of very-long-period seismicity accompanying summit activity at Kilauea Volcano, Hawai`i, 2007–2013: Journal of Volcanology and Geothermal Research, v. 278–279, p. 59–85.

Dawson, P.B., Dietel, C., Chouet, B.A., Honma, K., Ohminato, T., and Okubo, P., 1998, Digitally telemetered broadband seismic network at Kīlauea Volcano, Hawaii: U.S. Geological Survey Open File Report 98-108, 121 p.

Dayton, K., 2008, Volcano park evacuated: Honolulu Advertiser, April 9, 2008, accessed October 3, 2019, at http://the.honoluluadvertiser.com/article/2008/Apr/09/ln/hawaii804090433.html.

Denlinger, R.P., 1997, A dynamic balance between magma supply and eruption rate at Kilauea volcano, Hawaii: Journal of Geophysical Research, v. 102, p. 18,091–18,100.

Draper, J.W., 1847, On the production of light by heat: The London, Edinburgh, and Dublin Philosophical Magazine and Journal of Science, v. XXX, p. 345–359.

Eaton, J.P., and Murata, K.J., 1960, How volcanoes grow: Science, v. 132, no. 3432, p. 925–938.

Edmonds, M., and Gerlach, T.M., 2007, Vapor segregation and loss in basaltic melts: Geology, v. 35, p. 751–754.

Elias, T., and Sutton A.J., 2002, Sulfur dioxide emission rates of Kīlauea Volcano, Hawaii, an update, 1998–2001: U.S. Geological Survey Open-File Report 02-460, 29 p., available at http://pubs.usgs.gov/of/2002/of02-460.

Elias, T., and Sutton, A.J., 2007, Sulfur dioxide emission rates from Kīlauea Volcano, Hawaii, an update, 2002–2006: U.S. Geological Survey Open-File Report 2007-1114, 37 p.

Elias, T., and Sutton, A.J., 2012, Sulfur dioxide emission rates from Kīlauea Volcano, Hawai'i, 2007–2010: U.S. Geological Survey Open-File Report 2012–1107, 25 p., available at http://pubs.usgs.gov/of/2012/1107.

Elias, T., and Sutton, A.J., 2017, Volcanic air pollution hazards in Hawaii: U.S. Geological Survey Fact Sheet 2017-3017, 4 p., https://doi.org/10.3133/fs20173017.

Elias, T., Kern, C., Horton, K.A., Sutton, A.J., and Garbeil, H., 2018, Measuring $SO_2$ emission rates at Kilauea Volcano, Hawaii, using an array of upward-looking UV spectrometers, 2014-2017: Frontiers in Earth Science, v. 6, no. 214, https://doi.org/10.3389/feart.2018.00214.

Elias, T., Kern, C., Sutton, A.J., and Horton, K., 2020, Sulfur dioxide emission rates from Kīlauea Volcano, Hawaii, 2008-2013: U.S. Geological Survey data release, https://doi.org/10.5066/P9K0EZII.

Elias, T., Sutton A.J., Stokes, J.B., and Casadevall, T.J., 1998, Sulfur dioxide emission rates of Kīlauea Volcano, Hawaii, 1979–1997: U.S. Geological Survey Open-File Report 98-462, available at http://pubs.usgs.gov/of/1998/of98-462.

Ellis, W., 1825, Narrative of a tour through Hawaii, or, Owhyhee: H. Fisher, Son, and P. Jackson, London, p. 264. [Simultaneously published in Boston by Crocker & Brewster. Reprinted in 1826 and 1827 in London by Fisher and Jackson; reprinted 1917 by the Hawaiian Gazette Co., Ltd., Honolulu; reprinted 2004 by Mutual Publishing, Honolulu; 1827 London ed. reprinted in 1963 as Journal of William Ellis by the Advertiser Publishing Co., Ltd., Honolulu, 342 p.]

Endo, E.T., and Murray, T., 1991, Real-time seismic amplitude measurement (RSAM)—A volcano monitoring and prediction tool: Bulletin of Volcanology, v. 53, p. 533–545.

Eychenne, J., Houghton, B.F., Swanson, D.A., Carey, R.J., and Swavely, L., 2015, Dynamics of an open basaltic magma system—The 2008 activity of the Halema'uma'u Overlook vent, Kīlauea Caldera: Earth and Planetary Science Letters, v. 409, p. 49–60.

Fee, D., Garces, M., Orr, T.R., and Poland, M.P., 2011, Infrasound from the 2007 fissure eruptions of Kilauea Volcano, Hawai'i: Geophysical Research Letters, v. 38, 5 p., https://doi.org/10.1029/2010GL046422.

Fee, D., Garces, M., Patrick, M., Chouet, B., Dawson, P., and Swanson, D., 2010, Infrasonic harmonic tremor and degassing bursts from Halema'uma'u Crater, Kilauea Volcano, Hawaii: Journal of Geophysical Research, v. 115, no. B11316, 15 p.

Finch, R.H., 1940, Engulfment at Kīlauea Volcano: Volcano Letter, no. 470, p. 1–2.

Flinders, A.F., Caudron, C., Johanson, I.A., Taira, T., Shiro, B., and Haney, M., 2020, Seismic velocity variations associated with the 2018 lower East Rift Zone eruption of Kīlauea, Hawai‘i: Bulletin of Volcanology, v. 82, no. 47, 13 p., https://doi.org/10.1007/s00445-020-01380-w.

Gaudin, D., Taddeucci, J., Houghton, B.F., Orr, T.R., Andronico, D., Del Bello, E., Kueppers, U., Ricci, T., and Scarlato, P., 2016, 3-D high-speed imaging of volcanic bomb trajectory in basaltic explosive eruptions: Geochemistry, Geophysics, Geosystems, v. 17, p. 4,268–4,275.

Guffanti, M., Diefenbach, A.K., Ewert, J.W., Ramsey, D.W., Cervelli, P.F., and Schilling, S.P., 2010, Volcano-monitoring instrumentation in the United States, 2008: U.S. Geological Survey Open-File Report 2009–1165, 32 p. text plus Volcano-Monitoring Instrumentation Database, available at https://pubs.usgs.gov/of/2009/1165.

Heliker, C., and Mattox, T.N., 2003, The first two decades of the Pu‘u ‘Ō‘ō–Kupaianaha eruption—Chronology and selected bibliography, *in* Heliker C., Swanson, D.A., Takahashi, T.J., eds., The Pu‘u ‘Ō‘ō–Kupaianaha eruption of Kīlauea Volcano, Hawai‘i—The first 20 years: U.S. Geological Survey Professional Paper 1676, p. 1–27.

Holcomb, R.T., 1987, Eruptive history and long-term behavior of Kīlauea Volcano, *in* Decker, R.W., Wright, T.L., and Stauffer, P.H., eds., Volcanism in Hawaii: U.S. Geological Survey Professional Paper 1350, p. 261–350.

Horton, K., Garbeil H., Sutton, A.J., Elias, T., and Businger, S., 2012, Early monitoring results from the Halema‘uma‘u vog measurement and prediction FLYSPEC array [abs.]: Extended Abstracts of the American Geophysical Union Chapman Conference [Waikoloa, Hawaii] on Hawaiian Volcanoes—From Source to Surface, p. 48, accessed June 16, 2020, at http://hilo.hawaii.edu/~kenhon/HawaiiChapman/documents/1HawaiiChapmanAbstracts.pdf.

Houghton, B.F., Swanson, D.A., Biass, S., Fagents, S.A., and Orr, T.R., 2017, Partitioning of pyroclasts between ballistic transport and a convective plume—Kīlauea volcano, 19 March 2008: Journal of Geophysical Research, v. 122, p. 3,379–3,391, https://doi.org/10.1002/2017JB014040.

Houghton, B.F., Swanson, D.A., Carey, R.J., Rausch, J., and Sutton, A.J., 2011, Pigeonholing pyroclasts—Insights from the 19 March 2008 explosive eruption of Kīlauea Volcano: Geology, v. 39, p. 263–266, https://doi.org/10.1130/G31509.1.

Houghton, B.F., Swanson, D.A., Raush, J., Carey, R.J., Fagents, S.A., and Orr, T.R., 2013, Pushing the Volcanic Explosivity Index to its limit and beyond—Constraints from exceptionally weak explosive eruptions at Kīlauea in 2008: Geology, v. 41, p. 627–630, https://doi.org/10.1130/G34146.1.

Hsieh, P.A., and Ingebritsen, S.E., 2019, Groundwater Inflow toward a preheated volcanic conduit—Application to the 2018 Eruption at Kīlauea Volcano, Hawai‘i: Journal of Geophysical Research, Solid Earth, v. 124, p. 1,498–1,506.

Jaggar, T.A., 1917, Volcanological investigations at Kilauea: American Journal of Science, ser. 4, v. 44, p. 160–218.

Jaggar, T.A., 1924, May 1924: Monthly Bulletin of the Hawaiian Volcano Observatory, v. 12, no. 5, p. 29–55. [Reprinted in Bevens, D., Takahashi, T.J., and Wright, T.L., eds., 1988, The early serial publications of the Hawaiian Volcano Observatory: Hawaii National Park, Hawaii Natural History Association, v. X, p. 529–560.]

Jaggar, T.A., 1947, Origin and development of craters: Geological Society of America Memoir 21, 508 p.

Jaggar, T.A., and Finch, R.H., 1924, The explosive eruption of Kīlauea in Hawaii, 1924: American Journal of Science, v. 8, p. 353–374.

James, M.R., Lane, S.J., and Chouet, B.A., 2006, Gas slug ascent through changes in conduit diameter—Laboratory insights into a volcano-seismic source process in low-viscosity magmas: Journal of Geophysical Research, v. 111, no. B05201, https://doi.org/10.1029/2005JB003718.

Jo, M-J., Jung, H-P., Won, J-S., 2015, Detecting the source location of recent summit inflation via three-dimensional InSAR observation of Kīlauea Volcano: Remote Sensing, v. 7, p. 14,386–14,402.

Johnson, D.J., Eggers, A.A., Bagnardi, M., Battaglia, M., Poland, M.P., and Miklius, A., 2010, Shallow magma accumulation at Kilauea Volcano, Hawai‘i, revealed by microgravity surveys: Geology, v. 38, p. 1,139–1,142.

Johnson, J.H., and Poland, M.P., 2013, Seismic detection of increased degassing before Kīlauea's 2008 summit explosion: Nature Communications, v. 4, no. 1668, https://doi.org/10.1038/ncomms2703.

Kern, C., Lerner, A.H., Elias, T., Nadeau, P.A., Holland, L., Kelly, P.J., Werner, C., Clor, L.E., and Cappos, M., 2020, Quantifying gas emissions associated with the 2018 rift eruption of Kīlauea Volcano using ground based DOAS measurements: Bulletin of Volcanology, v. 82, no. 55, 24 p., https://doi.org/10.1007/s00445-020-01390-8.

Kern, C., Sutton, J., Elias, T., Lee, L., Kamibayashi, K., Antolik, L., and Werner, C., 2015, An automated $SO_2$ camera system for continuous, real-time monitoring of gas emissions from Kīlauea Volcano's summit Overlook: Journal of Volcanology and Geothermal Research, v. 300, p. 81–94, https://doi.org/10.1016/j.jvolgeores.2014.12.004.

Kinoshita, W.T., Koyanagi, R.Y., Wright, T.L., and Fiske, R.S., 1969, Kīlauea Volcano—The 1967–68 summit eruption: Science, v. 166, p. 459–468.

LeWinter, A.L., 2014, Characterization of the Overlook crater and lava lake of Kīlauea volcano through terrestrial laser scanning: Greeley, Colo., University of Northern Colorado, M.A. thesis, 203 p.

Liu, C., Lay, T., and Xiong, X., 2018, Rupture in the 4 May 2018 Mw 6.9 earthquake seaward of the Kilauea East Rift Zone fissure eruption in Hawaii: Geophysical Research Letters, vol. 45, p. 9,508–9,515, https://doi.org/10.1029/2018GL079349.

Longo, B.M., 2013, Adverse health effects associated with increased activity at Kīlauea Volcano—A repeated population-based survey: International Scholarly Research Notices, v. 2013, 10 p., http://dx.doi.org/10.1155/2013/475962.

Longo, B.M., Yang, W., Green, J.B., Crosby, F.L., and Crosby, V.L., 2010, Acute health effects associated with exposure to volcanic air pollution (vog) from increased activity at Kīlauea Volcano in 2008: Journal of Toxicology and Environmental Health, Part A, v. 73, , no. 20, p. 1,370–1,381, https://doi.org/10.1080/15287394.2010.497440.

Lowenstern, J.B., Sisson, T.W., and Hurwitz, S., 2017, Probing magma reservoirs to improve volcano forecasts: Eos, v. 98, https://doi.org/10.1029/2017EO085189.

Mastin, L.G., 1997, Evidence for water influx from a caldera lake during the explosive hydromagmatic eruption of 1790, Kīlauea volcano, Hawaii: Journal of Geophysical Research, v. 102, no. B9, p. 20,093–20,109.

McPhie, J., Walker, G.P.L., and Christiansen, R.L., 1990, Phreatomagmatic and phreatic fall and surge deposits from explosions at Kīlauea volcano, Hawaii, 1790 A.D.—Keanakakoi Ash Member: Bulletin of Volcanology, v. 52, p. 334–354.

Miklius, A., Cervelli, C., Sako, M., Lisowski, M., Owen, S., Segal, P., Foster, J., Kamibayashi, K., and Brooks, B., 2005, Global Positioning System measurements on the Island of Hawai‘i—1997 through 2004: U.S. Geological Open File Report 2005-1425, 48 p.

Nadeau, P.A., Palma, J.L., and Waite, G.P., 2011, Linking volcanic tremor, degassing and eruption dynamics via $SO_2$ imaging: Geophysical Research Letters, v. 38, no. L01304, http://dx.doi.org/10.1029/2010GL045820.

Nadeau, P.A., Werner, C.A., Waite, G.P., Carn, S.A., Brewer, I.D., Elias, T., Sutton, A.J., and Kern, C., 2015, Using $SO_2$ camera imagery and seismicity to examine degassing and gas accumulation at Kīlauea Volcano, May 2010: Journal of Volcanology and Geothermal Research, v. 300, p. 70–80, https://doi.org/10.1016/j.jvolgeores.2014.12.005.

Neal, C.A., Brantley, S.R,, Antolik, L., Babb, J., Burgess, M., Calles, K., Cappos, M., Chang, J.C., Conway, S., Desmither, L., Dotray, P., Elias, T., Fukunaga, P., Fuke, S., Johanson, I.A., Kamibayashi, K., Kauahikaua, J., Lee, R.L., Pekalib, S., Miklius, A., Million, W., Moniz, C.J., Nadeau, P.A., Okubo, P., Parcheta, C., Patrick, M.R., Shiro, B., Swanson, D.A., Tollett, W., Trusdell, F., Younger, E.F., Zoeller, M.H., Montgomery-Brown, E.K., Anderson, K.R., Poland, M.P., Ball, J., Bard, J., Coombs, M., Dietterich, H.R., Kern, C., Thelen, W.A., Cervelli, P.F., Orr, T., Houghton, B.F., Gansecki, C., Hazlett, R., Lundgren, P., Diefenbach, A.K., Lerner, A.H., Waite, G., Kelly, P., Clor, L., Werner, C., Mulliken, K., and Fisher, G., 2019, The 2018 rift eruption and summit collapse of Kilauea Volcano: Science, v. 363, no. 6425, p. 367–374, https://doi.org/10.1126/science.aav7046.

Okubo, C.H., and Martel, S.J., 1998, Pit crater formation on Kilauea Volcano, Hawaii: Journal of Volcanology and Geothermal Research, v. 86, p. 1–18.

Okubo, P.G., Nakata, J.S., and Koyanagi, R.Y., 2014, The evolution of seismic monitoring systems at the Hawaiian Volcano Observatory, *in* Poland, M.P., Takahashi, T.J., and Landowski, C.M., eds., Characteristics of Hawaiian Volcanoes: U.S. Geological Survey Professional Paper 1801, p. 67–94.

Orr, T., Bleacher, J., Patrick, M., and Wooten, K., 2015b, A sinuous elongate tumulus over an active lava tube at Kīlauea Volcano—Evolution, analogs, and hazard forecasts: Journal of Volcanology and Geothermal Research, v. 291, p. 35–48.

Orr, T.R., Houghton, B.F., Taddeucci, F., Del Bello, E., Scarlato, P., and Patrick, M.R., 2014, The bubble's wake—Localized rebound of Kilauea's summit lava lake following minor bubble bursts [abs.]: American Geophysical Union Fall Meeting abstract no. V41D-05.

Orr, T.R., Poland, M.P., Patrick, M.R., Thelen, W.A., Sutton, J., Elias, T., Thornber, C.T., Parcheta, C., and Wooten, K.M., 2015a, Kīlauea's 5–9 March 2011 Kamoamoa fissure eruption and its relation to 30+ years of activity from Pu‘u ‘Ō‘ō, *in* Carey, R., Poland, M., Cayol, V., and Weis, D., eds, Hawaiian Volcanism—From Source to Surface: American Geophysical Union Geophysical Monograph 208, 28 p.

Orr, T.R., and Rea, J.C., 2012, Time-lapse camera observations of gas piston activity at Pu‘u ‘Ō‘ō, Kīlauea volcano, Hawai‘i: Bulletin of Volcanology, v. 74, p. 2,353–2,362.

Orr, T.R., Thelen, W.A., Patrick, M.R., Swanson, D.A., and Wilson, D.C., 2013, Explosive eruptions triggered by rockfalls at Kīlauea Volcano, Hawai‘i: Geology, v. 41, p. 207–210, https://doi.org/10.1130/G33564.1.

Palma, J.L., Calder, E.S., Basualto, D., Blake, S., and Rothery, D., 2008, Correlations between $SO_2$ flux, seismicity and outgassing activity at the open vent of Villarrica volcano, Chile: Journal of Geophysical Research, v. 113, no. B10201, 23 p.

Patrick, M.R., Anderson, K.R., Poland, M.P., Orr, T., and Swanson, D., 2015a, Lava lake level as a gauge of magma reservoir pressure and eruptive hazard: Geology, v. 43, p. 831–834, https://doi.org/10.1130/G36896.1.

Patrick, M.R., Kauahikaua, J., Orr, T., Davies, A., and Ramsey, M., 2015b, Operational thermal remote sensing and lava flow monitoring at the Hawaiian Volcano Observatory, *in* Harris, A.J.L., De Groeve, T., Garel, F., and Carn, S.A., eds., Detecting, Modelling and Responding to Effusive Eruptions: Geological Society of London Special Publications, v. 426, p. 489–503.

Patrick, M.R., Orr, T., Anderson, K., Swanson, D.A., 2019b, Eruptions in sync—Improved constraints on Kīlauea Volcano’s hydraulic connection: Earth and Planetary Science Letters, v. 507, p. 60–61.

Patrick, M.R., Orr, T., Fisher, G., Trusdell, F., and Kauahikaua, J., 2017, Thermal mapping of a pāhoehoe lava flow, Kīlauea Volcano: Journal of Volcanology and Geothermal Research, v. 332, p. 71–87, https://doi.org/10.1016/j.jvolgeores.2016.12.007.

Patrick, M.R., Orr, T., Lee, L., Antolik, L., and Kamibayashi, K., 2014, Continuous monitoring of Hawaiian volcanoes with thermal cameras: Journal of Applied Volcanology, v. 3, no. 1, https://doi.org/10.1186/2191-5040-3-1.

Patrick, M.R., Orr, T., Lee, L., and Moniz, C., 2015c, A multipurpose camera system for monitoring Kilauea Volcano, Hawai‘i: U.S. Geological Survey Techniques and Methods, book 13, chap. A2, 25 p., https://doi.org/10.3133/tm13A2.

Patrick, M.R., Orr, T., Sutton, A.J., Lev, E., and Fee, D., 2016b, Shallowly driven fluctuations in lava lake outgassing (gas pistoning), Kīlauea Volcano, Hawai‘i: Earth and Planetary Science Letters, v. 433, p. 326–338, https://doi.org/10.1016/j.epsl.2015.10.052.

Patrick, M.R., Orr, T.R., Swanson, D.A., Elias, T., and Shiro, B., 2018, Lava lake activity at the summit of Kīlauea Volcano in 2016: U.S. Geological Survey Scientific Investigations Report 2018–5008, 58 p., https://doi.org/10.3133/sir20185008.

Patrick, M.R., Orr, T., Swanson, D.A., and Lev, E., 2016a, Shallow and deep controls on lava lake surface motion at Kīlauea Volcano: Journal of Volcanology and Geothermal Research, v. 328, p. 247–261, https://doi.org/10.1016/j.jvolgeores.2016.11.010.

Patrick, M.R., Swanson, D.A., and Orr, T., 2019a, A review of controls on lava lake level—Insights from Halema‘uma‘u Crater, Kilauea Volcano: Bulletin of Volcanology, v. 81, 26 p.

Patrick, M.R., Wilson, D., Fee, D., Orr, T., and Swanson, D., 2011, Shallow degassing events as a trigger for very-long-period seismicity at Kīlauea Volcano, Hawai‘i: Bulletin of Volcanology, v. 73, p. 1,179–1,186, https://doi.org/10.1007/s00445-011-0475-y.

Patrick, M.R., Wilson, D., Fee, D., Orr, T., Swanson, D., Sutton, A., and Elias, T., 2008, Gas-pistoning associated with the 2008 summit eruption of Kīlauea Volcano, Hawai‘i [abs.]: Eos Transactions, v. 89, no. 53, American Geophysical Union Fall Meeting Supplement abstract no. V51E-2082.

Patrick, M.R., Younger, E.F., and Tollett, W., 2019c, Lava level and crater geometry data during the 2018 lava lake draining at Kilauea Volcano, Hawaii: U.S. Geological Survey data release, https://doi.org/10.5066/P9MJY24N.

Perret, F.A., 1913a, The lava fountains of Kīlauea: American Journal of Science, ser. 4, v. 35, p. 139–148.

Perret, F.A., 1913b, The circulatory system in the Halemaumau lake during the summer of 1911: American Journal of Science, ser. 4, v. 35, p. 337–349.

Peters, N.J., Oppenheimer, C., Brennan, P., Lokk, L.B., Ash, M., and Kyle, P., 2018, Radar altimetry as a robust tool for monitoring the active lava lake at Erebus Volcano, Antarctica: Geophysical Research Letters, v. 45, p. 8,897–8,904, https://doi.org/10.1029/2018GL079177.

Poland, M.P., 2014, Time-averaged discharge rate of subaerial lava at Kīlauea Volcano, Hawai‘i, measured from TanDEM-X interferometry—Implications for magma supply and storage during 2011–2013: Journal of Geophysical Research, v. 119, p. 5,464–5,481.

Poland, M.P., and Anderson, K.R., 2020, Partly cloudy with a chance of lava flows—Forecasting volcanic eruptions in the twenty-first century: Journal of Geophysical Research Solid Earth, v. 125, 32 p.

Poland, M.P., and Carbone, D., 2016, Insights into shallow magmatic processes at Kīlauea Volcano, Hawai‘i, from a multiyear continuous gravity time series: Journal of Geophysical Research, v. 121, p. 5,477–5,492, https://doi.org/10.1002/2016JB013057.

Poland, M.P., and Carbone, D., 2018, Continuous gravity and tilt reveal anomalous pressure and density changes associated with gas pistoning within the summit lava lake of Kīlauea Volcano, Hawai‘i: Geophysical Research Letters, v. 45, p. 2,319–2,327, https://doi.org/10.1002/2017GL076936.

Poland, M.P., Miklius, A., and Montgomery-Brown, E.K., 2014, Magma supply, storage and transport at shield-stage Hawaiian volcanoes, *in* Poland, M.P., Takahashi, T.J., and Landowski, C.M., eds., Characteristics of Hawaiian Volcanoes: U.S. Geological Survey Professional Paper 1801, p. 179–234.

Poland, M.P., Miklius, A., Orr, T., Sutton, J., Thornber, C., and Wilson, D., 2008, New episodes of volcanism at Kīlauea Volcano, Hawaii: Eos, v. 89, p. 37–48.

Poland, M.P., Miklius, A.M., Sutton, A.J., and Thornber, C.R., 2012, A mantle-driven surge in magma supply to Kīlauea Volcano during 2003-2007: Nature Geoscience, v. 5, p. 295–300, https://doi.org/10.1038/ngeo1426.

Poland, M.P., Orr, T.R., Kauahikaua, J.P., Brantley, S.R., Babb, J.L., Patrick, M.R., Neal, C.A., Anderson, K.R., Antolik, L., Burgess, M., Elias, T., Fuke, S., Fukunaga, P., Johanson, I.A., Kagimoto, M., Kamibayashi, K., Lee, L., Miklius, A., Million, W., Moniz, C., Okubo, P.G., Sutton, A.J., Takahashi, T.J., Thelen, W.A., Tollett, W., and Trusdell, F.A., 2016a, The 2014–2015 Pāhoa lava flow crisis at Kīlauea Volcano, Hawaiʻi—Disaster avoided and lessons learned: Geological Society of America Today, v. 26, p. 4–10.

Poland, M.P., Pritchard, M.E., Anderson, K.R., Furtney, M., and Carn, S.A., 2016b, Monitoring and modeling—The future of volcanic eruption forecasting [abs.]: American Geophysical Union Fall Meeting abstract no. NH44A-01.

Poland, M.P., Sutton, A.J., and Gerlach, T.M., 2009, Magma degassing triggered by static decompression at Kīlauea Volcano, Hawaiʻi: Geophysical Research Letters, v. 36, https://doi.org/10.1029/2009GL039214.

Ripepe, M., Poggi, P., Braun, T., and Gordeev, E., 1996, Infrasonic waves and volcanic tremor at Stromboli: Geophysical Research Letters, v. 23, p. 181–184.

Rowe, M.C., Thornber, C.R., and Orr, T.R., 2015, Primitive components, crustal assimilation, and magmatic degassing during the early 2008 Kīlauea summit eruptive activity, *in* Carey, R.J., Cayol, V., Poland, M., and Weis, D., eds., Hawaiian Volcanoes—From Source to Surface: American Geophysical Union Geophysical Monograph 208, p. 439–455.

Rowland, S., and Munro, D.C., 1993, The 1919–1920 eruption of Mauna Iki, Kīlauea—Chronology, geologic mapping and magma transport mechanisms: Bulletin of Volcanology, v. 55, p. 190–203.

Spampinato, L., Oppenheimer, C., Cannata, A., Montalto, P., Salerno, G.G., and Calvari, S., 2012, On the time-scale of thermal cycles associated with open-vent degassing: Bulletin of Volcanology, v. 74, p. 1,281–1,292.

Sur, P., 2011, Lava on the rise at Kilauea: Hawaii Tribune Herald, February 13, 2011.

Sutton, A.J., and Elias, T., 2014, One hundred volatile years of volcanic gas studies at the Hawaiian Volcano Observatory, *in* Poland, M.P., Takahashi, T.J., and Landowski, C.M., eds., Characteristics of Hawaiian Volcanoes: U.S. Geological Survey Professional Paper 1801, p. 295–320.

Sutton, A.J., Elias, T., and Kauahikaua, J., 2003, Lava effusion rates for the Puʻu ʻŌʻō–Kupaianaha eruption derived from $SO_2$ emissions and Very Low Frequency (VLF) measurements, *in* Heliker, C., Swanson, D.A., and Takahashi, T.J., eds., The Puʻu ʻŌʻō-Kūpaianaha Eruption of Kīlauea Volcano, Hawaiʻi—The First 20 Years: U.S. Geological Survey Professional Paper 1676, p. 137–148.

Sutton, A.J., Elias, T., Orr, T., Patrick, M.R., Poland, M.P., and Thornber, C., 2015, Is Kīlauea's East Rift Zone eruption running out of gas? [abs.]: American Geophysical Union Fall Meeting abstract no. V31B-3025.

Swanson, D.A., 2008, Hawaiian oral tradition describes 400 years of volcanic activity at Kīlauea: Journal of Volcanology and Geothermal Research, v. 176, p. 427–431.

Swanson, D.A., Duffield, W.A., Jackson, D.B., and Peterson, D.W., 1979, Chronological narrative of the 1969–71 Mauna Ulu eruption of Kīlauea volcano, Hawaii: U.S. Geological Survey Professional Paper 1056, 55 p.

Swanson, D.A., and Houghton, B., 2018, Products, processes, and implications of Keanakākoʻi volcanism, Kīlauea Volcano, Hawaiʻi, *in* Poland, M.P., Garcia, M.O., Camp, V.E., and Grunder, A., eds., Field Volcanology—A Tribute to the Distinguished Career of Don Swanson: Geological Society of America Special Paper 538, p. 159–190, https://doi.org/10.1130/2018.2538(07).

Swanson, D.A., Orr, T., and Patrick, M.R., 2016, Changes in the mass flux of tephra from the lava lake in Overlook crater, Kīlauea Volcano, Hawaiʻi [abs.]: American Geophysical Union Fall Meeting abstract no. V43A-3122.

Swanson, D.A., Rose, T.R., Fiske, R.S., and McGeehin, J.P., 2012, Keanakākoʻi Tephra produced by 300 years of explosive eruptions following collapse of Kīlauea Caldera in about 1500 CE: Journal of Volcanology and Geothermal Research, v. 215–216, p. 8–25, https://doi.org/10.1016/j.jvolgeores.2011.11.009.

Swanson, D.A., Weaver, S.J., and Houghton, B.F., 2015, Reconstructing the deadly eruptive events of 1790 CE at Kīlauea Volcano, Hawaiʻi: Geological Society of America Bulletin, v. 127, p. 503–515, https://doi.org/10.1130/B31116.1.

Swanson, D.A., Wooten, K., and Orr, T., 2009, Buckets of ash track tephra flux from Halemaʻumaʻu Crater, Hawaiʻi: Eos, v. 90, no. 46, p. 427–428.

Tam, E., Miike, R., Labrenz, S., Sutton, A.J., Elias, T., Davis, J., Chen, Y-L., Tantisira, K., Dockery, D., and Avol, E., 2016, Volcanic air pollution over the Island of Hawaiʻi—Emissions, dispersal, and composition; Association with respiratory systems and lung function in Hawaiʻi Island school children: Environment International, v. 92–93, p. 543–552, https://doi.org/10.1016/j.envint.2016.03.025.

Tazieff, H., 1977, An exceptional eruption—Mt. Niragongo, Jan. 10th, 1977: Bulletin of Volcanology, v. 40, p. 189–200.

Thornber, C., Orr, T., Heliker, C., and Hoblitt, R., 2015, Petrologic testament to changes in shallow magma storage and transport during 30+ years of recharge and eruption at Kilauea Volcano, Hawai‘i, *in* Carey, R.J., Cayol, V., Poland, M., and Weis, D., eds., Hawaiian Volcanoes—From Source to Surface: American Geophysical Union Geophysical Monograph 208, p. 147–188.

Tilling, R.I., 1987, Fluctuations in surface height of active lava lakes during 1972–1974 Mauna Ulu eruption, Kīlauea Volcano, Hawai‘i: Journal of Geophysical Research, v. 92, p. 13,721–13,730.

Tilling, R.I., Kauahikaua, J.P., Brantley, S.R., and Neal, C.A., 2014, The Hawaiian Volcano Observatory—A natural laboratory for studying basaltic volcanism, *in* Poland, M.P., Takahashi, J., and Landowski, C.M., eds., Characteristics of Hawaiian volcanoes: U.S. Geological Survey Professional Paper 1801, p. 1–64.

Valade, S., Ripepe, M., Giuffrida, G., Karume, K., and Tedesco, D., 2018, Dynamics of Mount Nyiragongo lava lake inferred from thermal imaging and infrasound array: Earth and Planetary Science Letters, v. 500, p. 192–204.

Vergniolle, S., and Jaupart, C., 1990, Dynamics of degassing at Kīlauea volcano, Hawaii: Journal of Geophysical Research, v. 95, p. 2,793–2,809.

Wilson, D., Elias, T., Orr, T., Patrick, M., Sutton, A.J., and Swanson, D., 2008, Small explosion from new vent at Kīlauea's summit: EOS, v. 89, p. 203.

Witham, F., Woods, A.W., and Gladstone, C., 2006, An analogue experimental model of depth fluctuations in lava lakes: Bulletin of Volcanology, v. 69, p. 51–56.

Wooten, K.M., Thornber, C.R., Orr, T.R., Ellis, J.F., and Trusdell, F.A., 2009, Catalog of tephra samples from Kīlauea's summit eruption, March–December 2008: U.S. Geological Survey Open-File Report 2009–1134, 26 p.

Wright, T.L., and Klein, F.W., 2014, Two hundred years of magma transport and storage at Kīlauea Volcano, Hawai‘i, 1790–2008: U.S. Geological Survey Professional Paper 1806, 240 p.

Menlo Park Publishing Service Center, California
Manuscript approved September 4, 2020
Edited by Monica Erdman
Illustration support by Kimber Petersen
Layout and design by Cory Hurd

Patrick and others—**Kīlauea's 2008–2018 Summit Lava Lake—Chronology and Eruption Insights**—Professional Paper 1867

ISSN 1044-9612 (print)
ISSN 2330-7102 (online)
https://doi.org/10.3133/pp1867A